MMNSA

Mathematical Modelling and Numerical Simulation with Applications

ISSN Online : 2791-8564

Year : 2021

Volume : 1

Issue : 1

www.mmnsa.org

VOLUME: 1 ISSUE: 1
ISSN ONLINE: 2791-8564

September 2021
http://mmnsa.org

MATHEMATICAL MODELLING AND NUMERICAL SIMULATION WITH APPLICATIONS

Contents

Research Articles

1 A numerical approach to the coupled atmospheric ocean model using a fractional operator
Pundikala Veeresha **1-10**

2 Numerical solutions and synchronization of a variable-order fractional chaotic system
Zakia Hammouch, Mehmet Yavuz, Necati Özdemir **11-23**

3 Construction of different types of traveling wave solutions of the relativistic wave equation associated with the Schrödinger equation
Asıf Yokuş **24-31**

4 The Hermite-Hadamard type inequality and its estimations via generalized convex functions of Raina type
Muhammad Tariq, Hijaz Ahmad, Soubhagya Kumar Sahoo **32-43**

5 Stability analysis of an incommensurate fractional-order SIR model
Bahatdin Daşbaşı **44-55**

Mathematical Modelling and Numerical Simulation with Applications, 2021, 1(1), 1–10

https://www.mmnsa.org
ISSN Online: 2791-8564 / Open Access
https://doi.org/10.53391/mmnsa.2021.01.001

RESEARCH PAPER

A numerical approach to the coupled atmospheric ocean model using a fractional operator

Pundikala Veeresha [1,*,†]

[1]Center for Mathematical Needs, Department of Mathematics, CHRIST (Deemed to be University), Bengaluru-560029, India

*Corresponding Author
†pundikala.veeresha@christuniversity.in & pveeresha.maths@gmail.com

Abstract

In the present framework, the coupled mathematical model of the atmosphere-ocean system called El Nino-Southern Oscillation (ENSO) is analyzed with the aid Adams-Bashforth numerical scheme. The fundamental aim of the present work is to demonstrate the chaotic behaviour of the coupled fractional-order system. The existence and uniqueness are demonstrated within the frame of the fixed-point hypothesis with the Caputo-Fabrizio fractional operator. Moreover, we captured the chaotic behaviour for the attained results with diverse order. The effect of the perturbation parameter and others associated with the model is captured. The obtained results elucidate that, the present study helps to understand the importance of fractional order and also initial conditions for the nonlinear models to analyze and capture the corresponding consequence of the fractional-order dynamical systems.

Key words: Caputo-Fabrizio derivative; El Nino-Southern oscillation model; fixed point theorem
AMS 2020 Classification: 34A08; 26A33; 65L05

1 Introduction

The study of mathematical models is always a venue for innovation. It attracted researchers to illustrate their viewpoints and forecast the future significances of the associated phenomena. In this regard, the most efficient and reliable tool is calculus with both integral and differential operators. Most of the phenomena associated with the rate of change are modelled to assist these operators in the modernization of day-day life. For instance, the security of the country, biological processes, economic status, physical mechanism, chemical reaction, weather forecast, coastal and ocean engineering, and many others are examined as well moderated with the aid of mathematical modelling. Moreover, it becomes an interdisciplinary subject due to its ability to exemplify complex phenomena, and also it plays a vital role in creating a bridge between diverse areas. However, many researchers proved that the generalization of classical calculus is very essential to capture the more complex nature of the nonlinear problems associated with daily life. Later, they suggest the concept of calculus with fractional order called fractional calculus (FC) [1, 2, 3, 4, 5]. Even though it originated earlier, it recently fascinated scholars to investigate more essential behaviours the mathematical models described by differential equations [6, 7, 8, 9, 10].
On the other hand, the study of climate with irregularly intervallic changes in sea surface and wind temperatures is a hot topic in the present era due to its significance in diverse fields associated with living beings. Here, we consider the mathematical model exemplifying the atmospheric component coupled with the sea temperature change high air surface pressure, called El Nino-Southern Oscillation (ENSO) [11, 12, 13, 14]. In the tropical western Pacific, La Niña is with low air surface pressure and El Niño with high air surface pressure. The dynamics of recount the oscillating physical mechanism of the ENSO model with the

➤ **Received:** 24.06.2021 ➤ **Revised:** 11.08.2021 ➤ **Accepted:** 13.08.2021 ➤ **Published:** 15.08.2021

thermocline depth anomaly $v(t)$ and temperature of the eastern equatorial Pacific Sea surface $u(t)$ is presented with perturbation coefficient ε as [15, 16, 17, 18] follows

$$\frac{du(t)}{dt} = \beta u + \eta v - \varepsilon u^3,$$
$$\frac{dv(t)}{dt} = -\theta u - \gamma v, \tag{1}$$

where β, η, θ and γ are physical constants. The projected coupled system plays an important role in various phenomena. The projected system is analysed by many researchers to present their viewpoints and also capture linear and complex nature using many semi-analytical and numerical schemes [11, 12, 13, 14, 15, 16, 17, 18]. In the literature, we have distinct fractional operators, each one has its own limitation while examining the complex phenomena. In the present investigation, we consider the fractional operator without singular kernel, called Caputo-Fabrizio (CF) operator in Caputo sense [6], to examine the projected system. Due to more ability to capture the complex nature associated with history-based consequences and memory-related properties, FC is an interdisciplinary subject. Its fundamentals and theories are considered to study diverse real-world problems and attain numerous essential results [19, 20, 21, 22, 23, 24, 25, 26, 27, 28, 29]. Notably, results associated with hereditary, memory, random walk, long-range memory, non-Markovian processes, anomalous diffusion, and others highly necessitate the concept of FC. In this regard, authors in [36], the effect of generalizing the classical concept with the newly defined fractional operator to investigate about the HBV infection with antibody immune response, the nature of Belousov–Zhabotinskii reaction systems have been captured within the frame of Atangana–Baleanu fractional-order derivative by researchers in [37], some ingesting results are derived by authors in [38] about the vector born disease with the help of efficient scheme and Caputo–Fabrizio derivative, the strong interacting internal waves model has been examined with the reliable numerical method with a novel fractional operator in [39], and authors in [40, 41, 42, 43, 44, 45] derived some essential properties of the fractional operators.

Here, we consider Eq. (1) with the CF operator as follows

$${}_0^{CF}D_t^{\mu}u(t) = \beta u + \eta v - \varepsilon u^3,$$
$${}_0^{CF}D_t^{\mu}v(t) = -\theta u - \gamma v, \tag{2}$$

where ${}_0^{CF}D_t^{\mu}$ is a CF derivative with order μ.

The rest of the investigation is organized as follows: we recalled basic definitions of the considered fractional operator in the next section. In Section 3, the basic algorithm of the considered method is presented, and in the next section, the condition for the existence and uniqueness of solutions for the projected system is illustrated. The results and discussion on the derived results are illustrated in Section 5, and concluding remarks are presented in the lost section.

2 Preliminaries

The basic notions of FC are recalled in the present segment [30, 31].
A real function $f(t), t > 0$ is said to be in space C_ν, $\nu \in \mathbb{R}$ if there exists a real number $k(> \nu)$, such that $f(t) = t^k f_1$, where $f_1(t) \in C[0, \infty)$, which is also in space if and only if $u^{(n)} \in C_\nu, n \in \mathbb{N}$.
Definition 1. The Caputo fractional derivative of $f \in C_{-1}^n$ is presented as

$$D_t^{\mu} f(t) = \frac{1}{\Gamma(n-\mu)} \int_0^t (t-\vartheta)^{n-\mu-1} \frac{d^n}{dt^n} f(\vartheta)\, d\vartheta. \tag{3}$$

Definition 2. The Caputo-Fabrizio (CF) fractional derivative in Caputo sense for a function $f \in H^1(a,\ b)\,(\ b > a)$ is [6]

$${}_0^{CF}D_{0,t}^{\mu}(f(t)) = \frac{\mathcal{N}[\mu]}{1-\mu} \int_0^t f'(\vartheta) \exp\left[-\frac{\mu(t-\vartheta)}{1-\mu}\right] d\vartheta, \tag{4}$$

where $\mathcal{N}[\mu]$ $(\mathcal{N}[0] = \mathcal{N}[1] = 1)$ is normalization function.
But, in case the function u does not belong to $H^1(a, b)$, the CF derivative for this version is defined as

$${}_0^{CF}D_{0,t}^{\mu}(f(t)) = \frac{\mu\mathcal{N}[\mu]}{1-\mu} \int_0^t f(t) - f(\vartheta) \exp\left[-\frac{\mu(t-\vartheta)}{1-\mu}\right] d\vartheta. \tag{5}$$

Later, Losada and Nieto in [20] modified the above CF fractional derivative as follows

$${}_0^{CF}D_{0,t}^{\mu}(f(t)) = \frac{(2-\mu)\mathcal{N}[\mu]}{2(1-\mu)} \int_0^t f'(\vartheta) \exp\left[-\frac{\mu(t-\vartheta)}{1-\mu}\right] d\vartheta. \tag{6}$$

Definition 3. The Caputo-Fabrizio (CF) fractional integral for $\mu \in (0, 1)$ is defined as

$${}_0^{CF}I_t^{\mu}(f(t)) = \frac{1-\mu}{\mathcal{N}[\mu]} f(t) + \frac{\mu}{\mathcal{N}[\mu]} \int_0^t f(\vartheta)\, d\vartheta, t \geq 0. \tag{7}$$

3 Numerical method

In this segment, with the Caputo–Fabrizio operator, the two-step Adams–Bashforth method is hired [32, 33, 34]

$$ {}_{0}^{CF}D_t^{\mu}(u(t)) = \frac{\mathcal{N}[\mu]}{1-\mu}\int_0^t u'(\vartheta)\exp\left[-\mu\frac{t-\vartheta}{1-\mu}\right]d\vartheta\,. \tag{8} $$

Now, the grid size for some integer N for finite difference method is $k = \frac{1}{N}$. Further, the grid points are presented in the time interval $[0,\ T]$ as $t_n = nk, \quad n = 0, 1, 2, \ \ldots, TN$. At the grid point, the value of the function $u_i = u(t_i)$. For the fractional-order Caputo–Fabrizio derivative, a discrete approximation is presented as [34]

$$ {}_{0}^{CF}D_t^{\mu}(u(t_n)) = \frac{\mathcal{N}[\mu]}{1-\mu}\int_0^{t_n} u'(\vartheta)\exp\left[-\mu\frac{t_n-\vartheta}{1-\mu}\right]d\vartheta\,. \tag{9} $$

By the assist of first-order approximation, the above equation simplifies

$$ {}_{0}^{CF}D_t^{\mu}\left(u\left(t_j\right)\right) = \frac{\mathcal{N}[\mu]}{1-\mu}\sum_{j=1}^{n}\int_{(j-1)k}^{jk}\left(\frac{u^{k+1}-u^k}{\Delta t}+\mathcal{O}(\Delta t)\right)\exp\left[-\mu\frac{t_j-\vartheta}{1-\mu}\right]d\vartheta\,. \tag{10} $$

But

$$ \frac{\mathcal{N}[\mu]}{1-\mu}\sum_{j=1}^{n}\left(\frac{u^{j+1}-u^j}{\Delta t}+\mathcal{O}(\Delta t)\right)\int_{(j-1)k}^{jk}\exp\left[-\mu\frac{t_j-\vartheta}{1-\mu}\right]d\vartheta\,, \tag{11} $$

$$ {}_{0}^{CF}D_t^{\mu}\left(u\left(t_j\right)\right) = \frac{\mathcal{N}[\mu]}{\mu}\sum_{j=1}^{n}\left(\frac{u^{j+1}-u^j}{\Delta t}+\mathcal{O}(\Delta t)\right)d_{j,k}, \tag{12} $$

where

$$ d_{j,k} = \exp\left[-\mu\frac{k}{1-\mu}(n-j+1)\right] - \exp\left[-\mu\frac{k}{1-\mu}(n-j)\right]. \tag{13} $$

Finally, we obtained

$$ {}_{0}^{CF}D_t^{\mu}(u(t_n)) = \frac{\mathcal{N}[\mu]}{\mu}\sum_{j=1}^{n}\left(\frac{u^{j+1}-u^j}{\Delta t}\right)d_{j,k} + \frac{\mathcal{N}[\mu]}{\mu}\sum_{j=1}^{n}d_{j,k}\mathcal{O}(\Delta t). \tag{14} $$

4 Existence and uniqueness of solutions

Here, present the existence and uniqueness of the hired model within the frame of the fixed-point theorem. The system defined in Eq. (2) hired as follows

$$ \begin{cases} {}_{0}^{CF}D_t^{\mu}[u(t)] = \mathcal{G}_1(t,\ u) = \beta u + \eta v - \varepsilon u^3, \\ {}_{0}^{CF}D_t^{\mu}[v(t)] = \mathcal{G}_2(t, v) = -\theta u - \gamma v. \end{cases} \tag{15} $$

Now, using Eq. (2), we have

$$ \begin{aligned} u(t) - u(0) &= {}_{0}^{CF}I_t^{\mu}\left\{\beta u + \eta v - \varepsilon u^3\right\}, \\ v(t) - v(0) &= {}_{0}^{CF}I_t^{\mu}\{-\theta u - \gamma v\}. \end{aligned} \tag{16} $$

Then we have from [35] as follows

$$ \begin{aligned} u(t) - u(0) &= \frac{2\mu}{(2-\mu)\mathcal{N}(\mu)}\int_0^t \mathcal{G}_1(\zeta, u)\,d\zeta + \frac{2(1-\mu)}{(2-\mu)\mathcal{N}(\mu)}\mathcal{G}_1(t, u), \\ v(t) - v(0) &= \frac{2\mu}{(2-\mu)\mathcal{N}(\mu)}\int_0^t \mathcal{G}_2(\zeta, v)\,d\zeta + \frac{2(1-\mu)}{(2-\mu)\mathcal{N}(\mu)}\mathcal{G}_2(t, v). \end{aligned} \tag{17} $$

Theorem 1. The kernels $\mathcal{G}_1$ and $\mathcal{G}_2$ satisfies the Lipschitz condition and contraction if $0 \ \le \left(\beta + \eta\lambda_2 - \varepsilon\left(a^2 + b^2 + ab\right)\right) < 1$ and $0 \ \le (\theta\lambda_1 + \gamma) < 1$, satisfies respectively.

Proof. We consider the two functions u and u_1 to prove the required result, then

$$\begin{aligned}
\|\mathcal{G}_1(t,\ u)-\mathcal{G}_1(t,\ u_1)\| &= \left\|\left(\beta\left[u(t)-u(t_1)\right]+\eta v(t)-\varepsilon[u^3(t)-u^3(t_1)]\right)\right\| \\
&= \left\|\left(\beta\left[u(t)-u(t_1)\right]+\eta v(t)-\varepsilon[u^2(t)+u^2(t_1)+u(t)u(t_1)]\left[u(t)-u(t_1)\right]\right)\right\| \\
&\leq \left\|\beta+\eta v(t)-\varepsilon\left(a^2+b^2+ab\right)\right\|\|u(t)-u(t_1)\| \\
&\leq \left(\beta+\eta\lambda_2-\varepsilon\left(a^2+b^2+ab\right)\right)\|u(t)-u(t_1)\|,
\end{aligned} \tag{18}$$

where $\|v(t)\|\leq\lambda_2$ be the bounded function. Since u and u_1 are bounded, we have $\|u(t)\|\leq a$ and $\|u(t_1)\|\leq b$. Setting $\rho_1=\beta+\eta\lambda_2-\varepsilon\left(a^2+b^2+ab\right)$ in the above inequality, then we have

$$\|\mathcal{G}_1(t,\ u)-\mathcal{G}_1(t,\ u_1)\|\leq\rho_1\|u(t)-u(t_1)\|. \tag{19}$$

Eq. (19) provides the Lipschitz condition for $\mathcal{G}_1$. Similarly, we can see that if $0\leq\left(\beta+\eta\lambda_2-\varepsilon\left(a^2+b^2+ab\right)\right)<1$, then it implies the contraction. In the same way for $\rho_2=\theta\lambda_1+\gamma$, we can prove

$$\|\mathcal{G}_2(t,\ v)-\mathcal{G}_2(t,v_1)\|\leq\rho_2\|v(t)-v(t_1)\|. \tag{20}$$

By the assist of Eq. (20), Eq. (17) gives

$$\begin{aligned}
u(t)&=u(0)+\frac{2\mu}{(2-\mu)\mathcal{N}(\mu)}\int_0^t\mathcal{G}_1(\ \zeta,u)\,d\zeta+\frac{2(1-\mu)}{(2-\mu)\mathcal{N}(\mu)}\mathcal{G}_1(\ t,u),\\
v(t)&=v(0)+\frac{2\mu}{(2-\mu)\mathcal{N}(\mu)}\int_0^t\mathcal{G}_2(\ \zeta,v)\,d\zeta+\frac{2(1-\mu)}{(2-\mu)\mathcal{N}(\mu)}\mathcal{G}_2(\ t,v).
\end{aligned} \tag{21}$$

Then obtain the recursive form as

$$\begin{aligned}
u_n(t)&=\frac{2\mu}{(2-\mu)\mathcal{N}(\mu)}\int_0^t\mathcal{G}_1(\zeta,u_{n-1})\,d\zeta+\frac{2(1-\mu)}{(2-\mu)\mathcal{N}(\mu)}\mathcal{G}_1(t,u_{n-1}),\\
v_n(t)&=\frac{2\mu}{(2-\mu)\mathcal{N}(\mu)}\int_0^t\mathcal{G}_1(\zeta,v_{n-1})\,d\zeta+\frac{2(1-\mu)}{(2-\mu)\mathcal{N}(\mu)}\mathcal{G}_1(t,v_{n-1}).
\end{aligned} \tag{22}$$

The associated initial conditions are

$$u(0)=u_0(t)\ \ \textit{and}\ v(0)=v_0(t). \tag{23}$$

Now, between the terms the successive difference is presented as

$$\begin{aligned}
\phi_{1n}(t)=u_n(t)-u_{n-1}(t)&=\frac{2(1-\mu)}{(2-\mu)\mathcal{N}(\mu)}\left(\mathcal{G}_1(t,u_{n-1})-\mathcal{G}_1(t,u_{n-2})\right)+\frac{2\mu}{(2-\mu)\mathcal{N}(\mu)}\int_0^t\left(\mathcal{G}_1(t,u_{n-1})-\mathcal{G}_1(t,u_{n-2})\right)d\zeta,\\
\phi_{2n}(t)=v_n(t)-v_{n-1}(t)&=\frac{2(1-\mu)}{(2-\mu)\mathcal{N}(\mu)}\left(\mathcal{G}_2(t,v_{n-1})-\mathcal{G}_2(t,v_{n-2})\right)+\frac{2\mu}{(2-\mu)\mathcal{N}(\mu)}\int_0^t\left(\mathcal{G}_2(t,v_{n-1})-\mathcal{G}_2(t,v_{n-2})\right)d\zeta.
\end{aligned} \tag{24}$$

Notice that

$$\begin{aligned}
u_n(t)&=\sum_{i=1}^{n}\phi_{1i}(t),\\
v_n(t)&=\sum_{i=1}^{n}\phi_{2i}(t).
\end{aligned} \tag{25}$$

Therefore

$$\|\phi_{1n}(t)\|=\|u_n(t)-u_{n-1}(t)\|=\left\|\frac{2(1-\mu)}{(2-\mu)\mathcal{N}(\mu)}\left(\mathcal{G}_1(t,u_{n-1})-\mathcal{G}_1(t,u_{n-2})\right)+\frac{2\mu}{(2-\mu)\mathcal{N}(\mu)}\int_0^t\left(\mathcal{G}_1(t,u_{n-1})-\mathcal{G}_1(t,u_{n-2})\right)d\zeta\right\|. \tag{26}$$

The above equation simplifies with the assist of the triangular inequality, as

$$\|\phi_{1n}(t)\|=\|u_n(t)-u_{n-1}(t)\|=\frac{2(1-\mu)}{(2-\mu)\mathcal{N}(\mu)}\|(\mathcal{G}_1(t,u_{n-1})-\mathcal{G}_1(t,u_{n-2}))\|+\frac{2\mu}{(2-\mu)\mathcal{N}(\mu)}\left\|\int_0^t\left(\mathcal{G}_1(t,u_{n-1})-\mathcal{G}_1(t,u_{n-2})\right)d\zeta\right\|. \tag{27}$$

Then we have for u admitting the Lipschitz condition

$$\|\phi_{1n}(t)\|=\|u_n(t)-u_{n-1}(t)\|\leq\frac{2(1-\mu)}{(2-\mu)\mathcal{N}(\mu)}\rho_1\left\|\phi_{1(n-1)}(t)\right\|+\frac{2\mu}{(2-\mu)\mathcal{N}(\mu)}\rho_1\int_0^t\left\|\phi_{1(n-1)}(t)\right\|d\zeta. \tag{28}$$

Similarly, one can get

$$\|\phi_{2n}(t)\| \leq \frac{2\mu}{(2-\mu)\mathcal{N}(\mu)}\rho_2\int_0^t \left\|\phi_{2(n-1)}(\zeta)\right\| d\zeta + \frac{2(1-\mu)}{(2-\mu)\mathcal{N}(\mu)}\rho_2\left\|\phi_{2(n-1)}(t)\right\|. \tag{29}$$

Now, we state the following theorem with the assist of the above attained results:
Theorem 2. If we have specific t_0 , then the solution for Eq. (2) will exist and be unique. Further, we have for $i = 1, 2$.

$$\frac{2(1-\mu)}{(2-\mu)\mathcal{N}(\mu)}\rho_i + \frac{2\mu}{(2-\mu)\mathcal{N}(\mu)}\rho_i t_0 < 1,$$

Proof. Let $u(t)$ and $v(t)$ be the bounded functions admitting the Lipschitz condition. Then, we get by Eqs. (28) and (29)

$$\begin{aligned}\left\|\phi_{1i}(t)\right\| &\leq \|u(0)\|\left[\frac{2\mu}{(2-\mu)\mathcal{N}(\mu)}\rho_1 t + \frac{2(1-\mu)}{(2-\mu)\mathcal{N}(\mu)}\rho_1\right]^n,\\ \left\|\phi_{2i}(t)\right\| &\leq \|v_n(0)\|\left[\frac{2\mu}{(2-\mu)\mathcal{N}(\mu)}\rho_2 t + \frac{2(1-\mu)}{(2-\mu)\mathcal{N}(\mu)}\rho_2\right]^n.\end{aligned} \tag{30}$$

Therefore, for the obtained solutions, continuity and existence are verified. Now, to prove the Eq. (30) is a solution for Eq. (2), we consider

$$\begin{aligned}u(t) - u(0) &= u_n(t) - \mathcal{K}_{1n}(t),\\ v(t) - v(0) &= v_n(t) - \mathcal{K}_{2n}(t).\end{aligned} \tag{31}$$

Let us consider

$$\begin{aligned}\|\mathcal{K}_{1n}(t)\| &= \left\|\frac{2(1-\mu)}{(2-\mu)\mathcal{N}(\mu)}\left(\mathcal{G}_1(t,u) - \mathcal{G}_1(t, u_{n-1})\right) + \frac{2\mu}{(2-\mu)\mathcal{N}(\mu)}\int_0^t \left(\mathcal{G}_1(\zeta,u) - \mathcal{G}_1(\zeta,u_{n-1})\right)d\zeta\right\|\\ &\leq \frac{2(1-\mu)}{(2-\mu)\mathcal{N}(\mu)}\left\|\left(\mathcal{G}_1(t,u) - \mathcal{G}_1(t, u_{n-1})\right)\right\| + \frac{2\mu}{(2-\mu)\mathcal{N}(\mu)}\int_0^t \left\|\left(\mathcal{G}_1(\zeta,u) - \mathcal{G}_1(\zeta,u_{n-1})\right)\right\| d\zeta\\ &\leq \frac{2(1-\mu)}{(2-\mu)\mathcal{N}(\mu)}\rho_1\|u-u_{n-1}\| + \frac{2\mu}{(2-\mu)\mathcal{N}(\mu)}\rho_1\|u-u_{n-1}\|\, t.\end{aligned} \tag{32}$$

This process gives

$$\|\mathcal{K}_{1n}(t)\| \leq \left(\frac{2\mu}{(2-\mu)\mathcal{N}(\mu)}t + \frac{2(1-\mu)}{(2-\mu)\mathcal{N}(\mu)}\right)^{n+1}\rho_1^{n+1}M.$$

Similarly, at $t_0$we can obtain

$$\|\mathcal{K}_{1n}(t)\| \leq \left(\frac{2\mu}{(2-\mu)\mathcal{N}(\mu)}t_0 + \frac{2(1-\mu)}{(2-\mu)\mathcal{N}(\mu)}\right)^{n+1}\rho_1^{n+1}M. \tag{33}$$

As $n\to\infty$ and from Eq. (33), $\|\mathcal{K}_{1n}(t)\|\to 0$. Similarly, we can verify for $\|\mathcal{K}_{2n}(t)\|$. Next, for the solution of the projected model, we prove its uniqueness. Suppose $u^*(t)$ and $v^*(t)$, be the set of other solutions, then

$$u(t) - u^*(t) = \frac{2(1-\mu)}{(2-\mu)\mathcal{N}(\mu)}\left(\mathcal{G}_1(t,u) - \mathcal{G}_1(t, u^*)\right) + \frac{2\mu}{(2-\mu)\mathcal{N}(\mu)}\int_0^t \left(\mathcal{G}_1(\zeta,u) - \mathcal{G}_1(\zeta,u^*)\right)d\zeta. \tag{34}$$

Now, employing the norm on the above equation, we get

$$\begin{aligned}\left\|u(t) - u^*(t)\right\| &= \left\|\frac{2(1-\mu)}{(2-\mu)\mathcal{N}(\mu)}\left(\mathcal{G}_1(t,u) - \mathcal{G}_1(t, u^*)\right) + \frac{2\mu}{(2-\mu)\mathcal{N}(\mu)}\int_0^t \left(\mathcal{G}_1(\zeta,u) - \mathcal{G}_1(\zeta,u^*)\right)d\zeta\right\|\\ &\leq \frac{2\mu}{(2-\mu)\mathcal{N}(\mu)}\rho_1 t\left\|u(t) - u^*(t)\right\| + \frac{2(1-\mu)}{(2-\mu)\mathcal{N}(\mu)}\rho_1\left\|u(t) - u^*(t)\right\|.\end{aligned} \tag{35}$$

On solving

$$\left\|u(t) - u^*(t)\right\|\left(1 - \frac{2\mu}{(2-\mu)\mathcal{N}(\mu)}\rho_1 t - \frac{2(1-\mu)}{(2-\mu)\mathcal{N}(\mu)}\rho_1\right) \leq 0. \tag{36}$$

From Eq. (36), it is clear that $u(t) = u^*(t)$, if

$$\left(1 - \frac{2\mu}{(2-\mu)\mathcal{N}(\mu)}\rho_1 t - \frac{2(1-\mu)}{(2-\mu)\mathcal{N}(\mu)}\rho_1\right) \geq 0. \tag{37}$$

Hence, Eq. (37) proves our required proof.

5 Results and discussion

The study of complex nature associated with real-world models always attracted young researchers to present their viewpoints and illustrated novel properties of the corresponding system. In this work, we hired coupled system exemplifying the atmospheric ocean, namely ENSO model using a novel fractional derivative. The considered coupled system is analysed with the initial conditions $u(0) = u_0(t) = 1$ and $v(0) = v_0(t) = 1$. The nature of hired model for different μ is captured in Figure 1. From these figures, we can observe that as order increase, the complex nature reduces, specifically for $\mu = 0.85$ we can observe more cycles in the plots. For different values of the perturbation parameter, the response of the achieved results is captured and cited in Figure 2. For $\eta = 4$, we can evidence the more complex nature as compared to $\eta = 2$. Similarly, we captured the nature for distinct θ and presented it in Figure 3. The present investigation confirms that the slight changes in the physical parameters associated to systems and furthers will help us investigate and predict the corresponding essential behaviour of the system. The fractional operator allows us to capture the more complex nature of the same system associated with time-based properties.

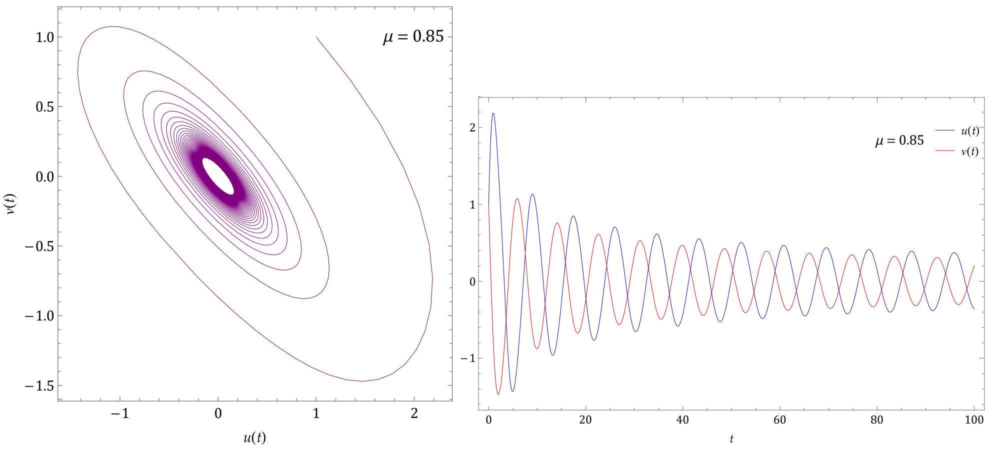

(a)

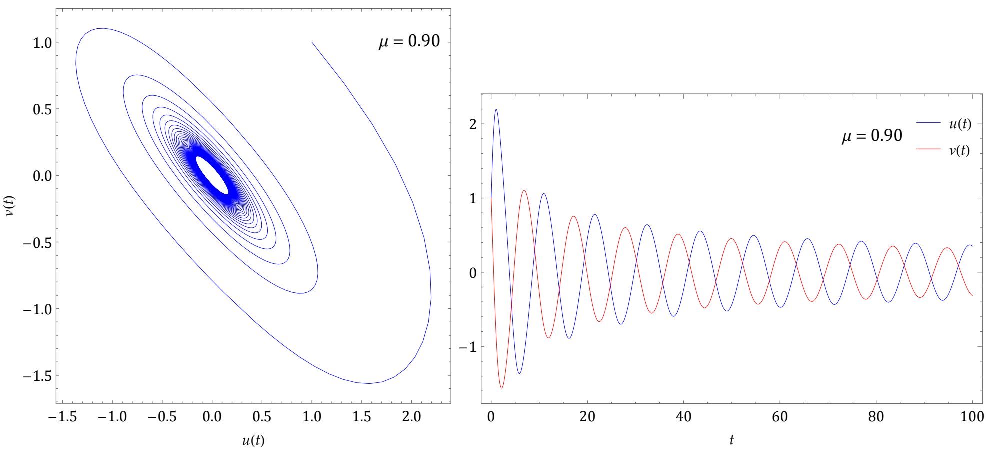

(b)

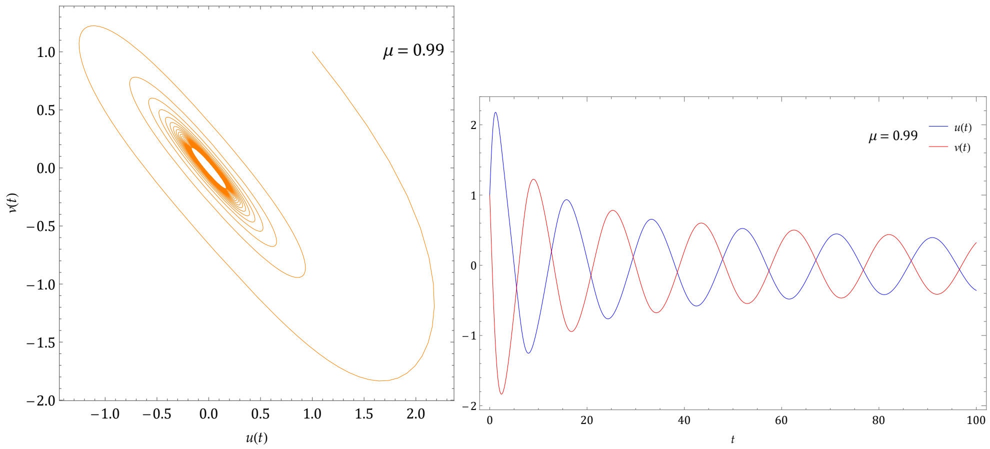

(c)

Figure 1. Behaviour of the results achieved for (a) $\mu = 0.85$, (b) $\mu = 0.90$ and (c) $\mu = 0.99$ at $\beta = 1$, $\eta = 1$, $\theta = 1$, $\gamma = 1$ and $\epsilon = 0.1$.

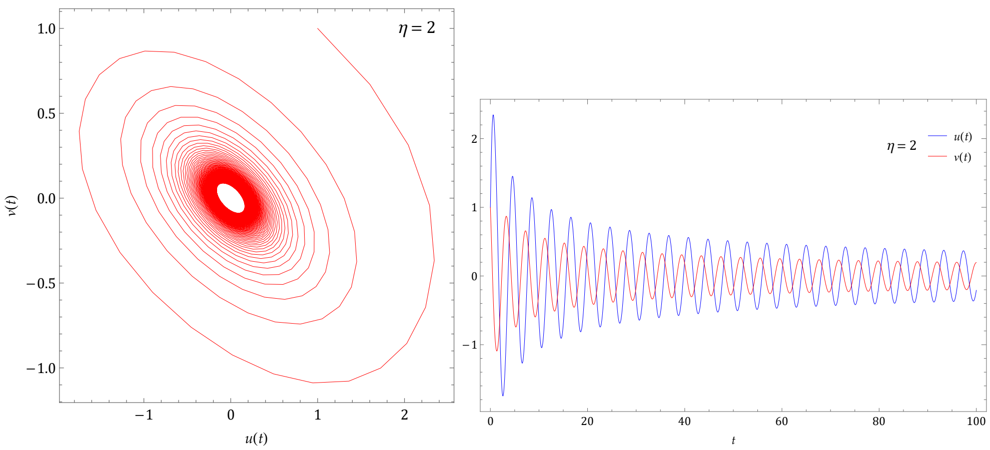

(a)

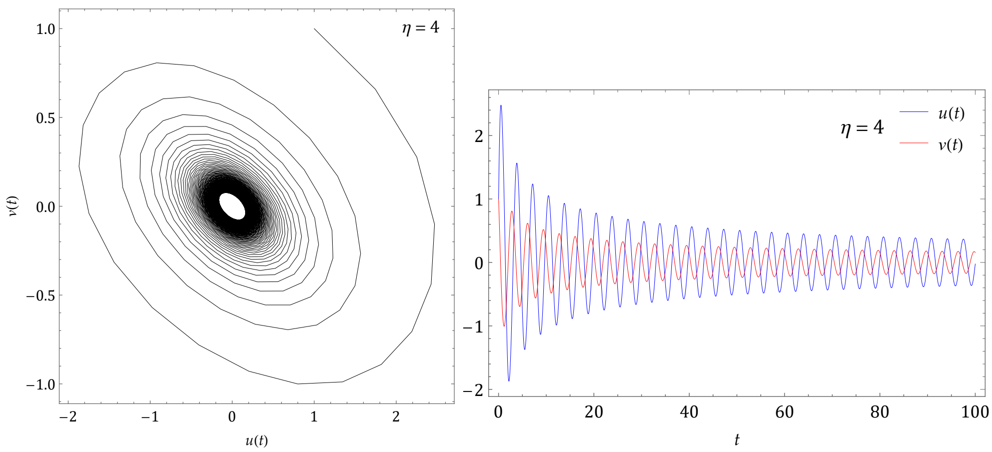

(b)

Figure 2. Nature of the results achieved for (a) $\eta = 2$ and (b) $\mu = 4$ at $\beta = 1$, $\mu = 0.95$, $\theta = 1$, $\gamma = 1$ and $\epsilon = 0.1$.

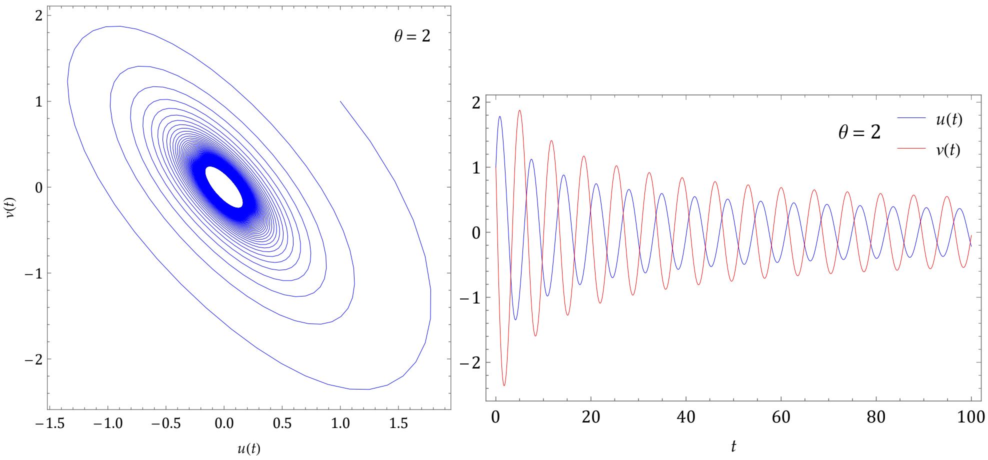

(a)

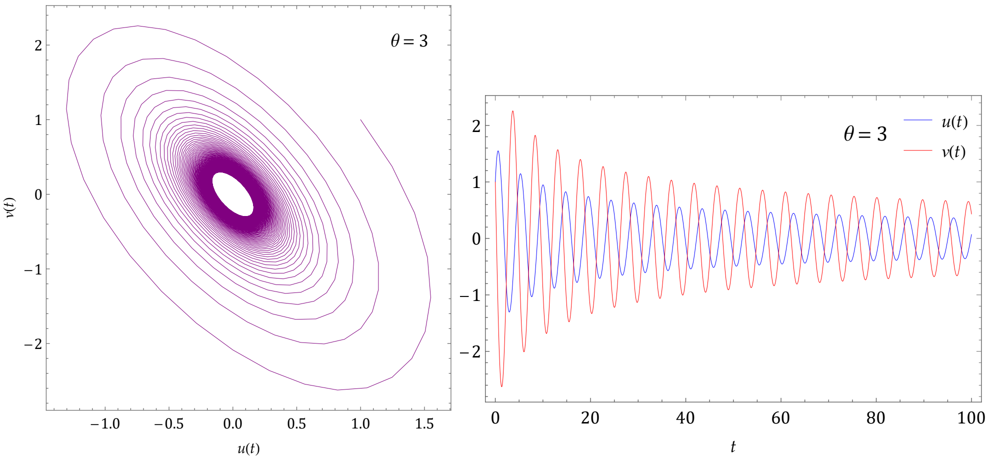

(b)

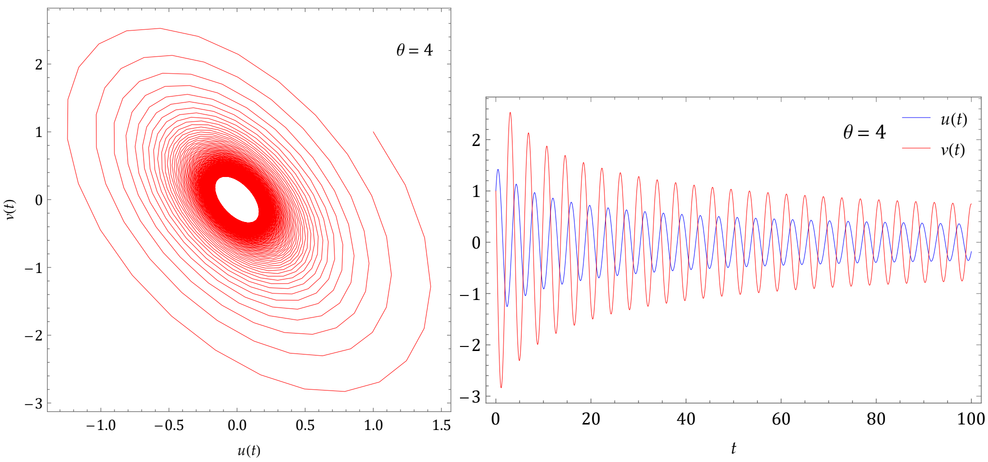

(c)

Figure 3. Response of the results achieved for (a) $\theta = 2$, (b) $\theta = 3$ and (c) $\theta = 4$ at $\beta = 1$, $\eta = 1$, $\mu = 0.95$, $\gamma = 1$ and $\epsilon = 0.1$.

6 Conclusion

In the present study, we analysed the atmospheric ocean model within the frame of the novel fractional operator using an efferent numerical scheme. The complex nature of the considered ENSO model captured for distinct fractional order in parametric plots.

The behaviour for different parameters associated with coupled system is analysed and presented in plots. The conditions for both existence and uniqueness are archived in the present study for the considered system with the aid of Fixed-point theory and Banach space.

The capture plots show that the hired system is exceptionally reliant on the fractional operator. The projected method finds the solution for the employed system without making any perturbation, transformations, or discretization. The consequences attained in the present study are simulating as related to results available in the literature. Moreover, the hired system plays an important part in weather forecast and ocean consequences related to the daily life of the living beings. Hence, the present investigation can aid the researchers to investigate more regarding the model and opens the door for innovation. Finally, the efficiency and reliability of both considered operator and algorithm can be evidence with the help of the present investigation and further, they can employ for the complex model to study corresponding consequences.

Declarations

Consent for publication

Not applicable.

Conflicts of interest

The author declares that he has no conflict of interests.

Funding

Not applicable.

Acknowledgements

The author is thankful to the reviewers and editor for their valuable suggestions to improve the quality of the manuscript.

References

[1] M. Caputo, Elasticita e Dissipazione, Zanichelli, Bologna, (1969).

[2] K. S. Miller, B. Ross, An introduction to fractional calculus and fractional differential equations, A Wiley, New York, (1993).

[3] I. Podlubny, Fractional Differential Equations, Academic Press, New York, (1999).

[4] A. A. Kilbas, H. M. Srivastava, J. J. Trujillo, Theory and applications of fractional differential equations, Elsevier, Amsterdam, (2006).

[5] D. Baleanu, Z.B. Guvenc, J.A. Tenreiro Machado, New trends in nanotechnology and fractional calculus applications, Springer Dordrecht Heidelberg, London New York, (2010).

[6] M. Caputo, M. Fabrizio, A new definition of fractional derivative without singular kernel, Progr. Fract. Diff. Appl., 1 (2) (2015), 73-85.

[7] K. M. Safare, et.al., A mathematical analysis of ongoing outbreak COVID-19 in India through nonsingular derivative, Numerical Methods for Partial Differential Equations 37 (2) (2021), 1282-1298.

[8] M. Yavuz, European option pricing models described by fractional operators with classical and generalized Mittag-Leffler kernels, Numerical Methods for Partial Differential Equations, (2021), DOI: 10.1002/num.22645.

[9] L. Akinyemi, M. Şenol, S. N. Huseen, Modified homotopy methods for generalized fractional perturbed Zakharov–Kuznetsov equation in dusty plasma, Adv. Differ. Equ., 45 (2021), DOI: 10.1186/s13662-020-03208-5.

[10] C. Baishya, S. J. Achar, P. Veeresha, D. G. Prakasha, Dynamics of a fractional epidemiological model with disease infection in both the populations, Chaos, 31 (2021), DOI: 10.1063/5.0028905.

[11] J. Fei-Fei, An equatorial ocean recharge paradigm for ENSO. Part I: conceptual model, J. Atmos. Sci., 54 (7) (1996), 811-829.

[12] Y. Zen, The Laplace-Adomian-Pade technique for the ENSO model, Math. Probl. Eng, 4 (2013), DOI:10.1155/2013/954857.

[13] J. Q. Mo, W. T. Lin, J. Zhu, The variational iteration solving method for El Nino/La Nino-Southern Oscillation model, Adv. Math., 35 (2) (2006), 232–236.

[14] J. Q. Mo, W. T. Lin, Generalized variation iteration solution of an atmosphere-ocean oscillator model for global climate, J. Syst. Sci. Complex, 24 (2) (2011), 271-276.

[15] Z. Xian-Chun, L. Yi-Hua, W. T. Lin, J. Q. Mo, Homotopic mapping solution of an oscillator for the El nino/La Nina-Southern Oscillation, Chin. Phys. B, 18 (11) (2009), 4603-4605.

[16] J. Singh, D. Kumar, J. J. Nieto, Analysis of an El Nino-Southern Oscillation model with a new fractional derivative, Chaos Solitons Fractals, 99 (2017), 109-115.

[17] M. Gubes, H. A. Peker, G. Oturanc, Application of differential transform method for El Nino Southern Oscillation (ENSO) model with compared Adomian decomposition and variational iteration methods. J. Math. Comput. Sci., 15 (2015), 167–178.

[18] J. Q. Mo JQ, W. T. Lin, Perturbed solution for the ENSO nonlinear model, Acta Phys. Sinica., 53 (4) (2004), 996-998.

[19] L. Akinyemi, O.S. Iyiola, A reliable technique to study nonlinear time-fractional coupled Korteweg-de Vries equations, Adv. Differ. Equ., 2020 (2020), 1-27, DOI: 10.1186/s13662-020-02625-w.

[20] E. K. Akgül, A. Akgül, M. Yavuz, New Illustrative Applications of Integral Transforms to Financial Models with Different Fractional Derivatives, Chaos Solitons Fractals 146 (2021), 110877.

[21] P. Veeresha, E. Ilhan, H. M. Baskonus, Fractional approach for analysis of the model describing wind- influenced projectile motion, Phys. Scr., 96 (2021), DOI: 10.1088/1402-4896/abf868.

[22] L. Akinyemi, A fractional analysis of Noyes–Field model for the nonlinear Belousov–Zhabotinsky reaction, Comp. Appl. Math., 39 (2020), 1-34, DOI: 10.1007/s40314-020-01212-9.

[23] P. Veeresha, D. G. Prakasha, A reliable analytical technique for fractional Caudrey-Dodd-Gibbon equation with Mittag-Leffler kernel, Nonlinear Eng., 9 (1) (2020), 319–328.

[24] M. Yavuz, N. Sene, Fundamental calculus of the fractional derivative defined with Rabotnov exponential kernel and application to nonlinear dispersive wave model, J. Ocean Eng. Sci., 6 (2) (2021), 196-205.

[25] S.-W. Yao, E. Ilhan, P. Veeresha, H. M. Baskonus, A powerful iterative approach for quintic complex Ginzburg-Landau equation within the frame of fractional operator, Fractals, (2021), DOI: 10.1142/S0218348X21400235.

[26] L. Akinyemi, P. Veeresha, M. Senol, Numerical solutions for coupled nonlinear Schrodinger-Korteweg-de Vries and Maccari's systems of equations, Modern Physics Letters B, (2021), 2150339, DOI: 10.1142/S0217984921503395.

[27] A. Atangana, R. T. Alqahtani, Numerical approximation of the space-time Caputo-Fabrizio fractional derivative and application to groundwater pollution equation, Adv. Diff. Equ., 1 (2016), 1–13.

[28] C. Baishya, Dynamics of a Fractional Stage Structured Predator-Prey model with Prey Refuge, Indian J. Ecol., 47 (4) (2020), 1118-1124.

[29] P. Veeresha, D.G. Prakasha, H.M. Baskonus, New numerical surfaces to the mathematical model of cancer chemotherapy effect in Caputo fractional derivatives, Chaos 29 (013119) (2019). DOI: 10.1063/1.5074099.

[30] K. M. Owolabi, A. Atangana, Analysis and application of new fractional Adams–Bashforth scheme with Caputo–Fabrizio derivative, Chaos, Solitons Fractals, 105 (2017), 111–119.

[31] A. Atangana, Derivative with a new parameter: theory, methods and applications, New York: Academic Press; 2016.

[32] A. Atangana, K. M. Owolabi, New numerical approach for fractional differential equations, Math. Model. Nat. Phenom., 13 (2018), DOI: 10.1051/mmnp/2018010.

[33] A. Atangana, J. J. Nieto, Numerical solution for the model of RLC circuit via the fractional derivative without singular kernel, Adv. Mech. Eng., 7(2015), 1–6.

[34] M. Caputo, M. Fabrizio, Applications of new time and spatial fractional derivatives with exponential kernels, Progr. Fract. Diff. Appl., 2 (2016), 1–11.

[35] J. Losada, J. J. Nieto, Properties of the new fractional derivative without singular kernel, Progr. Fract. Differ. Appl., 1 (2015), 87-92.

[36] J. Danane, K. Allali, Z. Hammouch, Mathematical analysis of a fractional differential model of HBV infection with antibody immune response, Chaos Solitons Fractals, 136 (2020).

[37] K. M. Owolabi, Z. Hammouch, Spatiotemporal patterns in the Belousov–Zhabotinskii reaction systems with Atangana–Baleanu fractional order derivative, Phys. A, 523 (2019), 1072-1090.

[38] F. Haq, I. Mahariq, T. Abdeljawad, N. Maliki, A new approach for the qualitative study of vector born disease using Caputo–Fabrizio derivative, Numer. Methods Partial Differ. Equ., 37 (2) (2021), 1809-1818.

[39] P. Veeresha, H. M. Baskonus, W. Gao, Strong interacting internal waves in rotating ocean: Novel fractional approach, Axioms, 10 (2) (2021).

[40] W. Zhong, L. Wang, T. Abdeljawad, Separation and stability of solutions to nonlinear systems involving Caputo–Fabrizio derivatives, Adv. Differ. Equ., 166 (2020). DOI: 10.1186/s13662-020-02632-x.

[41] R. Gul, M. Sarwar, K. Shah, T. Abdeljawad, F. Jarad, Qualitative Analysis of Implicit Dirichlet Boundary Value Problem for Caputo-Fabrizio Fractional Differential Equations, J. Funct. Spaces, (2020), DOI: 10.1155/2020/4714032.

[42] M. Yavuz, E. Bonyah, New approaches to the fractional dynamics of schistosomiasis disease model, Phys. A, 525 (2019), 373-393.

[43] P. Veeresha, D. G. Prakasha, Z. Hammouch, An efficient approach for the model of thrombin receptor activation mechanism with Mittag-Leffler function, Nonlinear Analysis: Problems, Applications and Computational Methods, (2020), 44–60.

[44] K. Shah, F. Jarad, T. Abdeljawad, On a nonlinear fractional order model of dengue fever disease under Caputo-Fabrizio derivative, Alexandria Eng. J., 59 (4) (2020), 2305-2313.

[45] M. Yavuz, N. Sene, Fundamental calculus of the fractional derivative defined with Rabotnov exponential kernel and application to nonlinear dispersive wave model, J. Ocean Eng. Sci., 6 (2) (2021), 196-205.

Mathematical Modelling and Numerical Simulation with Applications, 2021, 1(1), 11–23

https://www.mmnsa.org
ISSN Online: 2791-8564 / Open Access
https://doi.org/10.53391/mmnsa.2021.01.002

RESEARCH PAPER

Numerical solutions and synchronization of a variable-order fractional chaotic system

Zakia Hammouch [1,2,3,§], Mehmet Yavuz [4,5,§] and Necati Özdemir [6,*,§]

[1]Division of Applied Mathematics, Thu Dau Mot University, Binh Duong Province, Vietnam, [2]Department of Medical Research, China Medical University Hospital, Taichung, Taiwan, [3]Department of Sciences, École Normale Supérieure, Moulay Ismail University of Meknes, Morocco, [4]Department of Mathematics and Computer Sciences, Necmettin Erbakan University, 42090 Konya, Turkey, [5]Department of Mathematics, College of Engineering, Mathematics and Physical Sciences, University of Exeter, TR10, Cornwall, UK, [6]Department of Mathematics, Balikesir University, 10440 Balikesir, Turkey

[*]Corresponding Author
[§]hammouch_zakia@tdmu.edu.vn (Zakia Hammouch); mehmetyavuz@erbakan.edu.tr (Mehmet Yavuz); nozdemir@balikesir.edu.tr (Necati Özdemir)

Abstract

In the present paper, we implement a novel numerical method for solving differential equations with fractional variable-order in the Caputo sense to research the dynamics of a circulant Halvorsen system. Control laws are derived analytically to make synchronization of two identical commensurate Halvorsen systems with fractional variable-order time derivatives. The chaotic dynamics of the Halvorsen system with variable-order fractional derivatives are investigated and the identical synchronization between two systems is achieved. Moreover, graph simulations are provided to validate the theoretical analysis.

Key words: Variable-order fractional derivative; chaotic system; Lyapunov exponent; synchronization
AMS 2020 Classification: 34D06; 26A33; 34C28

1 Introduction

Recently chaos theory has attracted the scientific community. It has revalorized the evolution of science and technology immediately its appearance in 1963 [1]. This is primarily due to the unpredictable dynamic behavior and the sensitivity to initial conditions. The concept of chaotic science is extensively referred to the science of revelations, of the unpredictable and nonlinear. Therefore, when studying chaotic phenomena one should expect the unexpected. Besides, chaos theory has become an effective research area, because of the various applications of chaos in several disciplines like economy, chemistry, physics, engineering, ecology, robotics, secure communications etc [2]. In the literature, there are many familiar chaotic systems like: Lorenz system, Lu system, Ikeda system, Sprott-Linz system, Jerk system etc [3, 4, 5, 6, 7, 8, 9, 10, 11, 12, 13, 14, 15, 16, 17, 18, 19, 20, 21, 22, 23, 24, 25, 26, 27, 28, 29, 30, 31].
Moreover, the modeling of problems in physics, engineering, and real-life phenomena reflects the mathematical tools available at the time of their development. Therefore, most real-life problems have been described by means of differential equations with non-integer order derivatives [32]. Recently, many papers focused their attention on ODEs and PDEs with non-integer-order derivatives owing to their common aspect in assorted applications in finance, medical, fluid mechanics, viscoelasticity, biology, physics, and engineering [33, 34, 35, 36, 37]. Therefore, there is abundant literature developed touching the applications of fractional differential equations in non-linear dynamics [38, 39, 40, 41, 42, 43, 44]. Accordingly, considerable attention of fractional

➤ **Received:** 13.07.2021 ➤ **Revised:** 14.08.2021 ➤ **Accepted:** 17.08.2021 ➤ **Published:** 21.08.2021

equations and their solutions have been given [45, 46, 47, 48, 49, 50, 51, 52, 53, 54, 55, 56, 57, 58, 59, 60, 61]. Nowadays, the variable-order fractional calculus (VOFC) is becoming a very useful instrument, due to the numerous applications in science and engineering [62] and a few studies have been declared in the literature using derivatives with variable-order [63, 64]. More recently, in [65], a physical empirical study that includes the variable-order operators has been investigated.
In this paper, we will discuss a novel numerical method for obtaining the solutions of ODEs with variable-order time-fractional derivatives (VOFD). We then study the chaotic dynamics of a Halvorsen system with VOFD and achieve the identical synchronization between two systems.
Our paper organization is as follows: Section 2 deals with some fundamental definitions of VOFC and stability theory as well as it introduces a new numerical scheme for solving fractional-ordered DEs. Besides three illustrative examples explain the comparisons between solutions we obtained and the results in the literature in this section. In section 3, a circulant chaotic system with fractional-order derivatives is presented, its qualitative properties are explained in detail. Section 4 deals with the synchronization results. In section 5, numerical simulations are reported. Finally, in section 6, the main conclusions are outlined.

2 Preliminaries

Preliminaries for variable-order fractional calculus

In this section, we recall some definitions and properties of the VOFC; they are obtained by changing the order of the fractional derivation by a continuous bounded function in the counterparts.

Definition 1 *[66] For any bounded function $\kappa(t)$, the variable-order Caputo fractional derivative (VOCFD) of a function ϕ is given by*

$$D_C^{\kappa(t)}\phi(t) = \frac{1}{\Gamma(r-\kappa(t))}\int_0^t \left[\frac{\phi^{(r)}(s)}{(t-s)^{\kappa(s)+1-r}}\right] ds, \tag{1}$$

as long as the integral exists, with $r-1<\kappa(t)\leq r$, $r = \left[max_{0\leq t\leq T}\kappa(t)\right]+1$, where $[\rho]$ is the integer part of ρ, and $\Gamma(.)$ is the Gamma function. When $\kappa(t)$ is a constant, then we retrieve the constant-order fractional derivative in the Caputo sense.

Remark 1 Throughout this paper we think that the function $\kappa(t)$ is defined such that the integral in the previous definition exists.

Remark 2 Theoretical analysis on existence of solutions of various initial value problems with VOFDs has been given in some studies (see for instance [62] and [67]).

The stability theorem

Consider a general variable-order fractional (VOF) system

$$\begin{cases} D_c^{\kappa(t)}x(t) = \xi_1(x,y,z), \\ D_c^{\kappa(t)}y(t) = \xi_2(x,y,z), \\ D_c^{\kappa(t)}z(t) = \xi_3(x,y,z), \end{cases} \tag{2}$$

where $\kappa(t)\in(0,1]$ is the order function that is bounded and continuous, $t\geq 0$, and initial conditions $(x(0),y(0),z(0)) = (x_0,y_0,z_0)$. The equilibrium of system (2) can be deduced via solving the coupled equations

$$\begin{cases} \xi_1(x,y,z) = 0, \\ \xi_2(x,y,z) = 0, \\ \xi_3(x,y,z) = 0, \end{cases} \tag{3}$$

and the Jacobian of system (2) is shown as follows

$$J = \begin{bmatrix} \frac{\partial\xi_1}{\partial x} & \frac{\partial\xi_1}{\partial y} & \frac{\partial\xi_1}{\partial z} \\ \frac{\partial\xi_2}{\partial x} & \frac{\partial\xi_2}{\partial y} & \frac{\partial\xi_2}{\partial z} \\ \frac{\partial\xi_3}{\partial x} & \frac{\partial\xi_3}{\partial y} & \frac{\partial\xi_3}{\partial z} \end{bmatrix}. \tag{4}$$

The stability of system (2) counts on the stability of eigenvalues λ_i of the Jacobian J. To categorize the equilibrium point of system (2), we will use the extended necessary stability condition for VOF systems [66].
We denote $\kappa_R = \max_{0\leq t\leq T}\kappa(t)$ and $\kappa_r = \min_{0\leq t\leq T}\kappa(t)$.

Theorem 1 *Say that E is a given equilibrium point of the following autonomous system*

$$D_t^{\kappa(t)}X(t) = F(X), \tag{5}$$

where $X(0) = X_0$, $0 < \kappa(t) \leq 1$ is bounded and continuous and $X \in \mathbb{R}^n$.
If the λ_i values of $J = \frac{\partial F}{\partial X}|_E$ hold

$$|arg(\lambda_i)| > \frac{\pi}{2}\kappa_R, \tag{6}$$

in that case system (5) is locally asymptotically stable at the balance value E. Else, if $|arg(\lambda_i)| < \frac{\pi}{2}\kappa_r$ system (5) is unstable.

A numerical scheme for solving VOF differential equations

Taking into account that variable-order fractional differentiation is a generalization constant-order fractional differentiation (COFD), some well-known relations including composition and sequential derivative rules for COFD do not remain valid for VOFD. Consequently, solving differential equations under variable-order derivatives needs different methodologies, modifications, and/or generalizations for the known concepts. Inspired by the recent works [68] and [69], we introduce in what follows a new scheme for solving FDEs with variable-order.
Let us take the following VOF system:

$$\begin{cases} {}_0^C Dx^{\kappa(t)}(t) = F(t, x(t)) \quad \text{for } \; 0 < t \leq T, \\ x(0) = x_0, \end{cases} \tag{7}$$

where F is a general nonlinear function, $0 < \kappa(t) \leq 1$ and x_0 is the initial condition.
Applying the operator $I^{\kappa(t)}$ on both sides of equation (7) we get

$$x(t) = x_0 + \frac{1}{\Gamma(\kappa(t))}\int_0^t F(s, x(s))(t-s)^{\kappa(t)-1}ds. \tag{8}$$

Now we choose the following uniform grid:

$$h = \frac{T}{N}, \; t_n = nh, \; \text{for } n = 0, 1, 2, \ldots, N, \; t_0 = 0 \, \text{and} \, T_n = T.$$

For a given $t = t_{n+1}$, $n = 0, 1, 2 \ldots, N$ it yields

$$\begin{aligned} x(t_{n+1}) &= x_0 + \frac{1}{\Gamma(\kappa(t))}\int_0^{t_{n+1}} F(s, x(s))(t_{n+1}-s)^{\kappa(t)-1}ds \\ &= x_0 + \frac{1}{\Gamma(\kappa(t))}\sum_{k=0}^{n}\int_{t_k}^{t_{k+1}} F(s, x(s))(t_{n+1}-s)^{\kappa(t)-1}ds. \end{aligned} \tag{9}$$

It is well-known that composite Lagrange interpolation consists in splitting the interval into many subintervals, and uses a lower order Lagrange interpolation in each subinterval, in order to have a good approximation of a function. Therefore, on each subinterval $[t_k, t_{k+1}]$, we approximate $F(s, x(s))$ with a Lagrange interpolation polynomial:

$$\begin{aligned} P_k(\tau) &= \frac{s - t_{k-1}}{t_k - t_{k-1}} F(t_k, x(t_k)) - \frac{s - t_k}{t_k - t_{k-1}} F(t_{k-1}, x(t_{k-1})) \\ &= \frac{F(t_k, x(t_k))}{h}(s - t_{k-1}) - \frac{F(t_{k-1}, x(t_{k-1}))}{h}(s - t_k) \\ &\simeq \frac{F(t_k, x_k)}{h}(s - t_{k-1}) - \frac{F(t_{k-1}, x_{k-1})}{h}(s - t_k). \end{aligned}$$

Coming back to (9), we get the following

$$\begin{aligned} x_{n+1} &= x_0 + \frac{1}{\Gamma(\kappa(t))}\sum_{k=0}^{n}\frac{F(t_k, x_k)}{h}\int_{t_k}^{t_{k+1}}(s - t_{k-1})(t_{n+1}-s)^{\kappa(t)-1}ds \\ &\quad - \frac{1}{\Gamma(\kappa(t))}\sum_{k=0}^{n}\frac{F(t_{k-1}, x_{k-1})}{h}\int_{t_k}^{t_{k+1}}(s - t_k)(t_{n+1}-s)^{\kappa(t)-1}ds. \end{aligned} \tag{10}$$

Next, we compute the following coefficients

$$\mathcal{A}_{\kappa(t),k,1} = \int_{t_k}^{t_{k+1}}(s - t_{k-1})(t_{n+1}-s)^{\kappa(t)-1}ds,$$

and

$$\mathcal{B}_{\kappa(t),k,2} = \int_{t_k}^{t_{k+1}}(s - t_k)(t_{n+1}-s)^{\kappa(t)-1}ds.$$

A simple integration leads to

$$\mathcal{A}_{\kappa(t),k,1} = \frac{(n+1-k)^{\kappa(t)}\left(n-k+2+\kappa(t)\right) - (n-k)^{\kappa(t)}(n-k+2+2\kappa(t))}{\kappa(t)(\kappa(t)+1)}, \tag{11}$$

and

$$\mathcal{B}_{\kappa(t),k,2} = \frac{(n+1-k)^{\kappa(t)+1} - (n-k)^{\kappa(t)}(n-k+1+\kappa(t))}{\kappa(t)(\kappa(t)+1)}. \tag{12}$$

Inserting (11) and (12) in equation (10) gives the following approximation

$$\begin{aligned} x_{n+1} &= x_0 + \sum_{k=0}^{n} Q_k \left((n+1-k)^{\kappa(t)}\left(n-k+2+\kappa(t)\right) - (n-k)^{\kappa(t)}(n-k+2+2\kappa(t))\right) \\ &- \sum_{k=0}^{n} Q_{k-1}\left((n+1-k)^{\kappa(t)+1} - (n-k)^{\kappa(t)}(n-k+1+\kappa(t))\right). \end{aligned} \tag{13}$$

$Q_k = \frac{h^{\kappa(t)}F(t_k,x_k)}{\Gamma(\kappa(t)+2)}$ and $Q_{k-1} = \frac{h^{\kappa(t)}F(t_{k-1},x_{k-1})}{\Gamma(\kappa(t)+2)}$.

To prove the accuracy and the applicability of the above described method, we give some examples and find their solutions. The obtained numerical solutions are compared with the exact solutions if the case arises, otherwise, we made a comparison with obtained results via other known methods.

Example 1 *First we take the following linear FDE, where the fractional operator is taken in the Caputo sense:*

$$\begin{cases} D_c^{\kappa(t)}x(t) = \cos(2t), & t \in [0,T] \\ x(0) = 0. \end{cases} \tag{14}$$

The application of the fractional integral on both sides of (14) gives the following exact solution:

$$x(t) = \frac{-2^{3/2-\kappa(t)}t\alpha(t)\,\mathbf{LS}\left(\kappa(t)+1/2, 3/2, 2t\right) + 2t^{\kappa(t)+1/2}\kappa(t)}{2\Gamma(2+\kappa(t))\sqrt{t}} + \frac{2t^{\kappa(t)+1/2} - 2^{-\kappa(t)+1/2}\mathbf{LS}\left(\kappa(t)+3/2, 1/2, 2t\right)}{2\Gamma(2+\kappa(t))\sqrt{t}},$$

where **LS** *is the Lommel's function. Let us take $\kappa(t) = 0.9 - 0.05\frac{t}{1+t}$ solve equation (14) numerically using the above proposed scheme for a step-size $h = 0.01$, $N = 1000$ and $T = 10$. Figure 1 plots the profile of numerical solution vs exact solution of (14), it is clear that the suggested algorithm furnishes accurate numerical results.*

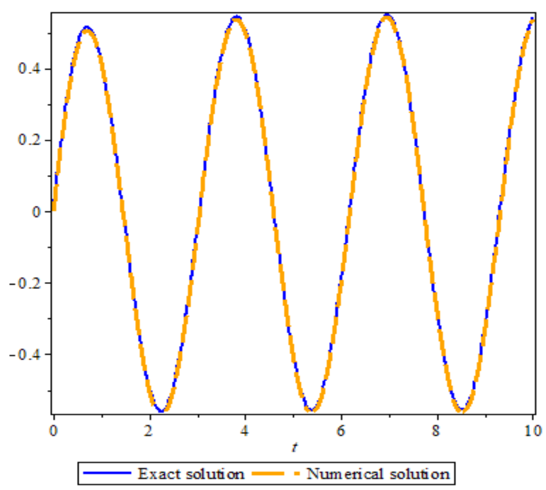

Figure 1. Exact vs numerical solution of (14) for $\kappa(t) = 0.9 - 0.05\frac{t}{1+t}$.

Example 2 *Now we take into account the following equation*

$$\begin{cases} D_C^{\kappa(t)} x(t) = e^{-\sqrt{t^2}}, & t \in [0, T] \\ x(0) = 0. \end{cases} \tag{15}$$

Similarly, we get the following exact solution for equation (15)

$$x(t) = \frac{t^{1/2\,\kappa(t)} e^{-1/2\,t} \mathbf{W}\left(-1/2\,\kappa(t),\, 1/2\,\kappa(t) + 1/2,\, t\right)}{t\,(1 + \kappa(t))\,\Gamma(\kappa(t))} + \frac{t^{1/2\,\kappa(t)} e^{-1/2\,t} \mathbf{W}\left(-1/2\,\kappa(t) + 1,\, 1/2\,\kappa(t) + 1/2,\, t\right)}{t\kappa(t)\,(1 + \kappa(t))\,\Gamma(\kappa(t))},$$

where **W** *is the Whittaker function.*
To prove the high accuracy of the novel method, we solve equation (15) by taking $\kappa(t) = 0.94 + \frac{1}{30}\sin\left(\frac{t}{6}\right)$, $h = 0.05$ *and* $T = 10$. *Figure 2 shows that an excellent agreement between the exact and numerical solution of (15).*

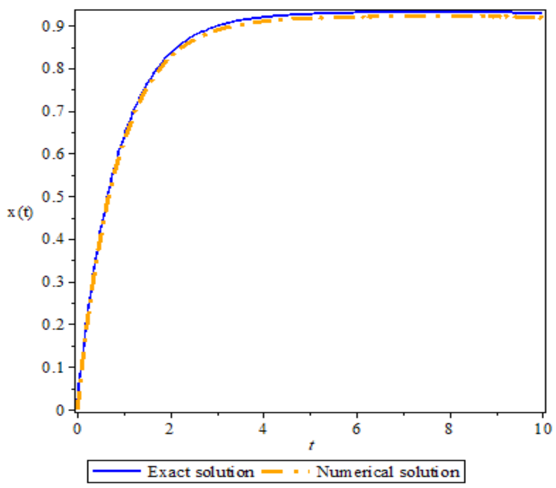

Figure 2. Exact vs numerical solution of (15) for $\kappa(t) = 0.94 + \frac{1}{30}\sin\left(\frac{t}{6}\right)$

Example 3 *Let us now consider the problem for the VFO Duffing oscillator [32]*

$$\begin{cases} x''(t) + 0.2 D_C^{\kappa(t)} x(t) + x(t) + x^3(t) = p(t), \\ x(0) = 0,\ x'(0) = 0, \end{cases} \tag{16}$$

where

$$\kappa(t) = 1 - exp(-t), \text{ and } p(t) = 2 + t^2 + t^6 + 0.4\,\frac{t^{1+e^{-t}} e^t}{\Gamma\left(e^{-t}\right)\left(1 + e^{-t}\right)}. \tag{17}$$

The exact solution of Eq. (16) is $x(t) = t^2$. *In Figure 3, we remark that the solution we obtained and the exact solution are in high agreement for* $h = 0.01$.

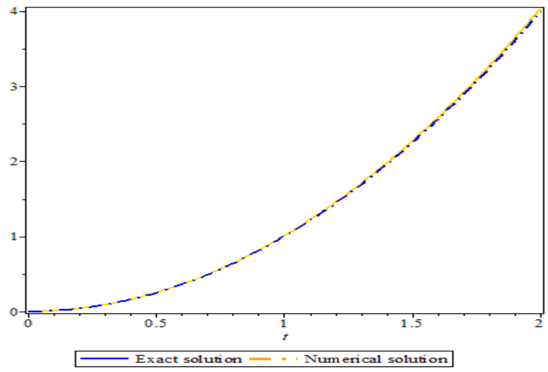

Figure 3. Exact vs numerical solution of (16) for $\kappa(t) = 1 - exp(-t)$.

3 A variable-order fractional Halvorsen system

This section aims to present a study of a 3D circulant system, called the Halvorsen system [3] with variable fractional-order derivative in Caputo sense, which is described by the following

$$\begin{cases} D_c^{q(t)}x = -ax - by - bz - y^2, \\ D_c^{q(t)}y = -ay - bz - bx - z^2, \\ D_c^{q(t)}z = -az - bx - by - x^2. \end{cases} \tag{18}$$

It is clear that system (18) is symmetric respectively to cyclic interchanges of the states x, y, and z. According to Halvorsen, system (18) is chaotic for the values of the parameters are given as $a = 1.3$ and $b = 4$ (for the classical case $q(t) = 1$). In what follows, we describe the qualitative properties of the Halvorsen chaotic system (18). Throughout this section we will take $q(t) = 0.7 + 0.2\frac{\exp(-t)}{1+\exp(-t)}$.

Dissipativity

As in [3], the Halvorsen system (18) can be written as

$$D_c^{q(t)}X(t) = F(X(t)), \tag{19}$$

where $X = \begin{bmatrix} x \\ y \\ z \end{bmatrix}$, $F = \begin{bmatrix} f_1(X) \\ f_2(X) \\ f_3(X) \end{bmatrix}$ and

$$\begin{cases} f_1(X) = -ax - by - bz - y^2, \\ f_2(X) = -ay - bz - bx - z^2, \\ f_3(X) = -az - bx - by - x^2. \end{cases}$$

The divergence of the vector field f on $\mathbb{R}^3$ is expressed as

$$\text{div}F = \frac{\partial f_1}{\partial x} + \frac{\partial f_2}{\partial y} + \frac{\partial f_3}{\partial z} = -3.9 < 0. \tag{20}$$

Let us denote by Ω a subset of $\mathbb{R}^3$ with a smooth boundary such that $\Omega(t) = \Phi_t(\Omega)$ where Φ_t is the flow of F. Additionally, let $V(t)$ refers to the hypervolume of $\Omega(t)$. By the Liouville's theorem, we get

$$\frac{dV}{dt} = \int_{\Omega(t)} \text{div}F dxdydz. \tag{21}$$

Replacing div$F$ from (20) into (21), we get

$$\frac{dV}{dt} = -3.9 \int_{\Omega(t)} dxdydz = -3.9V(t), \tag{22}$$

Integrating equation (22) we obtain

$$V(t) = V(0)\exp(-3.9t). \tag{23}$$

According to Eq. (23), $V(t)$ is converging to zero exponentially as t becomes infinite. Consequently, the VOF Halvorsen system (18) is a dissipative one.

Equilibrium point and the stability

The equilibria of the VOF Halvorsen system (18) are deduced by solving the following system

$$\begin{cases} -ax - by - bz - y^2 = 0, \\ -ay - bz - bx - z^2 = 0, \\ -az - bx - by - x^2 = 0. \end{cases} \tag{24}$$

We find that (24) has two equilibrium points, namely

$$E_0 = (0, 0, 0) \quad \text{and} \quad E_1 = (-9.27, -9.27, -9.27). \tag{25}$$

The Jacobian matrix of the VOF Halvorsen system (24) at E_0 is obtained as

$$J_{E_0} = \begin{bmatrix} -1.27 & -4 & -4 \\ -4 & -1.27 & -4 \\ -4 & -4 & -1.27 \end{bmatrix}. \tag{26}$$

The matrix J_{E_0} has the eigenvalues

$$\begin{bmatrix} \lambda_1 = 2.73, \\ \lambda_2 = -9.27, \\ \lambda_3 = 2.73. \end{bmatrix} \tag{27}$$

Similarly, the Jacobian matrix of system (24) at E_1 is given as

$$J_{E_1} = \begin{bmatrix} -1.27 & 14.54 & -4 \\ -4 & -1.27 & 14.54 \\ 14.54 & -4 & -1.27 \end{bmatrix}. \tag{28}$$

The eigenvalues of J_{E_1} are :

$$\begin{bmatrix} \kappa_1 = -6.54 + 16.0561109861635i, \\ \kappa_2 = -6.54 - 16.0561109861635i, \\ \kappa_3 = 9.27. \end{bmatrix} \tag{29}$$

We conclude that the equilibrium point E_0 is a saddle then it is unstable. Therefore, the necessary condition to ensure chaos is satisfied.

Quantitative characterization of VOFD Halvorsen system

The computation of Lyapunov exponents (LE) is a basic problem in the study of dynamical systems since they provide a quantification of the exponential divergence of initially close state-space trajectories and measure the amount of chaos in a given system [3]. Actually, a positive (LE) is sufficient to claim the presence of chaos in a dynamical system.
A numerical calculation using the Gram-Schmidt orthonormalization procedure for the initial conditions $(x, y, z) = (0.2, 0.6, 0.2)$ reveals that system (24) when $q(t) = 0.7 + 0.2\frac{\exp(-t)}{1+\exp(-t)}$, has the following Lyapunov exponents :

$$\begin{bmatrix} L_1 = 0.7935801, \\ L_2 = 0.0002090, \\ L_3 = -4.6037936. \end{bmatrix} \tag{30}$$

Since $L_1 + L_2 + L_3 = -3.8100045 < 0$, the VOF Halvorsen chaotic system (24) is dissipative.
Moreover, the Kaplan-Yorke dimension of the VOF Halvorsen chaotic system (24) is obtained as

$$D_{KY} = 2 + \frac{L_1 + L_2}{|L_3|} = 2.1724206533, \tag{31}$$

which is fractional.

4 Active control synchronization

The synchronization of two coupled chaotic systems is an important topic due to its applications in various fields of science and engineering, for instance, secure communication, cryptography, analog and digital signals, control processing, time series analysis, as well as earthquake dynamics [70]. Moreover, numerous techniques have been investigated for chaos synchronization like linear and nonlinear feedback control [71], back stepping nonlinear control approach [72], sliding mode control [73], adaptive control [74], etc. In this paper, we will design active nonlinear controllers to synchronize two identical Halvorsen systems with variable-order time-fractional derivatives.

To achieve synchronization, we define the drive-response scheme of two VOF identical Halvorsen systems, namely

$$\text{Drive}\begin{cases} D_t^{q(t)}x_1 = -ax_1 - by_1 - bz_1 - y_1^2, \\ D_t^{q(t)}y_1 = -ay_1 - bz_1 - bx_1 - z_1^2, \\ D_t^{q(t)}z_1 = -az_1 - bx_1 - by_1 - x_1^2. \end{cases} \tag{32}$$

$$\text{Response}\begin{cases} D_t^{q(t)}x_2 = -ax_2 - by_2 - bz_2 - y_2^2 + U_1(t), \\ D_t^{q(t)}y_2 = -ay_2 - bz_2 - bx_2 - z_2^2 + U_2(t), \\ D_t^{q(t)}z_2 = -az_2 - bx_2 - by_2 - x_2^2 + U_3(t), \end{cases} \tag{33}$$

where $U_i(t)$; $i = 1, 2, 3$ are unknown active control functions to be computer lated. Recall that the initial conditions $(x_{1,0}, y_{1,0}, z_{1,0})$ and $(x_{2,0}, y_{2,0}, z_{2,0})$ are different and we target to synchronize the signals even if there is discrepancy between the initial conditions. First, we define the error vector $\mathbf{e}(t)$ as the following

$$\begin{cases} e_1 = x_2 - x_1, \\ e_2 = y_2 - y_1, \\ e_3 = z_2 - z_1. \end{cases} \tag{34}$$

Subtracting (32) from (33) and using (34), we find

$$\begin{cases} D_t^{q(t)}e_1 = -ae_1 - be_2 - be_3 - (y_2^2 - y_1^2) + U_1(t), \\ D_t^{q(t)}e_2 = -ae_2 - be_3 - be_1 - (z_2^2 - z_1^2) + U_2(t), \\ D_t^{q(t)}e_3 = -ae_3 - be_1 - be_2 - (x_2^2 - x_1^2) + U_3(t). \end{cases} \tag{35}$$

Let

$$\begin{cases} U_1(t) = be_2 + be_3 + (y_2^2 - y_1^2), \\ U_2(t) = (z_2^2 - z_1^2) + be_3, \\ U_3(t) = (x_2^2 - x_1^2). \end{cases} \tag{36}$$

Consequently, the fractional-order error dynamical system is reduced to

$$\begin{cases} D_t^{q(t)}e_1 = -ae_1, \\ D_t^{q(t)}e_2 = -ae_2 - be_1, \\ D_t^{q(t)}e_2 = -be_1 - be_2 - ae_3. \end{cases} \tag{37}$$

Theorem 2 *For any initial conditions, the drive and response defined by the synchronization scheme (32) and (33) are with the control law (36).*

Proof The above error system (37) has a unique equilibrium point $(0, 0, 0)$ and the Jacobian matrix at this point is

$$J_{(0,0,0)} = \begin{bmatrix} -1.3 & 0 & 0 \\ -4 & -1.3 & -4 \\ 0 & 0 & -1.3 \end{bmatrix}.$$

Clearly, $\lambda = -1.3$ is triple eigenvalue of $J_{(0,0,0)}$ and $|\arg(\lambda)| = \pi$ which is always greater than $\frac{\pi}{2} q_M$. Therefore, based on the stability theorem, we conclude that it is direct to see that the error dynamics converge to the manifold $(e_1, e_2, e_3) = (0, 0, 0)$ as $t \to \infty$. Consequently, the synchronization between two identical systems (32) and (33) is achieved via the control law (36).

5 Numerical simulations

This section presents the numerical simulations of Sections 3 and 4. The time step is fixed to $h = 0.01$ and the calculations are carried out for $q(t) = 0.7 + 0.2\frac{\exp(-t)}{1+\exp(-t)}$.

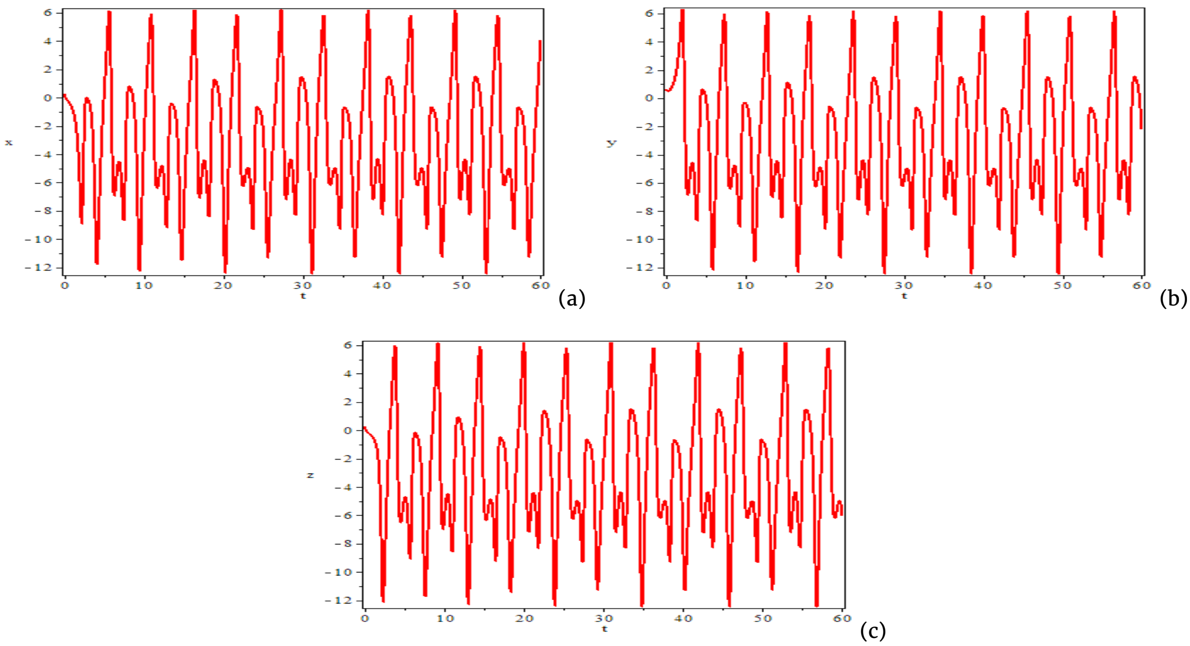

Figure 4. Time series of system (18) : (a) $x(t)$, (b) $y(t)$ and (c) $z(t)$.

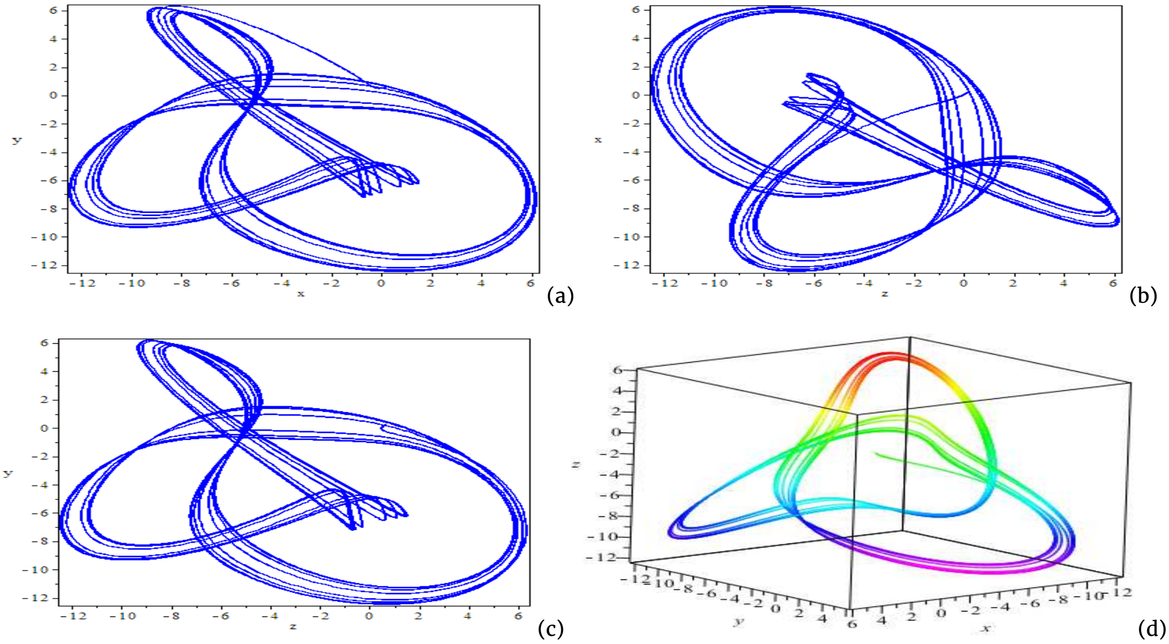

Figure 5. (a) Phase plane $x - y$, (b) Phase plane $x - z$, (c) Phase plane $y - z$ and (d) The attractor $x - y - z$.

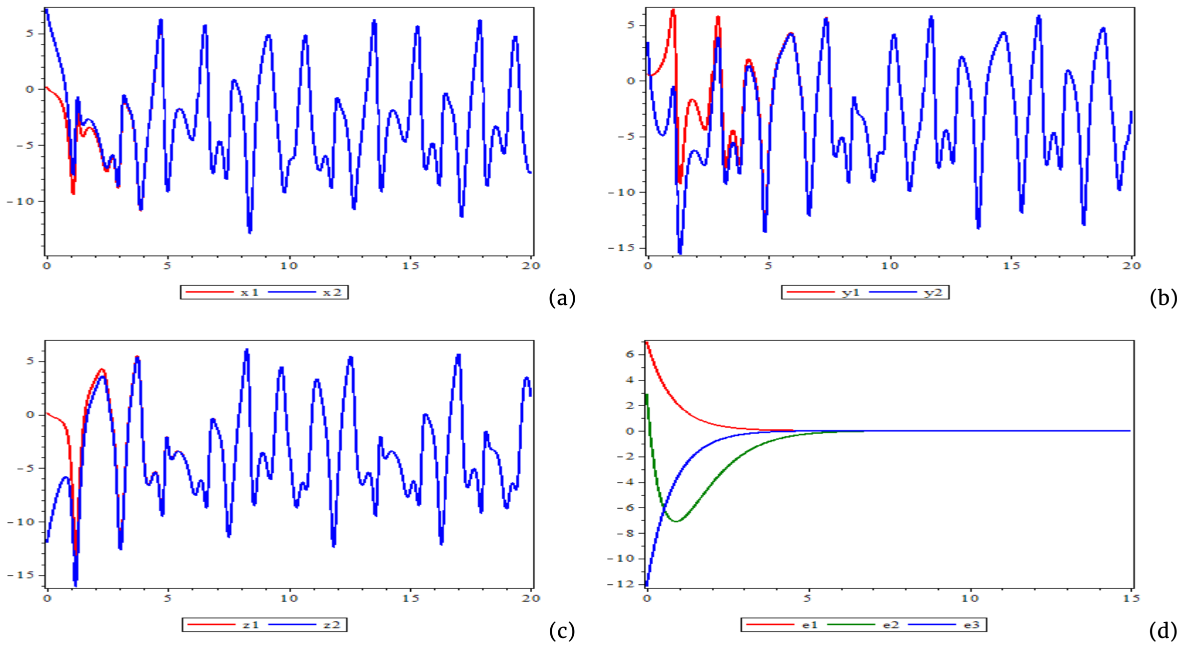

Figure 6. Synchronization of the VOF system (18): (a) $x_1(t)$ vs $x_2(t)$, (b) $y_1(t)$ vs $y_2(t)$, (c) $z_1(t)$ vs $z_2(t)$ and (d) The error functions $e_1(t)$, $e2(t)$, $e3(t) \to 0$ as $t \to \infty$.

6 Conclusion

This paper introduced a novel numerical method for solving ordinary differential equations with variable-order time-fractional derivatives. It is shown that there is no computational complexity in the algorithm, the method is easy to program. The accuracy of the method is demonstrated through numerical examples. Moreover, the chaotic dynamics of a Halvorsen system with variable-order fractional derivatives are investigated and the identical synchronization between two systems is achieved. Besides, the results of this paper reveal that the variable-order derivation can be very useful for describing chaotic phenomena, their control, and synchronization.

Declarations

Consent for publication

Not applicable.

Conflicts of interest

The authors declare that they have no conflict of interests.

Funding

Not applicable.

Author's contributions

Z.H.: Conceptualization, Methodology, Software, Writing-Original draft preparation. M.Y.: Data Curation, Validation, Writing-Reviewing and Editing. N.Ö.: Investigation, Visualization, Supervision. All authors discussed the results and contributed to the final manuscript.

Acknowledgements

The authors are very much thankful to the reviewers and editor for their valuable suggestions to improve the quality of the manuscript.

References

[1] Lorenz, E.N. Deterministic nonperiodic flow. *Journal of atmospheric sciences*, 20(2), 130-141, (1963).
[2] Azar, A.T., Sundarapandian, V. *Chaos modeling and control systems design* (Vol. 581). Germany: Springer, (2015).
[3] Azar, A.T., Sundarapandian, V., Ouannas, A. *Fractional order control and synchronization of chaotic systems* (Vol. 688). Springer, (2017).
[4] Effati, S., Saberi-Nadjafi, J., Saberi Nik, H. Optimal and adaptive control for a kind of 3D chaotic and 4D hyper-chaotic systems. *Applied Mathematical Modelling*, 38(2), 759-774, (2014).
[5] Yang, J., Dong-Lian, Q. The feedback control of fractional order unified chaotic system.*Chinese Physics B*, 19(2), 020508, (2010).
[6] Li, C., Tong, Y. Adaptive control and synchronization of a fractional-order chaotic system.*Pramana*, 80(4), 583-592, (2013).
[7] Li, C.G., Chen, G.R. Chaos in the fractional order Chen system and its control. *Chaos, Solitons and Fractals*, 22(3), 549-554, (2004).
[8] Li, Y., Chen, Y., Podlubny, I. Stability of fractional-order nonlinear dynamic systems: Lyapunov direct method and generalized Mittag-Leffler stability. *Computers and Mathematics with Applications*, 59(5), 1810-1821, (2010).
[9] Matignon, D. Stability results for fractional differential equations with applications to control processing.In *Computational Engineering in Systems Applications*, 963-968, (1996).
[10] Mekkaoui, T., Hammouch, Z., Belgacem, F., Abbassi, A.E. Fractional-order nonlinear systems: Chaotic dynamics, numerical simulation and circuits design. In *Fractional Dynamics*, (pp.343-356). Sciendo Migraiton, (2016).
[11] Auerbach, D., Grebogi, C., Ott, E., Yorke, J.A. Controlling chaos in high dimensional systems. *Physical review letters*, 69(24), 3479, (1992).
[12] Pyragas, V., Pyragas, K. Continuous pole placement method for time-delayed feedback controlled systems. *The European Physical Journal B*, 87(11), 1-10, (2014).
[13] Razminia, A., Baleanu, D. Fractional synchronization of chaotic systems with different orders.*Proceedings of the Romanian Academy*, 13, 14-321, (2012).
[14] Bai, E.W., Lonngren, K.E. Synchronization of two Lorenz systems using active control. *Chaos, Solitons Fractals*, 8(1), 51-58, (1997).
[15] Blokh, A., Cleveland, C., Misiurewicz, M. Expanding polymodials Modern Dynamical Systems and Applications ed M Brin, B Hasselblatt and Ya Pesin, 253-70, (2004).
[16] Champoué, A., Yamapi, R., Woafo, P. Bifurcations in a birhythmic biological system with time-delayed noise. *Nonlinear Dynamics*, 73(4), 2157-2173, (2013).
[17] Diethelm, K., Ford, N. Analysis of fractional differential equations. *Journal of Mathematical Analysis and Applications*, 265(2), 229-248, (2002).
[18] Diethelm, K., Ford, N., Freed, A., Luchko, Y. Algorithms for the fractional calculus: a selection of numerical method. *Computer Methods in Applied Mechanics and Engineering*, 194(6-8), 743-773, (2005).
[19] Frohlich, H. Long Range Coherence and energy storage in a Biological systems. *International Journal of Quantum Chemistry*, 2(5), 641-649, (1968).
[20] Frohlich, H. Quantum Mechanical Concepts in Biology. *Theoretical Physics and Biology*, 1, (1969).
[21] He, G., Luo, M. Dynamic behavior of fractional order Duffing chaotic system and its synchronization via singly active control. *Applied Mathematics and Mechanics*, 33(5), 567-582, (2012).

[22] Kadji, H.G., Orou, J.B., Yamapi, R., Woafo, P. Nonlinear Dynamics and Strange Attractors in the Biological System. *Chaos Solitons and Fractals*, 32(2), 862-882, (2007).
[23] Kaiser, F. Coherent Oscillations in Biological Systems I. Bifurcations Phenomena and Phase transitions in enzyme-substrate reaction with Ferroelectric behaviour, 294, 304-333, (1978).
[24] Kaiser, F. Coherent Oscillations in Biological Systems II. Lecture Notes in Mathematics 2007; 1907; Springer: Berlin.
[25] Miller, K.S., Rosso, B. An Introduction to the Fractional Calculus and Fractional Differential Equations. Wiley, New York, (1993).
[26] Pham, V.T., Frasca, M., Caponetto, R., Hoang, T.M., Fortuna, L. Control and synchronization of fractional-order differential equations of phase-locked-loop. *Chaotic Modeling and Simulation*, 4, 623-631, (2012).
[27] Pecora, L.M., Carroll, T.L. Synchronization in chaotic systems. *Phys Rev Lett*, 64, 821-824, (1990).
[28] Pikovsky, A. Synchronization: A Universal Concept in Nonlinear Sciences. *Cambridge University Press*, (2011).
[29] Strogatz, S.H. Nonlinear Dynamics and Chaos: With Applications to Physics, Biology, Chemistry and Engineering. *Perseus Books Pub*, (1994).
[30] Ucar, A., Lonngren, K.E., Bai, E.W. Synchronization of the unified chaotic systems via active control. *Chaos, Solitons and Fractals*, 27,1292-97, (2006).
[31] Zaslavsky, G. Hamiltonian Chaos and Fractional Dynamics. *Oxford University Press*, (2008).
[32] Katsikadelis, J.T. Numerical solution of variable order fractional differential equations.*arXiv preprint arXiv*, 1802.00519, (2018).
[33] Podlubny, I. Fractional Differential Equations. Academic Press: San Diego; Calif, USA, (1999).
[34] Erturk, V.S, Momani, S., Odibat, Z. Application of generalized differential transform method to multi-order fractional differential equations. *Communications in Nonlinear Science and Numerical Simulation*, 13(8), 1642-1654, (2008).
[35] Freihat, A., Momani, S. Application of Multistep Generalized Differential Transform Method for the Solutions of the Fractional-Order Chua's System. *Discrete Dynamics in Nature and Society*, 1-12, (2012).
[36] Hammouch, Z., Mekkaoui, T. Circuit design and simulation for the fractional-order chaotic behavior in a new dynamical system. *Complex and Intelligent Systems*, 4(4), 251-260, (2018).
[37] Hongwu, W., Junhai, M. Chaos Control and Synchronization of a Fractional-order Autonomous System. *WSEAS Trans. on Mathematics*, 11,700-711, (2012).
[38] Caponetto, R., Dongola, G., Fortuna, L. Fractional order systems: Modeling and control application. Singapore: World Scientific, (2010).
[39] Escalante-Martínez, J.E., Gómez-Aguilar, J.F., Calderón-Ramón, C., Aguilar-Meléndez, A. & Padilla-Longoria, P. A mathematical model of circadian rhythms synchronization using fractional differential equations system of coupled van der Pol oscillators.*International Journal of Biomathematics*, 11(01), 1850014, (2018).
[40] Coronel-Escamilla, A., Gómez-Aguilar, J.F., Torres, L., Escobar-Jiménez, R.F. & Valtierra-Rodríguez, M. Synchronization of chaotic systems involving fractional operators of Liouville-Caputo type with variable-order. Physica A. *Statistical Mechanics and its Applications*, 487, 1-21, (2017).
[41] Yavuz, M. European option pricing models described by fractional operators with classical and generalized Mittag-Leffler kernels. *Numerical Methods for Partial Differential Equations*, 10.1002/num.22645, (2021).
[42] Zúniga-Aguilar, C.J., Gómez-Aguilar, J.F., Escobar-Jiménez, R.F. & Romero-Ugalde, H.M. Robust control for fractional variable-order chaotic systems with non-singular kernel. *The European Physical Journal Plus*, 133(1), 1-13, (2018).
[43] Yavuz, M. Novel solution methods for initial boundary value problems of fractional order with conformable differentiation. *An International Journal of Optimization and Control: Theories & Applications (IJOCTA)*, 8(1), 1-7, (2018).
[44] Zúniga-Aguilar, C.J., Romero-Ugalde, H.M., Gómez-Aguilar, J.F., Escobar-Jiménez, R.F. & Valtierra-Rodríguez, M. Solving fractional differential equations of variable-order involving operators with Mittag-Leffler kernel using artificial neural networks. *Chaos, Solitons & Fractals*, 103, 382-403, (2017).
[45] Petras, I. A note on the fractional-order Chua's system. *Chaos Soliton and Fractals*, 38(1), 140-147, (2008).
[46] Petras, I. Fractional-Order Nonlinear Systems: Modeling, Analysis and Simulation. Springer, (2011).
[47] Caputo, M. Linear models of dissipation whose Q is almost frequency independent. *Geophysical Journal International*, 13(5), 529-539, (1967).
[48] Ucar, S., Ucar, E., Ozdemir, N., Hammouch, Z. Mathematical analysis and numerical simulation for a smoking model with Atangana-Baleanu derivative. *Chaos, Solitons and Fractals*, 118, 300-306, (2019).
[49] Chand, M., Hammouch, Z., Asamoa, J.K.K., Baleanu, D. Certain Fractional Integrals and Solutions of Fractional Kinetic Equations Involving the Product of S-Function. In Mathematical Methods in Engineering (pp. 213-244), Springer, Cham, (2019).
[50] Owolabi, K.M., Hammouch, Z. Mathematical modeling and analysis of two-variable system with noninteger-order derivative. *Chaos: An Interdisciplinary Journal of Nonlinear Science*, 29(1), 013145, (2019).
[51] Yavuz, M., Ozdemir, N. European vanilla option pricing model of fractional order without singular kernel. *Fractal and Fractional*, 2(1), 3, (2018).
[52] Yavuz, M., Ozdemir, N. On the solutions of fractional Cauchy problem featuring conformable derivative.In *ITM Web of Conferences*. 22, EDP Sciences, (2018).
[53] Yavuz, M., Ozdemir, N. Numerical inverse Laplace homotopy technique for fractional heat equations. *Thermal Science*, 22(1), 185-194, (2018).
[54] Toufik, M., Atangana, A. New numerical approximation of fractional derivative with non-local and non-singular kernel: Application to chaotic models. *The European Physical Journal Plus*, 132(10), 1-16, (2017).
[55] Naik, P.A., Yavuz, M., Qureshi, S., Zu, J., Townley, S. Modeling and analysis of COVID-19 epidemics with treatment in fractional derivatives using real data from Pakistan. *The European Physical Journal Plus*, 135(10), 1-42, (2020).
[56] Mirzazadeh, M., Akinyemi, L., Şenol, M., Hosseini, K. A variety of solitons to the sixth-order dispersive (3+1)-dimensional nonlinear time-fractional Schrödinger equation with cubic-quintic-septic nonlinearities. *Optik*, 241, 166318, (2021).
[57] Yavuz, M., Yokus, A. Analytical and numerical approaches to nerve impulse model of fractional-order. *Numerical Methods for Partial Differential Equations*, 36(6), 1348-1368, (2020).

[58] Matar, M.M., Abbas, M.I., Alzabut, J., Kaabar, M.K.A., Etemad, S., Rezapour, S. Investigation of the p-Laplacian nonperiodic nonlinear boundary value problem via generalized Caputo fractional derivatives. *Advances in Difference Equations,* 2021(1), 1-18, (2021).
[59] Kaabar, M.K., Martínez, F., Gómez-Aguilar, J.F., Ghanbari, B., Kaplan, M., Günerhan, H. New approximate analytical solutions for the nonlinear fractional Schrödinger equation with second-order spatio-temporal dispersion via double Laplace transform method. *Mathematical Methods in the Applied Sciences,* 44(14), 11138-11156, (2021).
[60] Yavuz, M., Sulaiman, T.A., Usta, F., Bulut, H. Analysis and numerical computations of the fractional regularized long-wave equation with damping term. *Mathematical Methods in the Applied Sciences,* 44(9), 7538-7555, (2021).
[61] Tariq, K.U., Younis, M., Rizvi, S.T.R., Bulut, H. M-truncated fractional optical solitons and other periodic wave structures with Schrödinger-Hirota equation. *Modern Physics Letters B,* 34(supp01), 2050427, (2020).
[62] Yaghoobi, S., Moghaddam, B.P., Ivaz, K. An efficient cubic spline approximation for variable-order fractional differential equations with time delay. *Nonlinear Dynamics*, 87(2), 815-826, (2017).
[63] Coronel-Escamilla, A., Gómez-Aguilar, J.F., Torres, L., Valtierra-Rodriguez, M. & Escobar-Jiménez, R.F. Design of a state observer to approximate signals by using the concept of fractional variable-order derivative. *Digital Signal Processing*, 69, 127-139, (2017).
[64] Gómez-Aguilar, J.F. Analytical and numerical solutions of a nonlinear alcoholism model via variable-order fractional differential equations. *Physica A: Statistical Mechanics and its Applications*, 494, 52-75, (2018).
[65] Gómez-Aguilar J.F. Chaos in a nonlinear Bloch system with Atangana-Baleanu fractional derivatives. *Numerical Methods for Partial Differential Equations*, 34(5), 1716-1738, (2018).
[66] Yufeng, X., Zhimin, H. Synchronization of variable-order fractional financial system via active control method. *Open Physics*, 11(6), 824-835, (2013).
[67] Razminia, A., Dizaji, A.F., Majd, V.J. Solution existence for non-autonomous variable-order fractional differential equations. *Mathematical and Computer Modelling*, 55(3-4), 1106-1117, (2012).
[68] Solís-Pérez, J.E., Gómez-Aguilar, J.F., Atangana, A. Novel numerical method for solving variable-order fractional differential equations with power, exponential and Mittag-Leffler laws.*Chaos, Solitons and Fractals*, 114, 175-185, (2018).
[69] Atangana, A., Owolabi, K.M. New numerical approach for fractional differential equations. *Mathematical Modelling of Natural Phenomena*, 13(1), 3, (2018).
[70] Hammouch, Z., Mekkaoui, T. Chaos synchronization of a fractional nonautonomous system. *Nonautononmous Dynamical Systems*, 1:61-71, (2014).
[71] Lu, L,. Zhang, C., Guo, Z.A. Synchronization between two different chaotic systems with nonlinear feedback control. *Chinese Physics*, 16, 1603-1607, (2007).
[72] Olusola, O., Vincent, E., Njah, N., Ali, E. Control and Synchronization of Chaos in Biological Systems Via Backsteping Design. *International Journal of Nonlinear Science and Numerical Simulation*, 11(1), 121-128, (2011).
[73] Haeri, M., Emadzadeh, A. Synchronizing different chaotic systems using active sliding mode control. *Chaos, Solitons and Fractals*, 31(1), 119-129, (2007).
[74] Wang, Y., Guan, Z.H., Wang, H.O. Feedback an adaptive control for the synchronization of Chen system via a single variable. *Physics Letters A*, 312(1-2), 34-40, (2003).

Mathematical Modelling and Numerical Simulation with Applications, 2021, 1(1), 24–31

https://www.mmnsa.org
ISSN Online: 2791-8564 / Open Access
https://doi.org/10.53391/mmnsa.2021.01.003

RESEARCH PAPER

Construction of different types of traveling wave solutions of the relativistic wave equation associated with the Schrödinger equation

Asıf Yokus [1,*,†]

[1]Department of Mathematics, Firat University, Elazig, 23200, Turkey

[*]Corresponding Author
[†]asfyokus@yahoo.com (Asıf Yokus)

Abstract

In this study, an alternative method has been applied to obtain the new wave solution of mathematical equations used in physics, engineering, and many applied sciences. We argue that this method can be used for some special nonlinear partial differential equations (NPDEs) in which the balancing methods are not integer. A number of new complex hyperbolic trigonometric traveling wave solutions have been successfully generated in the Eckhaus equation (EE) and nonlinear Klein-Gordon (nKG) equation models associated with the Schrödinger equation. The graphs representing the stationary wave are presented by giving specific values to the parameters contained in these solutions. Finally, some discussions about new complex solutions are given. It is discussed by giving physical meaning to the constants in traveling wave solutions, which are physically important as well as mathematically. These discussions are supported by three-dimensional simulation. In order to eliminate the complexity of the process and to save time, computer package programs have been utilized.

Key words: Eckhaus equation; nonlinear Klein Gordon equation; complex hyperbolic trigonometric travelling wave solutions; non-integer balancing term
AMS 2020 Classification: 35C07; 37M05; 83C15

1 Introduction

The proposed method has been shown to be an effective mathematical instrument to solve the nonlinear wave of equations in mathematics, physics, and engineering. So the discussion of NPDEs exact solutions in the nonlinear sciences is very important. Over the past few years, many researchers have used this beneficial method extensively, for example, the Jacobi elliptic expansion method [1], modified Kudryashov method [2, 3], the tanh method [4], sub-equation analytical method [5], the inverse scattering method [6], the first integral method[7, 8], the extended tanh-function method [9, 10], the Hirota's direct method [11], the auxiliary equation method [12], improved Bernoulli sub-equation function method [13], expansion method [14], $(G'/G, 1/G)$-expansion method [15, 16, 17], generalized exponential rational function method [18, 19, 24], Sinh-Gordon function method [20], Sine-Gordon expansion method [21], Bernoulli sub-equation method [22], (G'/G)-expansion method [23].
The equation of the Eckhaus is as follows [25]:

$$iu_t + u_{xx} + 2(|u|^2)_x u + |u|^4 u = 0, \tag{1}$$

where $u = u(x,t)$ is a complex function. Eq. (1) is of the Schrödinger nonlinear type and recognizes a linearization of the Schrödinger linear equation that depends on free time. The EE has been found as a multi-scale asymptotic reduction of certain classes of NPDE.

➤ **Received:** 11.07.2021 ➤ **Revised:** 17.08.2021 ➤ **Accepted:** 20.08.2021 ➤ **Published:** 25.08.2021

The EE was linearized by a variation of the dependent variable. Many scientists have worked with this equation for example, the first-integral method [25], weakly nonlinear effects [26], the Laplace transform [27], the EE was linearized by an appropriate change of variable [28], many of the properties of the EE were researched [29], the EE can be integrated by a change of dependent variable [30], the intent of this work is to discover exact solutions of the EE by expansion method.

In this work, we use the expansion method to contract several new cases with the exact solutions for some NPDEs such as the nKG equation, which in mathematical physics is very important and many researchers paid attention to the balance number, not integer. In this paper, we analyze the nKG equation [31] as follows:

$$u_{tt} - \omega^2 u_{xx} + \alpha u - \beta u^3 + \gamma u^5 = 0, \tag{2}$$

where ω, α, β , and γ are arbitrary constant. In many scientific applications, these equations play an important role, such as the quantum field theory [32], the solid state physics [33], the nKG equations, and found many types of exact traveling wave solutions including compact solutions, periodic solutions, soliton solution using the tanh-function method [34], generalized Kudryashov method [35], Homotopy Perturbation Method [36].
The nonlinear Klein-Godon equation, which is directly related to the Schrödinger equation, has become famous in the literature as the relativistic wave equation[37]. It is also one of the indispensable equations of relativistic quantum mechanics, which examines the behavior of particles exposed to high energy. Space and rocket industry, nuclear and medical waste treatment, earthquake, high energy, and plasma physics are the application areas.

2 The methodology of the $(1/G')$-expansion method

In this segment, general realities of the $(1/G')$-expansion method [38, 39, 40] are displayed. To start with, we consider the general type of nonlinear PDE that depends on t and x variables.

$$W(u, u_t, u_x, u_{xx}, \dots) = 0, \tag{3}$$

here is $u(x, t)$ a function that depends on x and t, $\xi = k(x - 2at)$ in the form of $u(x, t) = Ue^{i(ax+bt)}$ where k, a and b are constants that are not zero. PDE referred to as Eq. (3), using this conversions

$$Q(U, U', U'', \dots) = 0, \tag{4}$$

the ODE is shaped. On the other hand, the solution of the linear ODE is given below $G = G(\xi)$.

$$G'' + \lambda G' + \mu = 0. \tag{5}$$

The solution of nonlinear ODE given by Eq. (4) can be written as follows.

$$u(\xi) = \sum_{i=1}^{m} a_i \left(\frac{1}{G'}\right)^m, \tag{6}$$

here are $a_1, a_2, \dots, \lambda, \mu$ constants and m is the balancing term. The term balance is a fixed number obtained in any non-linear ODE between the highest order linear term and the highest order non - linear term. This number Eq. (6) is written in place and then the needful derivatives for the solution are obtained. In such derivatives, $G'' = -\lambda G - \mu$ taken as $(1/G')$ is a polynomial and homogeneous equation. Here $(1/G')^m$, $m \in Q$ equals the coefficients of the terms to zero and a system of algebraic equations is built. This algebraic system of equations is calculated by using computer technology. These constants are written in place in Eq. (6). The ξ-linked solution must provide Eq. (4). After the necessary controls, the wave transformation is reversed and we reach the solution of Eq. (3).

3 Application 1

In this section, the solution given by Eq. (1) with $(1/G')$-expansion method will be obtained. We can choose the following transformation of the wave for Eq. (1):

$$u(x, t) = U(\xi)e^{i(ax+bt)}, \quad \xi = k(x - 2at), \tag{7}$$

under Eq. (1) wave transformation, Eq. (1) is converted to ODE as follows:

$$k^2 U'' - (b + a^2)U + 4kU'U^2 + U^5 = 0. \tag{8}$$

In Eq. (8), the balancing constant between the highest order linear term U'' and the highest nonlinear term U^5 is that $m = \frac{1}{2}$ is not integer. The solution of the ODE obtained in the form of Eq. (8) can be given in the following way considering Eq. (6):

$$U(\xi) = a_1 \left(\frac{1}{G'}\right)^{\frac{1}{2}}, \tag{9}$$

we take the 1st and 2nd derivatives of Eq. (9) and put them in Eq. (8), we get a polynomial with $(1/G')^{\frac{r}{2}}$, $r \in N$ variable. $(1/G')^{\frac{r}{2}}$ the polynomial term coefficients equal to zero.

$$
\begin{aligned}
\left(\tfrac{1}{G'}\right)^{\frac{1}{2}} &: \quad -a^2 a_1 - b a_1 + \tfrac{1}{4} k^2 \lambda^2 a_1 = 0,\\
\left(\tfrac{1}{G'}\right)^{\frac{3}{2}} &: \quad k^2 \lambda \mu a_1 + 2k\lambda a_1^3 = 0,\\
\left(\tfrac{1}{G'}\right)^{\frac{5}{2}} &: \quad \tfrac{3}{4} k^2 \mu^2 a_1 + 2k\mu a_1^3 + a_1^5 = 0.
\end{aligned}
\tag{10}
$$

The system of Eq. (10) can be solved with the help of a computer package program. The solutions obtained here are put into Eq. (9). Finally, the conversion is reversed and a new complex hyperbolic trigonometric travelling wave solution for Eq. (1) is obtained. The results are as follows:

$$
a_1 = \mp \frac{\mathrm{i}\sqrt{k}\sqrt{\mu}}{\sqrt{2}}, \quad \lambda = \mp \frac{2\sqrt{a^2+b}}{k},
$$

$$
u(x,t) = -\frac{\mathrm{i}e^{\mathrm{i}(ax+bt)}\sqrt{k}\sqrt{\mu}}{\sqrt{2}} \left(\frac{1}{\frac{k\mu}{2\sqrt{a^2+b}} + A\cosh\left[2(x-2at)\sqrt{a^2+b}\right] + A\sinh\left[2(x-2at)\sqrt{a^2+b}\right]} \right)^{\frac{1}{2}}, \tag{11}
$$

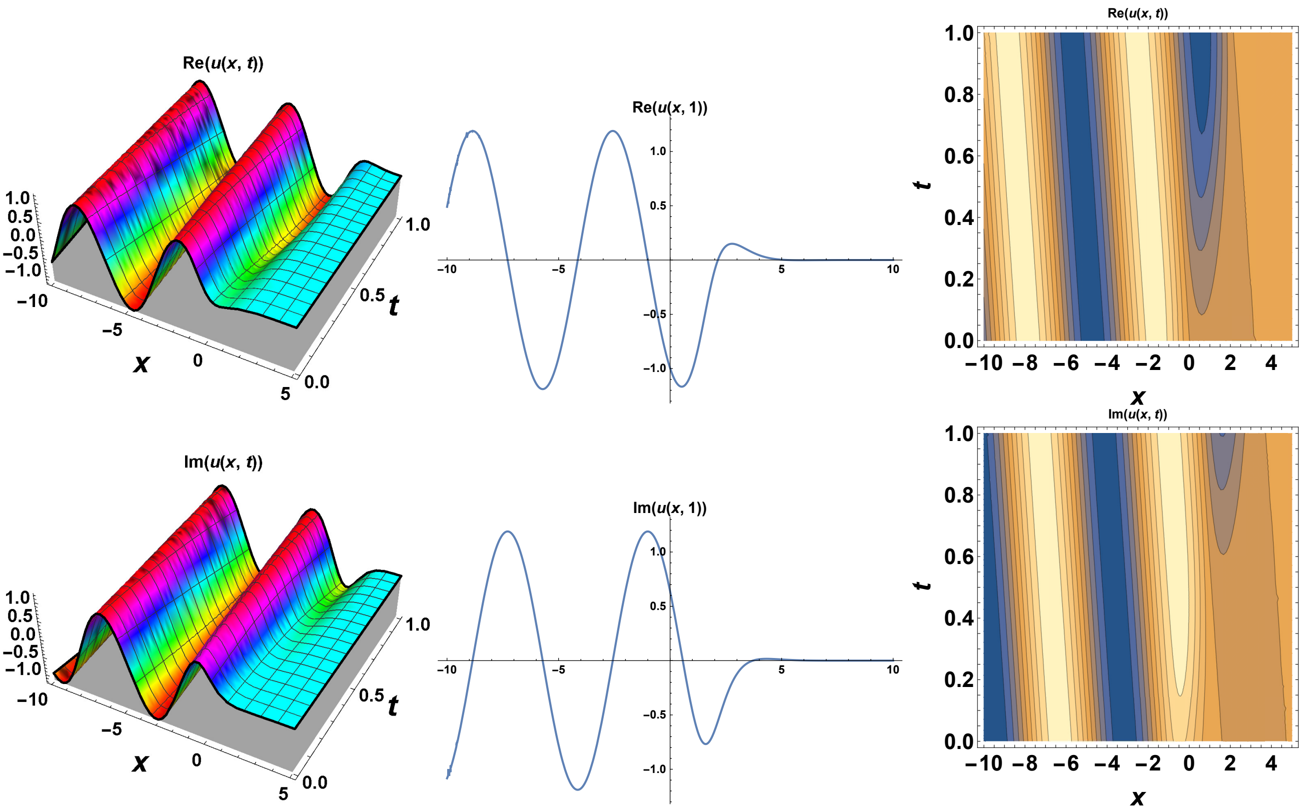

Figure 1. In terms of the Eq (11), for the constants $a = 1,\ b = 1,\ A = -5,\ k = -1,\ \mu = 6$ the new complex hyperbolic trigonometric travelling wave solution of Eq. (1).

4 Application 2

In this section, we use the proposed method to solve the nKG equation. We can choose the following transformation of the wave for Eq. (2):

$$
u(x,t) = U(\xi), \quad \xi = x - Vt \tag{12}
$$

where V is constant. The travelling wave variable Eq. (12) allows us to convert Eq. (2) to the following ODE for $U = U(\xi)$:

$$
\left(V^2 - \omega^2\right) U'' + \alpha U - \beta U^3 + \gamma U^5 = 0, \tag{13}
$$

In Eq. (13), the balancing constant between the highest order linear term U'' and the highest nonlinear term U^5 is that $m = \frac{1}{2}$ is not integer. The solution of the ODE obtained in the form of Eq. (13) can be given in the following way considering Eq. (6).

$$U(\xi) = a_1\left(\frac{1}{G'}\right)^{\frac{1}{2}}, \tag{14}$$

we take the 1st and 2nd derivatives of Eq. (14) and put them in Eq. (13), we get a polynomial with $(1/G')^{\frac{r}{2}}$, $r \in N$ variable. $(1/G')^{\frac{r}{2}}$ the polynomial term coefficients equal to zero.

$$\begin{aligned}
\left(\tfrac{1}{G'}\right)^{\frac{1}{2}} &: \quad \alpha a_1 - \tfrac{1}{4}\omega^2\lambda^2 a_1 + \tfrac{1}{4}v^2\lambda^2 a_1 = 0,\\
\left(\tfrac{1}{G'}\right)^{\frac{3}{2}} &: \quad -\omega^2\lambda\mu a_1 + v^2\lambda\mu a_1 - \beta a_1^3 = 0,\\
\left(\tfrac{1}{G'}\right)^{\frac{5}{2}} &: \quad -\tfrac{3}{4}\omega^2\mu^2 a_1 + \tfrac{3}{4}v^2\mu^2 a_1 + \gamma a_1^5 = 0,
\end{aligned} \tag{15}$$

The system of Eq. (15) can be solved with the help of a computer package program. The solutions obtained here are put into Eq. (14). Finally, the conversion is reversed and a new complex hyperbolic type trigonometric travelling wave solution to Eq. (2) is obtained. The results are as follows:

$$\begin{aligned}
&a_1 = \mp\frac{2i\sqrt{\alpha}\sqrt{\mu}}{\sqrt{\beta}\sqrt{\lambda}}, \quad \gamma = \frac{3\beta^2}{16\alpha}, \quad v = \mp\frac{\sqrt{-4\alpha+\omega^2\lambda^2}}{\lambda},\\
&u(x,t) = -\frac{2i\sqrt{\alpha}\sqrt{\mu}}{\sqrt{\beta}\sqrt{\lambda}\left[-\frac{\mu}{\lambda}+A\cosh\left[\lambda\left(x+\frac{t\sqrt{-4\alpha+\omega^2\lambda^2}}{\lambda}\right)\right]-A\sinh\left[\lambda\left(x+\frac{t\sqrt{-4\alpha+\omega^2\lambda^2}}{\lambda}\right)\right]\right]^{\frac{1}{2}}}.
\end{aligned} \tag{16}$$

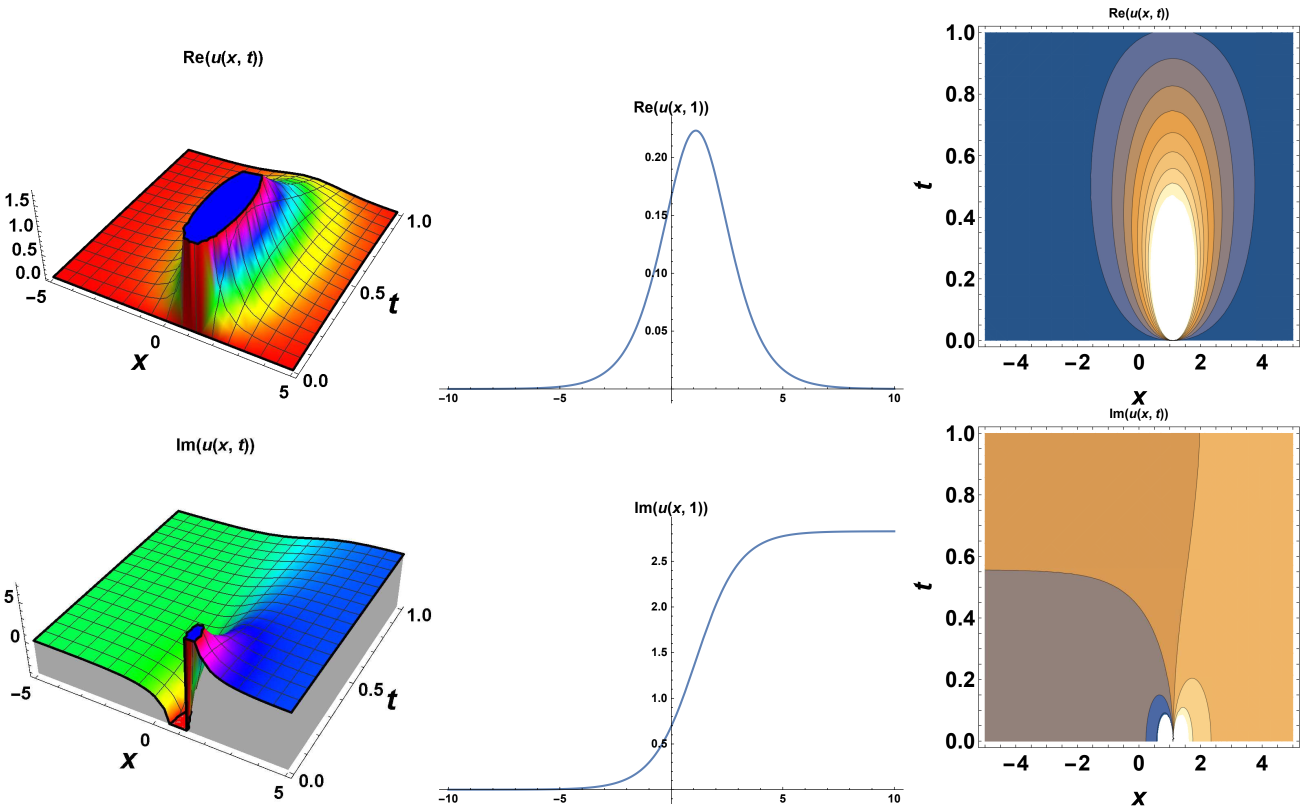

Figure 2. In terms of Eq. (16), for the constants $\alpha = 2$, $\beta = 1$, $A = 3$, $k = 2.5$, $\mu = 1$, $\lambda = 1$, $\omega = 0.001$ the new complex hyperbolic trigonometric travelling wave solution of Eq. (2).

5 Results and discussions

In this study, we have introduced a new method for a new complex hyperbolic trigonometric travelling wave solution of partial differential equations that are not integer in the balancing term. We have implemented the application here for the balancing term $m = \frac{1}{2}$. In next studies, both $m < 0$ and $m \neq \frac{1}{2}$ can be used for balancing terms that m is not integer. For Eq. (1), the complex hyperbolic trigonometric travelling wave solution presented in the form of Eq. (11), and for Eq. (2), the complex hyperbolic trigonometric travelling wave solution presented in the form of Eq. (16) is new and the solutions provide Eq. (1) and Eq. (2).

By giving special values to the parameters in these solutions, we can present the three-dimensional graphics representing the constant wave as follows.
The traveling wave solutions obtained in this study are valuable physically as well as mathematically. In order to understand its physical value, the constants in the obtained traveling wave solutions must be given physical meaning. In physics, the mathematical model representing the assumption that the envelope of a forward-moving wave pulse changes slowly in time and space compared to a period or wavelength can be represented by Eq. (7) [41]. In Eq. (7), $\xi = k(x - 2at)$ is the variable of the traveling wave. $U(\xi)$ represents an amplitude of the traveling wave solution. In addition, ka and a represent the velocity and frequency of the traveling wave, respectively, which is physically prominent in this study and whose different values will be analyzed for the behavior of the traveling wave. The a parameter is directly related to both the speed of the wave and the length of the wave. So let us analyze the behavior simulation of the traveling wave solution for different values of a in Eq. (11) traveling wave solution produced by the $(1/G')$-expansion method for Eq. (1).

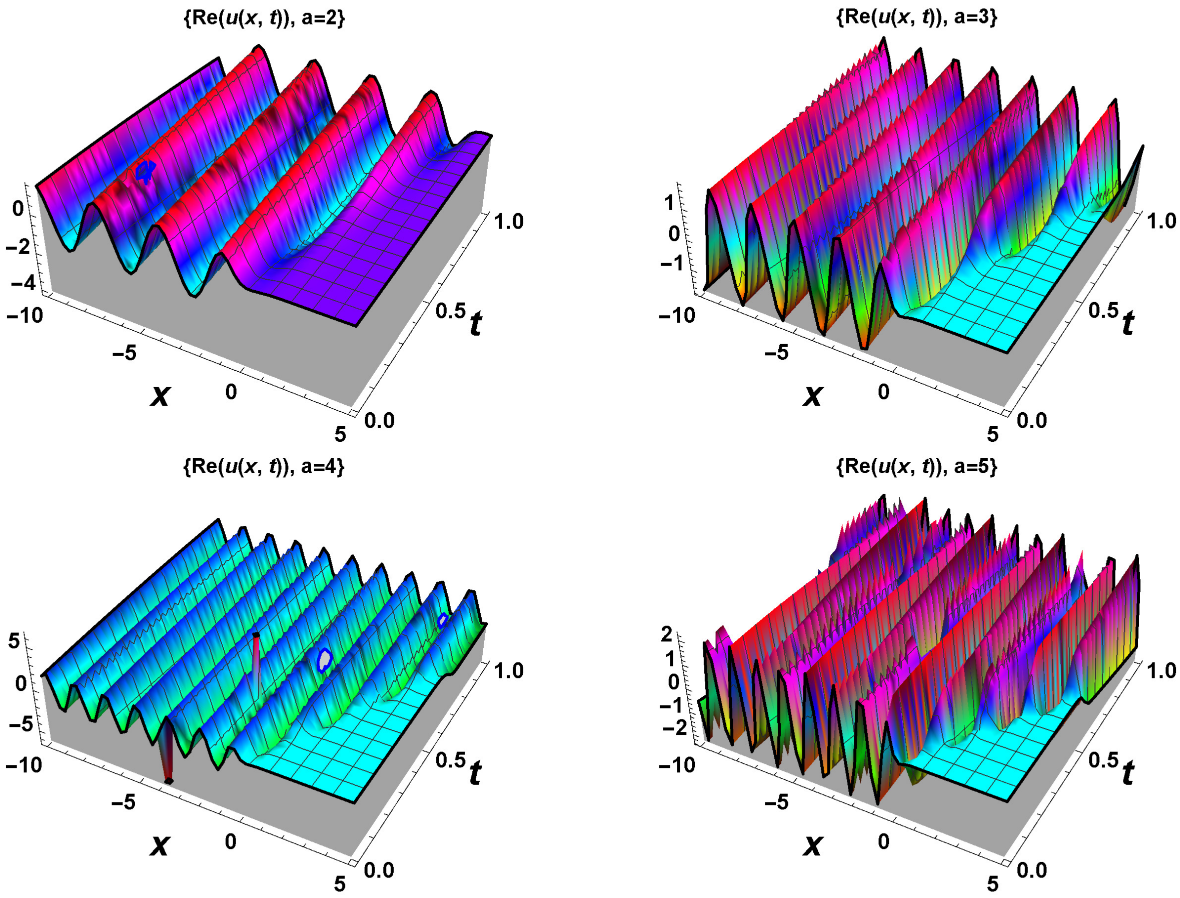

Figure 3. In terms real part of Eq. (11), for the constants $b = 1$, $A = -5$, $k = -1$, $\mu = 1$ the new complex hyperbolic trigonometric travelling wave solution of Eq. (1).

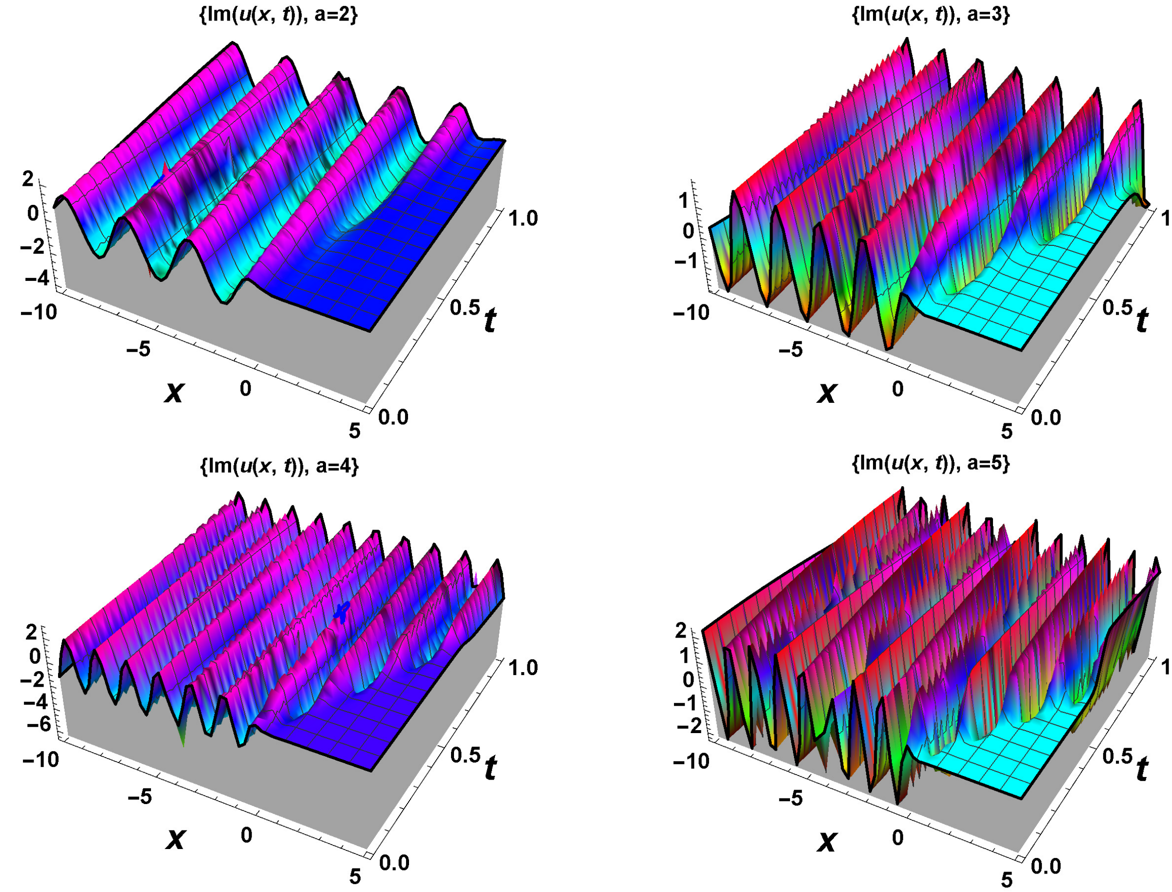

Figure 4. In terms imaginary part of Eq. (11), for the constants $b = 1$, $A = -5$, $k = -1$, $\mu = 1$ the new complex hyperbolic trigonometric travelling wave solution of Eq. (1).

Physically, we can observe in Figs. 3 and 4 that the parameter a is related to both the velocity and the frequency of the traveling wave. As the frequency increases, the wavelength of the traveling wave decreases while its speed increases. When a =, the traveling wave exhibits triangular wave behavior. The frequency of the traveling wave is directly related to the wave number. As the frequency increases, the number of waves increases. We can support the validity of this discussion with Figs. 3 and 4. In addition, the interpretations are similar as it exhibits similar behaviors for the real and imaginary parts.

The Klein-Gordon equation is related to the Schrödinger equation and is known as the relativistic wave equation. In physics, relativistic quantum mechanics studies the behavior of particles exposed to high energy [37]. We think that the Klein-Gordon equation, whose traveling wave solution is produced in this study, can be a mathematical model of a high-energy seismic wave. Traveling wave solutions, which play an important role in the transfer of energy from one point to another, may lead to different discussions about earthquakes in the future.

6 Conclusions

In this paper, we explored a new application $(1/G')$ -expansion method, we obtained exact solutions of the EE and nKG equation, and obtained new types of complex hyperbolic trigonometric travelling wave solution for the EE and nKG equation. Many scientists were less interested, when the balancing term used in the expansion methods was non-integer or negative. In order to increase this interest, the method can be applied for non-integer balancing terms of partial differential equations. This paper presented wider applicability using the $(1/G')$ -expansion method to handle nonlinear evolutionary equations. The parameters in the obtained traveling wave solution were given physical meaning. A three-dimensional simulation of the wave behavior is constructed for different values of the a parameter, which affects the frequency and speed of the traveling wave. The dynamics of the wave supported by simulation are discussed. Results show that this method was effective. The new wave solution obtained in this paper can present different perspectives on future researches.

Declarations

Consent for publication

Not applicable.

Conflicts of interest

The author declares that he has no known competing financial interests or personal relationships that could have appeared to influence the work reported in this paper.

Funding

The author declares that there is no funding source for the reported research.

Author's contributions

The research was carried out by the author and he accepts that the contributions and responsibilities belong to the author.

Acknowledgements

The author would like to thank Firat University for their unwavering support in the conduct of the research.

References

[1] Alquran, M., Jarrah, A., and Krishnan, E. Solitary Wave Solutions of the Phi-Four Equation and the Breaking Soliton System by Means of Jacobi Elliptic Sine-Cosine Expansion Method. *Nonlinear Dynamics and Systems Theory*, 18(3), 233-240, (2018).

[2] Durur, H., and Yokuş, A. Discussions on diffraction and the dispersion for traveling wave solutions of the (2+ 1)-dimensional paraxial wave equation. *Mathematical Sciences*, 1-11, (2021) https://link.springer.com/article/10.1007/s40096-021-00419-z.

[3] Yokuş, A., Durur, H., and Duran, S. Simulation and refraction event of complex hyperbolic type solitary wave in plasma and optical fiber for the perturbed Chen-Lee-Liu equation. *Optical and Quantum Electronics*, 53(402), (2021) https://doi.org/10.1007/s11082-021-03036-1.

[4] Malfliet, W. and Hereman, W. The tanh method: II. Perturbation technique for conservative systems. *Physica Scripta*, 54(6), 569, (1996).

[5] Duran, S., and Karabulut, B. Nematicons in liquid crystals with Kerr Law by sub-equation method. *Alexandria Engineering Journal*, (2021) https://doi.org/10.1016/j.aej.2021.06.077.

[6] Caudrelier, V.. Interplay between the Inverse Scattering Method and Fokas's Unified Transform with an Application. *Studies in Applied Mathematics*, 140(1), 3-26, (2018).

[7] Zhang, Q., Xiong, M., and Chen, L. The First Integral Method for Solving Exact Solutions of Two Higher Order Nonlinear Schrödinger Equations, *Journal of Advances in Applied Mathematics*, 4(1), (2019).

[8] Feng, Z. and Wang, X. The first integral method to the two-dimensional Burgers–Korteweg–de Vries equation. *Physics Letters A*, 308(2-3), 173-178, (2003).

[9] Fan, E. Extended tanh-function method and its applications to nonlinear equations. *Physics Letters A*, 277(4-5), 212-218, (2000).

[10] Tariq, H. et al. New travelling wave analytic and residual power series solutions of conformable Caudrey-Dodd-Gibbon-Sawada-Kotera equation. *Results in Physics*, 104591, (2021).

[11] Wazwaz, A.-M. The Hirota's direct method and the tanh–coth method for multiple-soliton solutions of the Sawada–Kotera–Ito seventh-order equation. *Applied Mathematics and Computation*, 199(1), 133-138, (2008).

[12] Akbulut, A. and Kaplan, M. Auxiliary equation method for time-fractional differential equations with conformable derivative. *Computers & Mathematics with Applications*, 75(3), 876-882, (2018).

[13] Baskonus, H.M. and Bulut, H. On the complex structures of Kundu-Eckhaus equation via improved Bernoulli sub-equation function method, *Waves in Random and Complex Media*, 25(4), 720-728, (2015).

[14] Wang, M., Li, X., and Zhang, J. The (G'/G)-expansion method and travelling wave solutions of nonlinear evolution equations in mathematical physics. *Physics Letters A*, 372(4), 417-423, (2018).

[15] Duran, S. Extractions of travelling wave solutions of (2+ 1)-dimensional Boiti–Leon–Pempinelli system via $(G'/G, 1/G)$-expansion method. *Optical and Quantum Electronics*, 53(6), 1-12, (2021).

[16] Duran, S. Solitary Wave Solutions of the Coupled Konno-Oono Equation by using the Functional Variable Method and the Two Variables $(G'/G, 1/G)$-Expansion Method. *Adıyaman University Journal of Science*, **10**(2), 585-594, (2020).

[17] Yokuş, A., and Durur, H. $(G'/G, 1/G)$-expansion method for analytical solutions of Jimbo-Miwa equation. *Cumhuriyet Science Journal*, **42**(1), 88-98, (2021).

[18] Durur, H. Energy-carrying wave simulation of the Lonngren-wave equation in semiconductor materials. *International Journal of Modern Physics B*, 2150213, (2021).

[19] Ali, K.K., Yilmazer, R., Bulut, H., Aktürk, T., and Osman, M.S. Abundant exact solutions to the strain wave equation in micro-structured solids. *Modern Physics Letters B*, 2150439, (2021).

[20] Yokuş, A., Durur, H., Nofal, T.A., Abu-Zinadah, H., Tuz, M., and Ahmad, H. Study on the applications of two analytical

methods for the construction of traveling wave solutions of the modified equal width equation. *Open Physics,* 18(1), 1003-1010, (2020).

[21] Ali, K K., Yilmazer, R., Baskonus, H.M., and Bulut, H. New wave behaviors and stability analysis of the Gilson-Pickering equation in plasma physics. *Indian Journal of Physics,* 95(5), 1003-1008, (2021).

[22] Ali, K.K., Yilmazer, R., Baskonus, H.M., and Bulut, H. Modulation instability analysis and analytical solutions to the system of equations for the ion sound and Langmuir waves. *Physica Scripta,* 95(6), 065602, (2020).

[23] Akinyemi, L., Şenol, M., Rezazadeh, H., Ahmad, H., and Wang, H. Abundant optical soliton solutions for an integrable (2+ 1)-dimensional nonlinear conformable Schrödinger system. Results in Physics, 25, 104177, (2021).

[24] Duran, S. Breaking theory of solitary waves for the Riemann wave equation in fluid dynamics. *International Journal of Modern Physics B,* 2150130, (2021).

[25] Taghizadeh, N., Mirzazadeh, M., and Tascan, F., The first-integral method applied to the Eckhaus equation, Applied Mathematics Letters, 25(5), 798-802, (2012).

[26] Calogero, F. and Eckhaus, W. Nonlinear evolution equations, rescalings, model PDEs and their integrability: II. *Inverse Problems,* 4(1), 11, (1988).

[27] Calogero, F. and De Lillo, S. Cauchy problems on the semiline and on a finite interval for the Eckhaus equation. *Inverse Problems,* 4(4), L33, (1988).

[28] Calogero, F. The evolution partial differential equation ut= uxxx+ 3 (uxxu 2+ 3 u 2 xu)+ 3 uxu 4. *Journal of mathematical physics,* 28(3), 538-555, (1987).

[29] Calogero, F. and De Lillo, S. The Eckhaus PDE $i\psi t + \psi xx + 2(|\psi|^2)x\psi + |\psi|4\psi = 0$. *Inverse Problems,* 3(4), 633, (1987).

[30] Calogero, F. and De Lillo, S. The Eckhaus equation in an external potential. *Journal of Physics A: Mathematical and General,* 25(7), L287, (1992).

[31] Zayed, E.M. and Gepreel, K.A. The modified (G'/G)-expansion method and its applications to construct exact solutions for nonlinear PDEs. *Wseas transactions on mathematics,* **10**(8), 270-278, (2011).

[32] Peskin, M.E. An introduction to quantum field theory, *CRC Press,* (2018).

[33] Khalatnikov, I.M. An introduction to the theory of superfluidity, *CRC Press,* (2018).

[34] Wazwaz, A.-M. Compactons, solitons and periodic solutions for some forms of nonlinear Klein-Gordon equations. *Chaos, Solitons & Fractals,* 2(4), 1005-1013, (2006).

[35] Baskonus, H.M. and Bulut, H. New hyperbolic function solutions for some nonlinear partial differential equation arising in mathematical physics, *Entropy,* 17(6), 4255-4270, (2015).

[36] Bulut, H. and Başkonus, H.M., On The Geometric Interpretations of The Klein-Gordon Equation And Solution of The Equation by Homotopy Perturbation Method. *Applications & Applied Mathematics*, 7(2), (2012).

[37] Orion, T. Klein-Gordon equation. Encyclopedia of Mathematics, (2012). https://encyclopediaofmath.org/wiki/Klein_Gordon-equation.

[38] Yokus, A. Comparison of Caputo and conformable derivatives for time-fractional Korteweg-de Vries equation via the finite difference method. *International Journal of Modern Physics B,* 32(29), 1850365, (2018).

[39] Yokus, A. and Kaya, D. Numerical and exact solutions for time fractional Burgers' equation. *Journal of Nonlinear Sciences and Applications,* 10(7), 3419-3428, (2017).

[40] Yokus, A. and Kaya, D. Conservation laws and a new expansion method for sixth order Boussinesq equation. in AIP Conference Proceedings, *AIP Publishing,* (2015).

[41] Arecchi, F. and Bonifacio, R. Theory of optical maser amplifiers. *IEEE Journal of Quantum Electronics,* 1(4), 169-178, (1965).

Mathematical Modelling and Numerical Simulation with Applications (MMNSA) (http://www.mmnsa.org)

Mathematical Modelling and Numerical Simulation with Applications, 2021, 1(1), 32–43

https://www.mmnsa.org
ISSN Online: 2791-8564 / Open Access
https://doi.org/10.53391/mmnsa.2021.01.004

RESEARCH PAPER

The Hermite-Hadamard type inequality and its estimations via generalized convex functions of Raina type

Muhammad Tariq [1,*,§], Hijaz Ahmad [2,§] and Soubhagya Kumar Sahoo [3,§]

[1]Department of Basic Sciences and Related Studies, Mehran University of Engineering and Technology, Jamshoro 76062, Pakistan, [2]Section of Mathematics, International Telematic University Uninettuno, Corso Vittorio Emanuele II, 39, 00186 Roma Italy, [3]Department of Mathematics, Institute of Technical Education and Research, Siksha O Anusandhan University, Bhubaneswar 751030, Odisha, India

[*]Corresponding Author
[§]captaintariq2187@gmail.com (Muhammad Tariq); hijaz555@gmail.com (Hijaz Ahmad); soubhagyalulu@gmail.com (Soubhagya Kumar Sahoo)

Abstract

The theory of convexity plays an important role in various branches of science and engineering. The main objective of this work is to introduce the idea of a generalized convex function by unifying s-type m-convex function and Raina type function. In addition, some beautiful algebraic properties and examples are discussed. Applying this new definition, we explore a new sort of Hermite-Hadamard inequality. Furthermore, to enhance the paper we investigate several new estimations of Hermite-Hadamard type inequality. The concepts and tools of this paper may invigorate and revitalize for additional research in this mesmerizing and absorbing field of mathematics.

Key words: Convex function; m-convex function; s-type convex function; Hölder's inequality; improved power-mean integral inequality
AMS 2020 Classification: 26A51; 26A33; 26D07; 26D10; 26D15

1 Introduction

The expression "convexity" is the main, intriguing, regular, and principal documentations in mathematical analysis. For the first time, it was utilized generally in a book by Hardy, Little, and Polya (see [1]). As of late, the hypothesis of convexity assumes an exceptionally entrancing and astonishing part in the realm of science, hence anyone working, especially in the field of inequalities cannot ignore its importance and significance. Numerous analysts consistently attempt to utilize novel thoughts for the pleasure and beautification of convexity theory. This hypothesis gives us fascinating and amazing mathematical strategies to tackle and to take care of a great deal of the issue which emerges in pure and applied sciences. During the last few decades, numerous scientists specially mathematicians have added to the advancement of the theory of convex analysis in different directions. For the attention of the readers, we encourage the references [2, 3, 4, 5, 6, 7] to see.

The theory of inequality is one of the most important aspects in many branches of mathematics such as functional analysis, theory of differential and integral equations, probability theory, mechanics, and other sciences. In this manner, the hypothesis of inequalities might be viewed as an autonomous field of mathematical analysis. As of late, the idea of convex analysis and the

➤ **Received:** 20.08.2021 ➤ **Revised:** 31.08.2021 ➤ **Accepted:** 01.09.2021 ➤ **Published:** 04.09.2021

concept of inequality have been generalized, improved and extended in many directions. The relationship between these two fields has roused numerous scientists specially mathematicians because of its broad applications. For some related papers on convexity, see the references [8, 9, 10, 11].
As everybody knows, there exists a class of numerical models depicted by differential equations, for example, Malthus population model. In any case, a great deal of a differential equation does not have a specific arrangement. Under this case, integral inequalities are critical for researching the boundedness, stability, asymptotic behavior of solutions to differential equations.
Motivated by the ongoing research activities, the aim of this paper is to introduce a new class of a convex function, called a generalized s–type $\mathfrak{m}$–convex function of Raina type. Next, we explore some of its algebraic properties and examples. As main results, a new version of Hermite–Hadamard inequality and its refinements in support of the new definition are presented.

2 Preliminaries

Definition 1 *[3] Let $\Upsilon : I \to \mathbb{R}$ be a real valued function. A function Υ is said to be convex, if*

$$\Upsilon\left(\flat\mathfrak{a}_1 + (1-\flat)\,\mathfrak{a}_2\right) \le \flat\Upsilon\left(\mathfrak{a}_1\right) + (1-\flat)\,\Upsilon\left(\mathfrak{a}_2\right) \tag{1}$$

holds for all $\mathfrak{a}_1, \mathfrak{a}_2 \in I$ and $\flat \in [0, 1]$.

The most important inequality concerning convex functions is Hermite–Hadamard inequality [12] given as:

Theorem 1 *If $\Upsilon : [\mathfrak{a}_1, \mathfrak{a}_2] \to \mathbb{R}$ is a convex function, then*

$$\Upsilon\left(\frac{\mathfrak{a}_1+\mathfrak{a}_2}{2}\right) \le \frac{1}{\mathfrak{a}_2-\mathfrak{a}_1}\int_{\mathfrak{a}_1}^{\mathfrak{a}_2}\Upsilon(x)dx \le \frac{\Upsilon(\mathfrak{a}_1)+\Upsilon(\mathfrak{a}_2)}{2}. \tag{2}$$

Since its discovery, many researchers have presented various generalizations and improvements with reference to different types of generalized convex functions like s- convex functions, m- convex functions, Harmonically convex functions, log-convex functions, exponentially convex functions, and many more. This inequality along with inequalities such as Ostrowski inequality, Simpson inequality, Bullen type inequality, Opial type inequality, and Mercer type inequality have accumulated a lot of attention among mathematicians due to their widespread view and applications in the field of mathematical analysis.
In 2005, Raina [13] introduced a new class of function defined formally by

$$\mathcal{F}^{\sigma}_{\rho,\lambda}(z) = \mathcal{F}^{\sigma(0),\,\sigma(1),\ldots}_{\rho,\lambda}(z) = \sum_{k=0}^{+\infty}\frac{\sigma(k)}{\Gamma(\rho k+\lambda)}z^k, \tag{3}$$

where $\sigma = (\sigma(0), \ldots, \sigma(k), \ldots)$ and $\rho, \lambda > 0$, $|z| < R$. The above class of functions is a generalization of the classical Mittag–Leffler function and the Kummer function.
Cortez [14, 15] established a new class of set and function involving the Raina's function, which is said to be a generalized convex set and a convex function.

Definition 2 *[15] Let $\sigma = (\sigma(0), \ldots, \sigma(k), \ldots)$ and $\rho, \lambda > 0$. A set $X \neq \emptyset$ is said to be generalized convex, if*

$$\mathfrak{a}_2 + \flat\,\mathcal{F}^{\sigma}_{\rho,\lambda}(\mathfrak{a}_1-\mathfrak{a}_2) \in X, \tag{4}$$

for all $\mathfrak{a}_1, \mathfrak{a}_2 \in X$ and $\flat \in [0, 1]$.

Definition 3 *[15] Let σ denote a bounded sequence, then $\sigma = (\sigma(0), \ldots, \sigma(k), \ldots)$ and $\rho, \lambda > 0$. If $\Upsilon : X \to \mathbb{R}$ satisfies the following inequality*

$$\Upsilon\left(\mathfrak{a}_2 + \flat\,\mathcal{F}^{\sigma}_{\rho,\lambda}(\mathfrak{a}_1-\mathfrak{a}_2)\right) \le \flat\Upsilon(\mathfrak{a}_1) + (1-\flat)\Upsilon(\mathfrak{a}_2), \tag{5}$$

for all $\mathfrak{a}_1, \mathfrak{a}_2 \in X$, where $\mathfrak{a}_1 < \mathfrak{a}_2$ and $\flat \in [0, 1]$, then Υ is called a generalized convex function.

Remark 1 *We have $\mathcal{F}^{\sigma}_{\rho,\lambda}(\mathfrak{a}_1-\mathfrak{a}_2) = \mathfrak{a}_1-\mathfrak{a}_2 > 0$, and so we obtain Definition 1.*

Condition A: Let $X \subseteq \mathbb{R}$ be an open generalized convex subset with respect to (w.r.t.) $\mathcal{F}^{\sigma}_{\rho,\lambda}(\cdot)$. For any $\mathfrak{a}_1, \mathfrak{a}_2 \in X$ and $\flat \in [0, 1]$,

$$\mathcal{F}^{\sigma}_{\rho,\lambda}\left(\mathfrak{a}_2 - (\mathfrak{a}_2 + \flat\,\mathcal{F}^{\sigma}_{\rho,\lambda}(\mathfrak{a}_1-\mathfrak{a}_2))\right) = -\flat\,\mathcal{F}^{\sigma}_{\rho,\lambda}(\mathfrak{a}_1-\mathfrak{a}_2),$$

$$\mathcal{F}^{\sigma}_{\rho,\lambda}\left(\mathfrak{a}_1 - \left(\mathfrak{a}_2 + \flat\,\mathcal{F}^{\sigma}_{\rho,\lambda}(\mathfrak{a}_1-\mathfrak{a}_2)\right)\right) = (1-\flat)\,\mathcal{F}^{\sigma}_{\rho,\lambda}(\mathfrak{a}_1-\mathfrak{a}_2).$$

Note that, for every $\mathfrak{a}_1$, $\mathfrak{a}_2 \in X$ and for all $\flat_1, \flat_2 \in [0, 1]$, using Condition A, we have

$$\mathcal{F}^{\sigma}_{\rho,\lambda}\left(\mathfrak{a}_2 + \flat_2\,\mathcal{F}^{\sigma}_{\rho,\lambda}(\mathfrak{a}_1-\mathfrak{a}_2) - (\mathfrak{a}_2 + \flat_1\,\mathcal{F}^{\sigma}_{\rho,\lambda}(\mathfrak{a}_1-\mathfrak{a}_2))\right) = (\flat_2-\flat_1)\,\mathcal{F}^{\sigma}_{\rho,\lambda}(\mathfrak{a}_1-\mathfrak{a}_2). \tag{6}$$

Definition 4 *[16] A non-negative function $\Upsilon : \mathbb{A} \to \mathbb{R}$ is said to be an s−type convex function if the following inequality for $\mathfrak{a}_1, \mathfrak{a}_2 \in \mathbb{A}$, $s \in [0,1]$ and $\flat \in [0,1]$ holds true:*

$$\Upsilon\left(\flat\mathfrak{a}_1 + (1-\flat)\,\mathfrak{a}_2\right) \leq \left[1 - (s(1-\flat))\right]\Upsilon\left(\mathfrak{a}_1\right) + \left[1 - s\flat\right]\Upsilon\left(\mathfrak{a}_2\right). \tag{7}$$

Definition 5 *[3] An inequality of the form*

$$(\Upsilon(\mathfrak{a}_1) - \Upsilon(\mathfrak{a}_2))(\Psi(\mathfrak{a}_1) - \Psi(\mathfrak{a}_2)) \geq 0, \quad \forall \mathfrak{a}_1, \mathfrak{a}_2 \in \mathbb{R}, \tag{8}$$

is said to be similarly ordered.

Inspired and excited by the ongoing research activities, the construction of this paper is marked as follows. First of all, in section 3, we discuss the new definition of the generalized s−type (m)−convex function of Raina type and its algebraic properties. In section 4, on the basis of a new identity, we attain the refinements of Hermite–Hadamard type inequality employing the new definition.

3 Generalized Preinvex function and its algebraic properties

In this section, we present the definition of a new class of convex functions called generalized s−type $\mathfrak{m}$−convex function of Raina type and also discuss its algebraic properties.

Definition 6 *Let $\mathbb{X}$ be a nonempty generalized convex set w.r.t. $\mathcal{F}^{\sigma}_{\rho,\lambda} : \mathbb{X} \times \mathbb{X} \to \mathbb{R}$.Then the nonnegative function $\Upsilon : \mathbb{X} \to \mathbb{R}$ is said to be a generalized s−type $\mathfrak{m}$−convex function of Raina type for fixed $\mathfrak{m}\mathfrak{m} \in (0,1] \times (0,1]$, if*

$$\Upsilon(\mathfrak{a}_2 + \flat\,\mathcal{F}^{\sigma}_{\rho,\lambda}(\mathfrak{a}_1 - \mathfrak{a}_2)) \leq (1 - s\flat)\,\Upsilon\left(\mathfrak{a}_2\right) + \left(1 - (s(1-\flat))\right)\mathfrak{m}\Upsilon\left(\frac{\mathfrak{a}_1}{\mathfrak{m}}\right) \tag{9}$$

holds for every $\mathfrak{a}_1, \mathfrak{a}_2 \in \mathbb{X}$, $\sigma = (\sigma(0), \ldots, \sigma(k), \ldots)$, $\rho, \lambda > 0$, $s \in [0,1]$, and $\flat \in [0,1]$.

Remark 2 *(i) Taking $s = \mathfrak{m} = 1$ in Definition 6, we attain the definition of a generalized convex function of Raina type which was explored by Cortez [14, 15].*
(ii) Taking $\mathfrak{m} = 1$ and $\mathcal{F}^{\sigma}_{\rho,\lambda}(\mathfrak{a}_1 - \mathfrak{a}_2) = \mathfrak{a}_1 - \mathfrak{a}_2$ in Definition 6, we attain the definition of s−type convex function which was given by İşcan et al. [16].
(iii) Taking $s = \mathfrak{m} = 1$ and $\mathcal{F}^{\sigma}_{\rho,\lambda}(\mathfrak{a}_1 - \mathfrak{a}_2) = \mathfrak{a}_1 - \mathfrak{a}_2$ in Definition 6, we obtain the definition, namely a convex function which was investigated by Niculescu et al. [3].

Lemma 1 *The following inequalities*

$$\flat \leq (1 - (s(1-\flat))) \quad \text{and} \quad 1 - \flat \leq 1 - s\flat$$

hold, for all $\flat \in [0,1]$, $\mathfrak{m} \in (0,1]$ and $s \in [0,1]$.

Proof The rest of the proof is clearly seen. ■

Proposition 1 *Every nonnegative generalized $\mathfrak{m}$−convex function of Raina type is a generalized s−type $\mathfrak{m}$−convex function of Raina type for $s \in [0,1]$, $\mathfrak{m} \in (0,1]$ and $\flat \in [0,1]$.*

Proof By using Lemma 1 and the definition of a generalized $\mathfrak{m}$−convex function of Raina type for $s \in [0,1]$, $\mathfrak{m} \in (0,1]$ and $\flat \in [0,1]$, we have

$$\Upsilon(\mathfrak{a}_2 + \flat\,\mathcal{F}^{\sigma}_{\rho,\lambda}(\mathfrak{a}_1 - \mathfrak{a}_2)) \leq (1-\flat)\Upsilon\left(\mathfrak{a}_2\right) + \mathfrak{m}\flat\Upsilon\left(\frac{\mathfrak{a}_1}{\mathfrak{m}}\right)$$

$$\leq (1 - s\flat)\,\Upsilon\left(\mathfrak{a}_2\right) + \left(1 - (s(1-\flat))\right)\mathfrak{m}\Upsilon\left(\frac{\mathfrak{a}_1}{\mathfrak{m}}\right).$$

Proposition 2 *Every non-negative generalized s−type $\mathfrak{m}$−convex function of Raina type for $s \in [0,1]$, $\mathfrak{m} \in (0,1]$, $n \in \mathbb{N}$ and $\flat \in [0,1]$, is a generalized $(h,\mathfrak{m})$−convex function of Raina type with $h(\flat) = (1 - (s(1-\flat)))$.*

Proof Using the definition of a generalized s−type $\mathfrak{m}$−convex function of Raina type for $s \in [0,1]$, $\mathfrak{m} \in (0,1]$ and $\flat \in [0,1]$ and in view of the condition $h(\flat) = (1 - (s(1-\flat)))$, we have

$$\Upsilon(\mathfrak{a}_2 + \flat\,\mathcal{F}^{\sigma}_{\rho,\lambda}(\mathfrak{a}_1 - \mathfrak{a}_2)) \leq (1 - s\flat)\,\Upsilon\left(\mathfrak{a}_2\right) + \left(1 - (s(1-\flat))\right)\mathfrak{m}\Upsilon\left(\frac{\mathfrak{a}_1}{\mathfrak{m}}\right),$$

$$\leq h(1-\flat)\Upsilon(\mathfrak{a}_2) + h\mathfrak{m}(\flat)\Upsilon(\frac{\mathfrak{a}_1}{\mathfrak{m}}).$$

■

Now, we will investigate some algebraic properties of the new definition.

Theorem 2 *Let $\Upsilon, \Psi : \mathbb{A} = [\mathfrak{a}_1, \mathfrak{a}_2] \to \mathbb{R}$. If Υ, Ψ are two generalized s−type $\mathfrak{m}$−convex functions of Raina type w.r.t. the same $\mathcal{F}^{\sigma}_{\rho,\lambda}$, then*
(i) The sum of Υ and Ψ is again a generalized s−type $\mathfrak{m}$−convex function of Raina type w.r.t. $\mathcal{F}^{\sigma}_{\rho,\lambda}$.
(ii) The scalar multiplication of the function Υ is a generalized s−type $\mathfrak{m}$−convex function of Raina type w.r.t. $\mathcal{F}^{\sigma}_{\rho,\lambda}$.

Proof (i) Let Υ, Ψ be generalized s-type $\mathfrak{m}$−convex functions of Raina type w.r.t. the $\mathcal{F}^{\sigma}_{\rho,\lambda}$, then for all $\mathfrak{a}_1, \mathfrak{a}_2 \in \mathbb{X}$, $s \in [0,1]$, $\mathfrak{m} \in (0,1]$ and $\flat \in [0,1]$, we have

$$\begin{aligned}
&(\Upsilon + \Psi)(\mathfrak{a}_2 + \flat\, \mathcal{F}^{\sigma}_{\rho,\lambda}(\mathfrak{a}_1 - \mathfrak{a}_2)) \\
&= \Upsilon(\mathfrak{a}_2 + \flat\, \mathcal{F}^{\sigma}_{\rho,\lambda}(\mathfrak{a}_1 - \mathfrak{a}_2)) + \Psi(\mathfrak{a}_2 + \flat\, \mathcal{F}^{\sigma}_{\rho,\lambda}(\mathfrak{a}_1 - \mathfrak{a}_2)) \\
&\leq (1 - s\flat)\,\Upsilon(\mathfrak{a}_2) + (1 - (s(1-\flat)))\, m\Upsilon\left(\frac{\mathfrak{a}_1}{\mathfrak{m}}\right) \\
&+ (1 - s\flat)\,\Psi(\mathfrak{a}_2) + (1 - (s(1-\flat)))\, \mathfrak{m}\Psi\left(\frac{\mathfrak{a}_1}{\mathfrak{m}}\right) \\
&= (1 - s\flat)[\Upsilon(\mathfrak{a}_2) + \Psi(\mathfrak{a}_2)] + (1 - (s(1-\flat)))\left[\mathfrak{m}\Upsilon\left(\frac{\mathfrak{a}_1}{\mathfrak{m}}\right) + \mathfrak{m}\Psi\left(\frac{\mathfrak{a}_1}{\mathfrak{m}}\right)\right] \\
&= (1 - s\flat)(\Upsilon + \Psi)(\mathfrak{a}_2) + (1 - (s(1-\flat)))\,\mathfrak{m}(\Upsilon + \Psi)(\frac{\mathfrak{a}_1}{\mathfrak{m}}).
\end{aligned}$$

(ii) Let Υ be a generalized s−type $\mathfrak{m}$−convex function of Raina type w.r.t. $\mathcal{F}^{\sigma}_{\rho,\lambda}$, then for all $\mathfrak{a}_1, \mathfrak{a}_2 \in \mathbb{A}$, $s \in [0,1]$, $c \in \mathbb{R}(c \geq 0)$, $\mathfrak{m} \in (0,1]$ and $\flat \in [0,1]$, we have

$$\begin{aligned}
&(c\Upsilon)(\mathfrak{a}_2 + \flat\, \mathcal{F}^{\sigma}_{\rho,\lambda}(\mathfrak{a}_1 - \mathfrak{a}_2)) \\
&\leq c\left[(1 - s\flat)\,\Upsilon(\mathfrak{a}_2) + (1 - (s(1-\flat)))\,\mathfrak{m}\Upsilon\left(\frac{\mathfrak{a}_1}{\mathfrak{m}}\right)\right] \\
&= (1 - s\flat)\,c\Upsilon(\mathfrak{a}_2) + (1 - (s(1-\flat)))\,c\mathfrak{m}\Upsilon\left(\frac{\mathfrak{a}_1}{\mathfrak{m}}\right) \\
&= (1 - s\flat)(c\Upsilon)(\mathfrak{a}_2) + (1 - (s(1-\flat)))\,\mathfrak{m}\,(c\Upsilon)\left(\frac{\mathfrak{a}_1}{\mathfrak{m}}\right).
\end{aligned}$$

It is the required proof. ■

Theorem 3 *Let $\Upsilon : \mathbb{A} \to \mathbb{Y}$ be a generalized s−type $\mathfrak{m}$−convex function of Raina type w.r.t. $\mathcal{F}^{\sigma}_{\rho,\lambda}$ and $\Psi : \mathbb{Y} \to \mathbb{R}$ be a non-decreasing function. Then the function $\Psi \circ \Upsilon$ is a generalized s−type $\mathfrak{m}$−convex function of Raina type w.r.t. $\mathcal{F}^{\sigma}_{\rho,\lambda}$ for $s \in [0,1]$, $\mathfrak{m} \in (0,1]$ and $\flat \in [0,1]$.*

Proof For all $\mathfrak{a}_1, \mathfrak{a}_2 \in \mathbb{A}$, $s \in [0,1]$, $\mathfrak{m} \in (0,1]$ and $\flat \in [0,1]$, we have

$$\begin{aligned}
&(\Psi \circ \Upsilon)(\mathfrak{a}_2 + \flat\, \mathcal{F}^{\sigma}_{\rho,\lambda}(\mathfrak{a}_1 - \mathfrak{a}_2)) \\
&= \Psi(\Upsilon(\mathfrak{a}_2 + \flat\, \mathcal{F}^{\sigma}_{\rho,\lambda}(\mathfrak{a}_1 - \mathfrak{a}_2))) \\
&\leq \Psi\left[(1 - s\flat)\,\Upsilon(\mathfrak{a}_2) + (1 - (s(1-\flat)))\,\mathfrak{m}\Upsilon\left(\frac{\mathfrak{a}_1}{\mathfrak{m}}\right)\right] \\
&\leq (1 - s\flat)\,\Psi(\Upsilon(\mathfrak{a}_2)) + (1 - (s(1-\flat)))\,\mathfrak{m}\Psi(\mathfrak{m}\Upsilon\left(\frac{\mathfrak{a}_1}{\mathfrak{m}}\right)) \\
&= (1 - s\flat)(\Psi \circ \Upsilon)(\mathfrak{a}_2) + (1 - (s(1-\flat)))\,\mathfrak{m}^2(\Psi \circ \Upsilon)\left(\frac{\mathfrak{a}_1}{\mathfrak{m}}\right).
\end{aligned}$$

It is the required proof. ■

Remark 3 *(i) If $n = s = 1$ in Theorem 3, then*

$$(\Psi \circ \Upsilon)(\mathfrak{m}\mathfrak{a}_2 + \flat\eta(\mathfrak{a}_1, \mathfrak{a}_2, \mathfrak{m})) \leq (1-\flat)(\Psi \circ \Upsilon)(\mathfrak{a}_2) + \flat\mathfrak{m}^2(\Psi \circ \Upsilon)\left(\frac{\mathfrak{a}_1}{\mathfrak{m}}\right).$$

(i) If $s = \mathfrak{m} = 1$ in Theorem 3, then

$$(\Psi \circ \Upsilon)(\mathfrak{a}_2 + \flat\, \mathcal{F}^{\sigma}_{\rho,\lambda}(\mathfrak{a}_1 - \mathfrak{a}_2)) \leq (1-\flat)(\Psi \circ \Upsilon)(\mathfrak{a}_2) + \flat(\Psi \circ \Upsilon)(\mathfrak{a}_1).$$

(ii) If we put $\mathfrak{m} = 1$ and $\eta(\mathfrak{a}_1, \mathfrak{a}_2, \mathfrak{m}) = \mathfrak{a}_1 - \mathfrak{m}\mathfrak{a}_2$ in Theorem 3, then

$$(\Psi \circ \Upsilon)(\flat\mathfrak{a}_1 + (1-\flat)\mathfrak{a}_2) \leq (1 - s\flat)(\Psi \circ \Upsilon)(\mathfrak{a}_2) + (1 - (s(1-\flat))(\Psi \circ \Upsilon)(\mathfrak{a}_1).$$

Theorem 4 *Let $0 < \mathfrak{a}_1 < \mathfrak{a}_2$, $\Upsilon_j : \mathbb{A} = [\mathfrak{a}_1, \mathfrak{a}_2] \to [0, +\infty)$ be a class of generalized s−type $\mathfrak{m}$−convex functions of Raina type w.r.t. $\mathcal{F}^{\sigma}_{\rho,\lambda}$ and $\Upsilon(u) = \sup_j \Upsilon_j(u)$. Then Υ is a generalized s−type $\mathfrak{m}$−convex function of Raina type for $s \in [0,1]$, $\mathfrak{m} \in (0,1]$ and $\flat \in [0,1]$, and $U = \{\tau \in [\mathfrak{a}_1, \mathfrak{a}_2] : \Upsilon(\tau_i) < \infty\}$ is an interval.*

Proof Let $\mathfrak{a}_1, \mathfrak{a}_2 \in U$, $s \in [0,1]$, $\mathfrak{m} \in (0,1]$ and $\flat \in [0,1]$, then

$$\begin{aligned}
&\Upsilon(\mathfrak{a}_2 + \flat\, \mathcal{F}^{\sigma}_{\rho,\lambda}(\mathfrak{a}_1 - \mathfrak{a}_2)) \\
&= \sup_j \Upsilon_j(\mathfrak{a}_2 + \flat\, \mathcal{F}^{\sigma}_{\rho,\lambda}(\mathfrak{a}_1 - \mathfrak{a}_2)) \\
&\leq (1 - s\flat) \sup_j \Upsilon_j(\mathfrak{a}_2) + (1 - (s(1-\flat)))\, \mathfrak{m} \sup_j \Upsilon_j\left(\frac{\mathfrak{a}_1}{\mathfrak{m}}\right) \\
&= (1 - s\flat)\, \Upsilon(\mathfrak{a}_2) + (1 - (s(1-\flat)))\, \mathfrak{m}\Upsilon\left(\frac{\mathfrak{a}_1}{\mathfrak{m}}\right) < \infty.
\end{aligned}$$

This is the required proof. ■

Theorem 5 *If $\Upsilon_i : \mathbb{R}^n \to \mathbb{R}$ is a generalized s−type $\mathfrak{m}$−convex function of Raina type w.r.t. $\mathcal{F}^{\sigma}_{\rho,\lambda}$ for $s \in [0,1]$, $\mathfrak{m} \in (0,1]$ and $\flat \in [0,1]$, then the set $\mathbb{M} = \{\tau \in \mathbb{R} : \Upsilon_i(\tau) \leq 0, i = 1,2,3,\ldots,n\}$ is a generalized $\mathfrak{m}$−convex set.*

Proof Since $\Upsilon_i(\tau)$, $(i = 1,2,3,\ldots,n)$ are generalized s−type $\mathfrak{m}$−convex functions of Raina type for $s \in [0,1]$, $\mathfrak{m} \in (0,1]$ and $\flat \in [0,1]$, then for all $\mathfrak{a}_1, \mathfrak{a}_2 \in \mathbb{R}^n$

$$\Upsilon_i(\mathfrak{a}_2 + \flat\, \mathcal{F}^{\sigma}_{\rho,\lambda}(\mathfrak{a}_1 - \mathfrak{a}_2)) \leq (1 - s\flat)\, \Upsilon(\mathfrak{a}_2) + (1 - (s(1-\flat)))\, \mathfrak{m}\Upsilon\left(\frac{\mathfrak{a}_1}{\mathfrak{m}}\right),$$

holds, where $i = 1,2,3,\ldots,n$
When $\mathfrak{a}_1, \mathfrak{a}_2 \in \mathbb{M}$, we know $\Upsilon_i(\mathfrak{a}_1) \leq 0$ and $\Upsilon_i(\mathfrak{a}_2) \leq 0$, from the above inequality, it yields that

$$\Upsilon_i(\mathfrak{a}_2 + \flat\, \mathcal{F}^{\sigma}_{\rho,\lambda}(\mathfrak{a}_1 - \mathfrak{a}_2)) \leq 0, \quad i = 1,2,3,\ldots,n.$$

That is $\mathfrak{a}_2 + \flat\, \mathcal{F}^{\sigma}_{\rho,\lambda}(\mathfrak{a}_1 - \mathfrak{a}_2) \in \mathbb{M}$. Hence, $\mathbb{M}$ is a generalized $\mathfrak{m}$−convex set. ■

Theorem 6 *If $\Upsilon : \mathbb{A} \subseteq \mathbb{R}^n \to \mathbb{R}$ is a generalized s−type $\mathfrak{m}$−convex function of Raina type w.r.t. $\mathcal{F}^{\sigma}_{\rho,\lambda}$ for $s \in [0,1]$, $\mathfrak{m} \in (0,1]$ and $\flat \in [0,1]$, then the function Υ is also a generalized quasi $\mathfrak{m}$−convex function of Raina type on a generalized $\mathfrak{m}$−convex set of Raina type $\mathbb{A}$ w.r.t. $\mathcal{F}^{\sigma}_{\rho,\lambda}$.*

Proof Since Υ is a generalized s−type $\mathfrak{m}$−convex function of Raina type w.r.t. $\mathcal{F}^{\sigma}_{\rho,\lambda}$ for $s \in [0,1]$, $\mathfrak{m} \in (0,1]$ and $\flat \in [0,1]$, and we assume that $m\Upsilon(\frac{\mathfrak{a}_1}{\mathfrak{m}}) \leq \Upsilon(\mathfrak{a}_2)$, then for all $\mathfrak{a}_1, \mathfrak{a}_2 \in \mathbb{A}$, we have

$$\begin{aligned}
&\Upsilon(\mathfrak{a}_2 + \flat\, \mathcal{F}^{\sigma}_{\rho,\lambda}(\mathfrak{a}_1 - \mathfrak{a}_2)) \\
&\leq (1 - s\flat)\, \Upsilon(\mathfrak{a}_2) + (1 - (s(1-\flat)))\, \mathfrak{m}\Upsilon\left(\frac{\mathfrak{a}_1}{\mathfrak{m}}\right) \\
&\leq \left[(1 - (s(1-\flat))) + (1 - s\flat)\right] \Upsilon(\mathfrak{a}_2) \\
&\leq \Upsilon(\mathfrak{a}_2).
\end{aligned}$$

In the same manner, let $\Upsilon(\mathfrak{a}_2) \leq \mathfrak{m}\Upsilon(\frac{\mathfrak{a}_1}{\mathfrak{m}})$, for all $\mathfrak{a}_1, \mathfrak{a}_2 \in \mathbb{A}$. We can also get

$$\Upsilon(\mathfrak{a}_2 + \flat\, \mathcal{F}^{\sigma}_{\rho,\lambda}(\mathfrak{a}_1 - \mathfrak{a}_2)) \leq \mathfrak{m}\Upsilon\left(\frac{\mathfrak{a}_1}{\mathfrak{m}}\right).$$

Consequently,

$$\Upsilon(\mathfrak{a}_2 + \flat\, \mathcal{F}^{\sigma}_{\rho,\lambda}(\mathfrak{a}_1 - \mathfrak{a}_2)) \leq \max\{\Upsilon(\mathfrak{a}_1), \Upsilon(\mathfrak{a}_2)\}.$$

That is, $\Upsilon : \mathbb{A} \subseteq \mathbb{R}^n \to \mathbb{R}$ is a generalized quasi $\mathfrak{m}$−convex function of Raina type on a generalized $\mathfrak{m}$−convex set of Raina type $\mathbb{A}$ w.r.t. $\mathcal{F}^{\sigma}_{\rho,\lambda}$. ■

Theorem 7 *If $\Upsilon : \mathbb{R}_\circ \to \mathbb{R}_\circ$ is a generalized s−type $\mathfrak{m}$−convex function of Raina type w.r.t. $\mathcal{F}^{\sigma}_{\rho,\lambda} : \mathbb{R}_\circ \times \mathbb{R}_\circ \times (0,1] \to \mathbb{R}_\circ$ for $s \in [0,1]$, $\mathfrak{m} \in (0,1]$ and $\flat \in [0,1]$. Assume that Υ is monotone decreasing, $\mathcal{F}^{\sigma}_{\rho,\lambda}$ is monotone increasing regarding $\mathfrak{m}$ for fixed $\mathfrak{a}_1, \mathfrak{a}_2 \in \mathbb{R}_\circ$ and $\mathfrak{m}_1 \leq \mathfrak{m}_2$ $(\mathfrak{m}_1, \mathfrak{m}_2 \in (0,1])$. If Υ is an s−type $\mathfrak{m}_1$−preinvex function on $\mathbb{R}_\circ$ w.r.t. $\mathcal{F}^{\sigma}_{\rho,\lambda}$, then Υ is an s−type $\mathfrak{m}_2$−preinvex function on $\mathbb{R}_\circ$ w.r.t. $\mathcal{F}^{\sigma}_{\rho,\lambda}$.*

Proof Since Υ is a generalized s−type m_1−convex function of Raina type, for all $\mathfrak{a}_1, \mathfrak{a}_2 \in \mathbb{R}_\circ$

$$\Upsilon(\mathfrak{a}_2 + \flat\, \mathcal{F}^{\sigma}_{\rho,\lambda}(\mathfrak{a}_1 - \mathfrak{a}_2)) \leq (1 - s\flat)\, \Upsilon(\mathfrak{a}_2) + (1 - (s(1-\flat)))\, \mathfrak{m}_1\Upsilon\left(\frac{\mathfrak{a}_1}{\mathfrak{m}_1}\right).$$

Combining the monotone decreasing of the function Υ with the monotone increasing of the mapping $\mathcal{F}^{\sigma}_{\rho,\lambda}$ regarding $\mathfrak{m}$ for fixed $\mathfrak{a}_1, \mathfrak{a}_2 \in \mathbb{R}_\circ$ and $m_1 \leq m_2$, it follows that

$$\begin{aligned}
&(1 - s\flat)\, \Upsilon(\mathfrak{a}_2) + (1 - (s(1-\flat)))\, \mathfrak{m}_1\Upsilon\left(\frac{\mathfrak{a}_1}{\mathfrak{m}_1}\right) \\
&\leq (1 - s\flat)\, \Upsilon(\mathfrak{a}_2) + (1 - (s(1-\flat)))\, \mathfrak{m}_2\Upsilon\left(\frac{\mathfrak{a}_1}{\mathfrak{m}_2}\right).
\end{aligned}$$

Finally, we have

$$\Upsilon(a_2 + \flat\, \mathcal{F}^{\sigma}_{\rho,\lambda}(a_1 - a_2)) \leq (1 - s\flat)\,\Upsilon(a_2) + (1 - (s(1 - \flat)))\, m_2 \Upsilon\left(\frac{a_1}{m_2}\right).$$

Hence, Υ is a generalized s−type m_2−convex function of Raina type on $\mathbb{R}_\circ$ w.r.t. η for fixed $s \in [0, 1]$ and $m \in [0, 1]$, which ends the proof. ■

Theorem 8 *Let $\Upsilon, \Psi : \mathbb{A} = [a_1, a_2] \to \mathbb{R}$. If Υ, Ψ are two generalized s−type m−convex functions of Raina type w.r.t. $\mathcal{F}^{\sigma}_{\rho,\lambda}$ and Υ, Ψ are similarly ordered functions and $[1 - (s(1 - \flat))] + [1 - s\flat] \leq 1$, then the product $\Upsilon\Psi$ is a generalized s−type m−convex function of Raina type w.r.t. $\mathcal{F}^{\sigma}_{\rho,\lambda}$ for $s \in [0, 1]$, $m \in (0, 1]$ and $\flat \in [0, 1]$.*

Proof Let Υ, Ψ be a generalized s−type m−convex function of Raina type w.r.t. same $\mathcal{F}^{\sigma}_{\rho,\lambda}$, $s \in [0, 1]$, $m \in (0, 1]$ and $\flat \in [0, 1]$, then

$$\begin{aligned}
&\Upsilon(a_2 + \flat\, \mathcal{F}^{\sigma}_{\rho,\lambda}(a_1 - a_2))\Psi(a_2 + \flat\, \mathcal{F}^{\sigma}_{\rho,\lambda}(a_1 - a_2)) \\
&\leq \left[(1 - s\flat)\,\Upsilon(a_2) + (1 - (s(1 - \flat)))\, m\Upsilon\left(\frac{a_1}{m}\right)\right] \\
&\times \left[(1 - s\flat)\,\Psi(a_2) + (1 - (s(1 - \flat)))\, m\Psi\left(\frac{a_1}{m}\right)\right] \\
&\leq (1 - s\flat)^2\, \Upsilon(a_2)\Psi(a_2) + (1 - (s(1 - \flat)))^2\, m^2\Upsilon(\frac{a_1}{m})\Psi(\frac{a_1}{m}) \\
&+ \frac{1}{n^2}\,(1 - (s(1 - \flat)))\,(1 - s\flat)\,[m\Upsilon(\frac{a_1}{m})\Psi(a_2) + \Upsilon(a_2)m\Psi(\frac{a_1}{m})] \\
&\leq (1 - s\flat)^2\, \Upsilon(a_2)\Psi(a_2) + [1 - (s(1 - \flat))]^2 m^2\Upsilon(\frac{a_1}{m})\Psi(\frac{a_1}{m}) \\
&+ (1 - (s(1 - \flat)))\,(1 - (s\flat))\,[m^2\Upsilon(\frac{a_1}{m})\Psi(\frac{a_1}{m}) + \Upsilon(a_2)\Psi(a_2)] \\
&= \left[(1 - s\flat)\,\Upsilon(a_2)\Psi(a_2) + (1 - (s(1 - \flat)))m^2\Upsilon(\frac{a_1}{m})\Psi(\frac{a_1}{m})\right] \\
&\times \left((1 - (s(1 - \flat))) + (1 - s\flat)\right) \\
&\leq (1 - s\flat)\,\Upsilon(a_2)\Psi(a_2) + (1 - (s(1 - \flat)))\, m^2\Upsilon(\frac{a_1}{m})\Psi(\frac{a_1}{m}).
\end{aligned}$$

This completes the proof. ■

Remark 4 *Taking $m = 1$ and $\mathcal{F}^{\sigma}_{\rho,\lambda}(a_1, a_2, m) = a_1 - ma_2$ in Theorem 8, then*

$$\Upsilon(\flat a_1 + (1 - \flat)a_2)\Psi(\flat a_1 + (1 - \flat)a_2) \leq [1 - (s(1 - \flat))]\Upsilon(a_1)\,\Psi(a_1) + [1 - s\flat]\Upsilon(a_2)\,\Psi(a_2).$$

4 Hermite–Hadamard type inequality via a generalized convex function of Raina type

The principal intention of this section is to establish a novel version of Hermite–Hadamard type inequality in the mode of the newly discussed concept.

Theorem 9 *Let $\Upsilon : [a_1, a_2] \in \mathbb{R}$ be a generalized s−type m−convex function of Raina type, if $a_1 < a_2$ and $\Upsilon \in L[a_1, a_2]$, then the following Hermite–Hadamard type inequalities hold:*

$$\begin{aligned}
\Upsilon(a_2 + \frac{1}{2}\, \mathcal{F}^{\sigma}_{\rho,\lambda}(a_1 - a_2)) &\leq \frac{(1 - \frac{s}{2})}{\mathcal{F}^{\sigma}_{\rho,\lambda}(a_1 - a_2)}\left[\int_{a_2}^{a_2 + \mathcal{F}^{\sigma}_{\rho,\lambda}(a_1 - a_2)} m\Upsilon(\frac{x}{m})dx + \int_{\frac{ma_2 + \mathcal{F}^{\sigma}_{\rho,\lambda}(a_1 - ma_2)}{m}}^{a_2} \Upsilon(x)dx\right] \\
&\leq (2 - s)\big[\Upsilon(a_2) + m\Upsilon(\frac{a_1}{m})\big].
\end{aligned}$$

Proof Since $a_1, a_2 \in \mathbb{X}^\circ$ and $\mathbb{X}^\circ$ is a generalized convex set with respect to $\mathcal{F}^{\sigma}_{\rho,\lambda}$ for every $m \in (0, 1]$ and $\flat \in [0, 1]$, we have $a_2 + \flat\, \mathcal{F}^{\sigma}_{\rho,\lambda}(a_1 - a_2) \in \mathbb{X}^\circ$. For the first inequality, using the Definition of generalized s-type m-convex function of Raina type, and condition C for $\mathcal{F}^{\sigma}_{\rho,\lambda}$ and integrating over $[0, 1]$,

$$\begin{aligned}
\Upsilon(y + \flat\, \mathcal{F}^{\sigma}_{\rho,\lambda}(x - y)) &\leq (1 - (s\flat))\Upsilon(y) + (1 - (s(1 - \flat)))m\Upsilon(\frac{x}{m}) \\
\Upsilon(y + \frac{1}{2}\, \mathcal{F}^{\sigma}_{\rho,\lambda}(x - y)) &\leq \left(1 - \frac{s}{2}\right)\left[m\Upsilon(\frac{x}{m}) + \Upsilon(y)\right].
\end{aligned}$$

Put $x = a_2 + \flat\, \mathcal{F}^{\sigma}_{\rho,\lambda}(a_1 - a_2)$ and $my = ma_2 + (1 - \flat)\, \mathcal{F}^{\sigma}_{\rho,\lambda}(a_1 - ma_2)$ in above inequality, the L.H.S of above inequality becomes

$$\Upsilon(y + \frac{1}{2}\, \mathcal{F}^{\sigma}_{\rho,\lambda}(x - y)) = \Upsilon(a_2 + \frac{1}{2}\, \mathcal{F}^{\sigma}_{\rho,\lambda}(a_1 - a_2)).$$

Now,

$$\begin{aligned}&\Upsilon(\mathfrak{a}_2+\frac{1}{2}\mathcal{F}^{\sigma}_{\rho,\lambda}(\mathfrak{a}_1-\mathfrak{a}_2))\\&\le\left(1-\frac{s}{2}\right)\left[\int_0^1 m\Upsilon(\frac{\mathfrak{a}_2+\flat\mathcal{F}^{\sigma}_{\rho,\lambda}(\mathfrak{a}_1-\mathfrak{a}_2)}{m})d\flat+\int_0^1\Upsilon(\mathfrak{a}_2+\frac{(1-\flat)}{m}\mathcal{F}^{\sigma}_{\rho,\lambda}(\mathfrak{a}_1-m\mathfrak{a}_2))d\flat\right]\\&\le\left(1-\frac{s}{2}\right)\frac{1}{\mathcal{F}^{\sigma}_{\rho,\lambda}(\mathfrak{a}_1-\mathfrak{a}_2)}\left[\int_{\mathfrak{a}_2}^{\mathfrak{a}_2+\mathcal{F}^{\sigma}_{\rho,\lambda}(\mathfrak{a}_1-\mathfrak{a}_2)}m\Upsilon(\frac{x}{m})dx+\int_{\frac{m\mathfrak{a}_2+\mathcal{F}^{\sigma}_{\rho,\lambda}(\mathfrak{a}_1-m\mathfrak{a}_2)}{m}}^{\mathfrak{a}_2}\Upsilon(x)dx\right].\end{aligned}$$

For the proof of the second inequality, using the definition of generalized s–type m convex function, as a result we attain

$$\begin{aligned}&\frac{1}{\mathcal{F}^{\sigma}_{\rho,\lambda}(\mathfrak{a}_1-\mathfrak{a}_2)}\left[\int_{\mathfrak{a}_2}^{\mathfrak{a}_2+\mathcal{F}^{\sigma}_{\rho,\lambda}(\mathfrak{a}_1-\mathfrak{a}_2)}m\Upsilon(\frac{x}{m})dx+\int_{\frac{m\mathfrak{a}_2+\mathcal{F}^{\sigma}_{\rho,\lambda}(\mathfrak{a}_1-m\mathfrak{a}_2)}{m}}^{\mathfrak{a}_2}\Upsilon(x)dx\right]\\&\le\left[\int_0^1\Upsilon(\mathfrak{a}_2+\flat\mathcal{F}^{\sigma}_{\rho,\lambda}(\mathfrak{a}_1-\mathfrak{a}_2))d\flat+\int_0^1\Upsilon(\mathfrak{a}_2+\frac{(1-\flat)}{m}\mathcal{F}^{\sigma}_{\rho,\lambda}(\mathfrak{a}_1-m\mathfrak{a}_2))d\flat\right]\\&\le\int_0^1(1-(s\flat))\Upsilon(\mathfrak{a}_2)d\flat+\int_0^1(1-(s(1-\flat)))m\Upsilon(\frac{\mathfrak{a}_1}{m})d\flat\\&+\int_0^1(1-(s(1-\flat)))\Upsilon(\mathfrak{a}_2)d\flat+\int_0^1(1-s\flat)m\Upsilon(\frac{\mathfrak{a}_1}{m})d\flat\\&\le\left(\frac{2-s}{2}\right)[\Upsilon(\mathfrak{a}_2)+\Upsilon(\mathfrak{a}_2)+m\Upsilon(\frac{\mathfrak{a}_1}{m})+m\Upsilon(\frac{\mathfrak{a}_1}{m})]\\&\le(2-s)[\Upsilon(\mathfrak{a}_2)+m\Upsilon(\frac{\mathfrak{a}_1}{m})].\end{aligned}$$

This completes the proof. ■

Corollary 1 *If $s=m=1$ and $\mathcal{F}^{\sigma}_{\rho,\lambda}(\mathfrak{a}_1-\mathfrak{a}_2)=\mathfrak{a}_1-\mathfrak{a}_2$ in Theorem 9, then as a result, we attain the classical Hermite-Hadamard type inequality in [12].*

5 Estimations of Hermite–Hadamard type inequality

The subjective aim of this section is to derive the estimations of (H–H) type inequality for a generalized s–type m–convex function of Raina type.

Lemma 2 *Let $X\subseteq\mathbb{R}$ be a generalized convex subset w.r.t. $\mathcal{F}^{\sigma}_{\rho,\lambda}:X\times X\to\mathbb{R}$ and $\mathfrak{a}_1,\mathfrak{a}_2\in X$ with $\mathcal{F}^{\sigma}_{\rho,\lambda}(\mathfrak{a}_1-\mathfrak{a}_2)\neq 0$. Suppose that $\Upsilon:X\to\mathbb{R}$ is a differentiable function. If Υ is integrable on the $\mathcal{F}^{\sigma}_{\rho,\lambda}$, then the following equality holds:*

$$\begin{aligned}&-\frac{\Upsilon(\mathfrak{a}_2)+\Upsilon(\mathfrak{a}_2+\mathcal{F}^{\sigma}_{\rho,\lambda}(\mathfrak{a}_1-\mathfrak{a}_2))}{2}+\frac{1}{\mathcal{F}^{\sigma}_{\rho,\lambda}(\mathfrak{a}_1-\mathfrak{a}_2)}\int_{\mathfrak{a}_2}^{\mathfrak{a}_2+\mathcal{F}^{\sigma}_{\rho,\lambda}(\mathfrak{a}_1-\mathfrak{a}_2)}\Upsilon(x)dx\\&=\frac{\mathcal{F}^{\sigma}_{\rho,\lambda}(\mathfrak{a}_1-\mathfrak{a}_2)}{2}\int_0^1(1-2\flat)\Upsilon'(\mathfrak{a}_2+\flat\mathcal{F}^{\sigma}_{\rho,\lambda}(\mathfrak{a}_1-\mathfrak{a}_2))d\flat.\end{aligned}$$

Proof Suppose that $\mathfrak{a}_1,\mathfrak{a}_2\in X$. Since X is a generalized convex set w.r.t. $\mathcal{F}^{\sigma}_{\rho,\lambda}$, for every $\flat\in[0,1]$, we have $\mathfrak{a}_2+\flat\mathcal{F}^{\sigma}_{\rho,\lambda}(\mathfrak{a}_1-\mathfrak{a}_2)\in X$. Integrating by parts

$$\begin{aligned}&\int_0^1(1-2\flat)\Upsilon'(\mathfrak{a}_2+\flat\mathcal{F}^{\sigma}_{\rho,\lambda}(\mathfrak{a}_1-\mathfrak{a}_2))d\flat\\&=\left[\frac{(1-2\flat)\Upsilon(\mathfrak{a}_2+\flat\mathcal{F}^{\sigma}_{\rho,\lambda}(\mathfrak{a}_1-\mathfrak{a}_2))}{\mathcal{F}^{\sigma}_{\rho,\lambda}(\mathfrak{a}_1-\mathfrak{a}_2)}\right]_0^1+\frac{2}{\mathcal{F}^{\sigma}_{\rho,\lambda}(\mathfrak{a}_1-\mathfrak{a}_2)}\int_0^1\Upsilon(\mathfrak{a}_2+\flat\mathcal{F}^{\sigma}_{\rho,\lambda}(\mathfrak{a}_1-\mathfrak{a}_2))d\flat\\&=-\frac{\Upsilon(\mathfrak{a}_2)+\Upsilon(\mathfrak{a}_2+\mathcal{F}^{\sigma}_{\rho,\lambda}(\mathfrak{a}_1-\mathfrak{a}_2))}{2}+\frac{1}{\mathcal{F}^{\sigma}_{\rho,\lambda}(\mathfrak{a}_1-\mathfrak{a}_2)}\int_{\mathfrak{a}_2}^{\mathfrak{a}_2+\mathcal{F}^{\sigma}_{\rho,\lambda}(\mathfrak{a}_1-\mathfrak{a}_2)}\Upsilon(x)dx.\end{aligned}$$

This completes the proof. ■

Theorem 10 *Suppose I° is a generalized convex set w.r.t. $\mathcal{F}^{\sigma}_{\rho,\lambda}$ and $\Upsilon:I^{\circ}\subseteq\mathbb{R}\to\mathbb{R}$ is a differentiable mapping on I°, $\mathfrak{a}_1,\mathfrak{a}_2\in I^{\circ}$ with $\mathfrak{a}_1<\mathfrak{a}_2$ and suppose that $\Upsilon'\in L[\mathfrak{a}_1,\mathfrak{a}_2]$. If $|\Upsilon'|$ is a generalized s–type m–convex function of Raina type on $L[\mathfrak{a}_1,\mathfrak{a}_2]$ for $\flat\in[0,1]$, $m\in(0,1]$ and $s\in[0,1]$, then*

$$\begin{aligned}&\left|\frac{\Upsilon(\mathfrak{a}_2)+\Upsilon(\mathfrak{a}_2+\mathcal{F}^{\sigma}_{\rho,\lambda}(\mathfrak{a}_1-\mathfrak{a}_2))}{2}-\frac{1}{\mathcal{F}^{\sigma}_{\rho,\lambda}(\mathfrak{a}_1-\mathfrak{a}_2)}\int_{\mathfrak{a}_2}^{\mathfrak{a}_2+\mathcal{F}^{\sigma}_{\rho,\lambda}(\mathfrak{a}_1-\mathfrak{a}_2)}\Upsilon(x)dx\right|\\&\le|\mathcal{F}^{\sigma}_{\rho,\lambda}(\mathfrak{a}_1-\mathfrak{a}_2)|\left(\frac{2-s}{4}\right)A\left(m|\Upsilon'(\frac{\mathfrak{a}_1}{m})|,|\Upsilon'(\mathfrak{a}_2)|\right),\end{aligned}$$

where A is the arithmetic mean.

Proof Assume that $\mathfrak{a}_1, \mathfrak{a}_2 \in I^\circ$. Since I° is a generalized convex set w.r.t. $\mathcal{F}^{\sigma}_{\rho,\lambda}$, for any $\flat \in [0,1]$, we have $\mathfrak{a}_2 + \flat\, \mathcal{F}^{\sigma}_{\rho,\lambda}(\mathfrak{a}_1 - \mathfrak{a}_2) \in I^\circ$. Using Lemma 2, generalized s−type $\mathfrak{m}$−convex function of Raina type of $|\Upsilon'|$ and properties of modulus, we have

$$\begin{aligned}
&\left|\frac{\Upsilon(\mathfrak{a}_2) + \Upsilon(\mathfrak{a}_2 + \mathcal{F}^{\sigma}_{\rho,\lambda}(\mathfrak{a}_1 - \mathfrak{a}_2))}{2} - \frac{1}{\mathcal{F}^{\sigma}_{\rho,\lambda}(\mathfrak{a}_1 - \mathfrak{a}_2)} \int_{\mathfrak{a}_2}^{\mathfrak{a}_2 + \mathcal{F}^{\sigma}_{\rho,\lambda}(\mathfrak{a}_1 - \mathfrak{a}_2)} \Upsilon(x)dx\right| \\
&\leq \left|\frac{\mathcal{F}^{\sigma}_{\rho,\lambda}(\mathfrak{a}_1 - \mathfrak{a}_2)}{2} \int_0^1 (1-2\flat)\Upsilon'(\mathfrak{a}_2 + \flat\, \mathcal{F}^{\sigma}_{\rho,\lambda}(\mathfrak{a}_1 - \mathfrak{a}_2))d\flat\right| \\
&\leq \frac{|\mathcal{F}^{\sigma}_{\rho,\lambda}(\mathfrak{a}_1 - \mathfrak{a}_2)|}{2} \int_0^1 |1-2\flat| \Big((1-(s\flat))|\Upsilon'(\mathfrak{a}_2)| + (1-(s(1-\flat)))\mathfrak{m}|\Upsilon'(\tfrac{\mathfrak{a}_1}{\mathfrak{m}})|\Big) d\flat \\
&\leq \frac{|\mathcal{F}^{\sigma}_{\rho,\lambda}(\mathfrak{a}_1 - \mathfrak{a}_2)|}{2} \Big(|\Upsilon'(\mathfrak{a}_2)| \int_0^1 |1-2\flat|(1-(s\flat))d\flat + \mathfrak{m}|\Upsilon'(\tfrac{\mathfrak{a}_1}{\mathfrak{m}})| \int_0^1 |1-2\flat|(1-(s(1-\flat)))d\flat\Big) \\
&\leq \frac{|\mathcal{F}^{\sigma}_{\rho,\lambda}(\mathfrak{a}_1 - \mathfrak{a}_2)|}{2} \Big(|\Upsilon'(\mathfrak{a}_2)|\Big(\frac{2-s}{4}\Big) + |\mathfrak{m}\Upsilon'(\tfrac{\mathfrak{a}_1}{\mathfrak{m}})|\Big(\frac{2-s}{4}\Big)\Big) \\
&\leq |\mathcal{F}^{\sigma}_{\rho,\lambda}(\mathfrak{a}_1 - \mathfrak{a}_2)| \Big(\frac{2-s}{4}\Big) A\Big(\mathfrak{m}|\Upsilon'(\tfrac{\mathfrak{a}_1}{\mathfrak{m}})|, |\Upsilon'(\mathfrak{a}_2)|\Big).
\end{aligned}$$

This is the required proof. ■

Corollary 2 *If we put $\mathfrak{m} = 1$ and $s = 1$ in Theorem 10, then we obtain Theorem (2.1) in [17].*

Corollary 3 *If we put $s = \mathfrak{m} = 1$ and $\mathcal{F}^{\sigma}_{\rho,\lambda}(\mathfrak{a}_1 - \mathfrak{a}_2) = \mathfrak{a}_1 - \mathfrak{a}_2$ in Theorem 10, we get inequality (4.1) in [18].*

Theorem 11 *Suppose I° is a generalized convex set w.r.t. $\mathcal{F}^{\sigma}_{\rho,\lambda}$ and $\Upsilon : I^\circ \subseteq \mathbb{R} \to \mathbb{R}$ be a differentiable mapping on I°, $\mathfrak{a}_1, \mathfrak{a}_2 \in I^\circ$ with $\mathfrak{a}_1 < \mathfrak{a}_2, q > 1, \frac{1}{p} + \frac{1}{q} = 1$ and suppose that $\Upsilon' \in L[\mathfrak{a}_1, \mathfrak{a}_2]$. If $|\Upsilon'|^q$ is a generalized s−type $\mathfrak{m}$−convex function of Raina type on $L[\mathfrak{a}_1, \mathfrak{a}_2]$ for $\flat \in [0,1]$, $\mathfrak{m} \in (0,1]$ and $s \in [0,1]$, then*

$$\begin{aligned}
&\left|\frac{\Upsilon(\mathfrak{a}_2) + \Upsilon(\mathfrak{a}_2 + \mathcal{F}^{\sigma}_{\rho,\lambda}(\mathfrak{a}_1 - \mathfrak{a}_2))}{2} - \frac{1}{\mathcal{F}^{\sigma}_{\rho,\lambda}(\mathfrak{a}_1 - \mathfrak{a}_2)} \int_{\mathfrak{a}_2}^{\mathfrak{a}_2 + \mathcal{F}^{\sigma}_{\rho,\lambda}(\mathfrak{a}_1 - \mathfrak{a}_2)} \Upsilon(x)dx\right| \\
&\leq \frac{|\mathcal{F}^{\sigma}_{\rho,\lambda}(\mathfrak{a}_1 - \mathfrak{a}_2)|}{2} \Big(\frac{1}{p+1}\Big)^{\frac{1}{p}} \Big(\frac{2-s}{2}\Big)^{\frac{1}{q}} A^{\frac{1}{q}}\Big(\mathfrak{m}|\Upsilon'(\tfrac{\mathfrak{a}_1}{\mathfrak{m}})|^q, |\Upsilon'(\mathfrak{a}_2)|^q\Big),
\end{aligned}$$

where A is the arithmetic mean.

Proof Assume that $\mathfrak{a}_1, \mathfrak{a}_2 \in I^\circ$. Since I° is a generalized convex set w.r.t. $\mathcal{F}^{\sigma}_{\rho,\lambda}$, for any $\flat \in [0,1]$, we have $\mathfrak{a}_2 + \flat\, \mathcal{F}^{\sigma}_{\rho,\lambda}(\mathfrak{a}_1 - \mathfrak{a}_2) \in I^\circ$. Using Lemma 2, Hölder's integral inequality and generalized s−type $\mathfrak{m}$−convex function of Raina type of $|\Upsilon'|^q$ and properties of modulus, we have

$$\begin{aligned}
&\left|\frac{\Upsilon(\mathfrak{a}_2) + \Upsilon(\mathfrak{a}_2 + \mathcal{F}^{\sigma}_{\rho,\lambda}(\mathfrak{a}_1 - \mathfrak{a}_2))}{2} - \frac{1}{\mathcal{F}^{\sigma}_{\rho,\lambda}(\mathfrak{a}_1 - \mathfrak{a}_2)} \int_{\mathfrak{a}_2}^{\mathfrak{a}_2 + \mathcal{F}^{\sigma}_{\rho,\lambda}(\mathfrak{a}_1 - \mathfrak{a}_2)} \Upsilon(x)dx\right| \\
&\leq \left|\frac{\mathcal{F}^{\sigma}_{\rho,\lambda}(\mathfrak{a}_1 - \mathfrak{a}_2)}{2} \int_0^1 (1-2\flat)\Upsilon'(\mathfrak{a}_2 + \flat\, \mathcal{F}^{\sigma}_{\rho,\lambda}(\mathfrak{a}_1 - \mathfrak{a}_2))d\flat\right| \\
&\leq \frac{|\mathcal{F}^{\sigma}_{\rho,\lambda}(\mathfrak{a}_1 - \mathfrak{a}_2)|}{2} \Big(\int_0^1 |1-2\flat|^p\Big)^{\frac{1}{p}} \Big(\int_0^1 |\Upsilon'(\mathfrak{a}_2 + \flat\, \mathcal{F}^{\sigma}_{\rho,\lambda}(\mathfrak{a}_1 - \mathfrak{a}_2))|^q d\flat\Big)^{\frac{1}{q}} \\
&\leq \frac{|\mathcal{F}^{\sigma}_{\rho,\lambda}(\mathfrak{a}_1 - \mathfrak{a}_2)|}{2} \Big(\frac{1}{p+1}\Big)^{\frac{1}{p}} \Big(|\Upsilon'(\mathfrak{a}_2)|^q \int_0^1 (1-(s\flat))d\flat + \int_0^1 \mathfrak{m}|\Upsilon'(\tfrac{\mathfrak{a}_1}{\mathfrak{m}})|^q(1-(s(1-\flat)))d\flat\Big)^{\frac{1}{q}} \\
&\leq \frac{|\mathcal{F}^{\sigma}_{\rho,\lambda}(\mathfrak{a}_1 - \mathfrak{a}_2)|}{2} \Big(\frac{1}{p+1}\Big)^{\frac{1}{p}} \Big(\frac{2-s}{2}\Big)^{\frac{1}{q}} A^{\frac{1}{q}}\Big(\mathfrak{m}|\Upsilon'(\tfrac{\mathfrak{a}_1}{\mathfrak{m}})|^q, |\Upsilon'(\mathfrak{a}_2)|^q\Big),
\end{aligned}$$

which is the required proof. ■

Corollary 4 *If $\mathfrak{m} = 1$ and $s = 1$ in Theorem 11, then we attain Theorem (2.2) in [17]*

Corollary 5 *If we put $\mathfrak{m} = s = 1$ and $\mathcal{F}^{\sigma}_{\rho,\lambda}(\mathfrak{a}_1 - \mathfrak{a}_2) = \mathfrak{a}_1 - \mathfrak{a}_2$ in Theorem 11, then we get inequality (4.2) [18]*

Theorem 12 *Suppose I° is a generalized convex set w.r.t. $\mathcal{F}^{\sigma}_{\rho,\lambda}$ and $\Upsilon : I^\circ \subseteq \mathbb{R} \to \mathbb{R}$ is a differentiable mapping on I°, $\mathfrak{a}_1, \mathfrak{a}_2 \in I^\circ$ with $\mathfrak{a}_1 < \mathfrak{a}_2, q \geq 1$, and suppose that $\Upsilon' \in L[\mathfrak{a}_1, \mathfrak{a}_2]$. If $|\Upsilon'|^q$ is a generalized s−type $\mathfrak{m}$−convex function of Raina type on $L[\mathfrak{a}_1, \mathfrak{a}_2]$ for for $\flat \in [0,1]$, $\mathfrak{m} \in (0,1]$ and $s \in [0,1]$, then*

$$\begin{aligned}
&\left|\frac{\Upsilon(\mathfrak{a}_2) + \Upsilon(\mathfrak{a}_2 + \mathcal{F}^{\sigma}_{\rho,\lambda}(\mathfrak{a}_1 - \mathfrak{a}_2))}{2} - \frac{1}{\mathcal{F}^{\sigma}_{\rho,\lambda}(\mathfrak{a}_1 - \mathfrak{a}_2)} \int_{\mathfrak{a}_2}^{\mathfrak{a}_2 + \mathcal{F}^{\sigma}_{\rho,\lambda}(\mathfrak{a}_1 - \mathfrak{a}_2)} \Upsilon(x)dx\right| \\
&\leq \frac{|\mathcal{F}^{\sigma}_{\rho,\lambda}(\mathfrak{a}_1 - \mathfrak{a}_2)|}{2} \Big(\frac{1}{2}\Big)^{1-\frac{2}{q}} \Big(\frac{2-s}{4}\Big)^{\frac{1}{q}} A^{\frac{1}{q}}\Big(\mathfrak{m}|\Upsilon'(\tfrac{\mathfrak{a}_1}{\mathfrak{m}})|^q, |\Upsilon'(\mathfrak{a}_2)|^q\Big),
\end{aligned}$$

where A is the arithmetic mean.

Proof Assume that $\mathfrak{a}_1, \mathfrak{a}_2 \in I^\circ$. Since I° is a generalized convex set w.r.t. $\mathcal{F}^{\sigma}_{\rho,\lambda}$, for any $\flat \in [0,1]$, we have $\mathfrak{a}_2 + \flat\, \mathcal{F}^{\sigma}_{\rho,\lambda}(\mathfrak{a}_1 - \mathfrak{a}_2) \in I^\circ$. Suppose that $q > 1$. Using Lemma 2, power-mean inequality and generalized s-type $\mathfrak{m}$-convex function of Raina type of $|\Upsilon'|^q$ and properties of modulus, we have

$$\begin{aligned}
&\left|\frac{\Upsilon(\mathfrak{a}_2) + \Upsilon(\mathfrak{a}_2 + \mathcal{F}^{\sigma}_{\rho,\lambda}(\mathfrak{a}_1 - \mathfrak{a}_2))}{2} - \frac{1}{\mathcal{F}^{\sigma}_{\rho,\lambda}(\mathfrak{a}_1 - \mathfrak{a}_2)}\int_{\mathfrak{a}_2}^{\mathfrak{a}_2 + \mathcal{F}^{\sigma}_{\rho,\lambda}(\mathfrak{a}_1 - \mathfrak{a}_2)} \Upsilon(x)dx\right| \\
&\leq \left|\frac{\mathcal{F}^{\sigma}_{\rho,\lambda}(\mathfrak{a}_1 - \mathfrak{a}_2)}{2}\int_0^1 (1-2\flat)\Upsilon'(\mathfrak{a}_2 + \flat\, \mathcal{F}^{\sigma}_{\rho,\lambda}(\mathfrak{a}_1 - \mathfrak{a}_2))d\flat\right| \\
&\leq \frac{|\mathcal{F}^{\sigma}_{\rho,\lambda}(\mathfrak{a}_1 - \mathfrak{a}_2)|}{2}\left(\int_0^1 |1-2\flat|d\flat\right)^{1-\frac{1}{q}}\left(\int_0^1 |1-2\flat||\Upsilon'(\mathfrak{a}_2 + \flat\, \mathcal{F}^{\sigma}_{\rho,\lambda}(\mathfrak{a}_1 - \mathfrak{a}_2))|^q d\flat\right)^{\frac{1}{q}} \\
&\leq \frac{|\mathcal{F}^{\sigma}_{\rho,\lambda}(\mathfrak{a}_1 - \mathfrak{a}_2)|}{2}\left(\frac{1}{2}\right)^{1-\frac{1}{q}}\left(\int_0^1 |1-2\flat|\left[(1-(s\flat))|\Upsilon'(\mathfrak{a}_2)|^q + (1-(s(1-\flat)))|\Upsilon'(\mathfrak{a}_1)|^q\right]d\flat\right)^{\frac{1}{q}} \\
&\leq \frac{|\mathcal{F}^{\sigma}_{\rho,\lambda}(\mathfrak{a}_1 - \mathfrak{a}_2)|}{2}\left(\frac{1}{2}\right)^{1-\frac{1}{q}} \\
&\times \left(|\Upsilon'(\mathfrak{a}_2)|^q\int_0^1 |1-2\flat|(1-(s\flat))d\flat + \int_0^1 |1-2\flat|\mathfrak{m}|\Upsilon'(\frac{\mathfrak{a}_1}{\mathfrak{m}})|^q(1-(s(1-\flat)))d\flat\right)^{\frac{1}{q}} \\
&= \frac{|\mathcal{F}^{\sigma}_{\rho,\lambda}(\mathfrak{a}_1 - \mathfrak{a}_2)|}{2}\left(\frac{1}{2}\right)^{1-\frac{2}{q}}\left(\frac{2-s}{4}\right)^{\frac{1}{q}}A^{\frac{1}{q}}\left(\mathfrak{m}|\Upsilon'(\frac{\mathfrak{a}_1}{\mathfrak{m}})|^q, |\Upsilon'(\mathfrak{a}_2)|^q\right).
\end{aligned}$$

For the case $q = 1$, we apply the same technique step by step as used in the Theorem 10. This completes the proof. ■

Corollary 6 *If we put $n = \mathfrak{m} = 1$ and $s = 1$ in Theorem 12, then*

$$\begin{aligned}
&\left|\frac{\Upsilon(\mathfrak{a}_2) + \Upsilon(\mathfrak{a}_2 + \mathcal{F}^{\sigma}_{\rho,\lambda}(\mathfrak{a}_1 - \mathfrak{a}_2))}{2} - \frac{1}{\mathcal{F}^{\sigma}_{\rho,\lambda}(\mathfrak{a}_1 - \mathfrak{a}_2)}\int_{\mathfrak{a}_2}^{\mathfrak{a}_2 + \mathcal{F}^{\sigma}_{\rho,\lambda}(\mathfrak{a}_1 - \mathfrak{a}_2)} \Upsilon(x)dx\right| \\
&\leq \frac{\mathcal{F}^{\sigma}_{\rho,\lambda}(\mathfrak{a}_1 - \mathfrak{a}_2)}{4}A^{\frac{1}{q}}\left[|\Upsilon'(\mathfrak{a}_1)|^q, |\Upsilon'(\mathfrak{a}_2)|^q\right].
\end{aligned}$$

Corollary 7 *If $s = \mathfrak{m} = 1$ and $\mathcal{F}^{\sigma}_{\rho,\lambda}(\mathfrak{a}_1 - \mathfrak{a}_2) = \mathfrak{a}_1 - \mathfrak{a}_2$ in Theorem 12, we get inequality (4.3) in [18].*

Theorem 13 *Suppose I° is a generalized convex set w.r.t. $\mathcal{F}^{\sigma}_{\rho,\lambda}$ and $\Upsilon : I^\circ \subseteq \mathbb{R} \to \mathbb{R}$ is a differentiable mapping on I°, $\mathfrak{a}_1, \mathfrak{a}_2 \in I^\circ$ with $\mathfrak{a}_1 < \mathfrak{a}_2, q > 1, \frac{1}{p} + \frac{1}{q} = 1$ and suppose that $\Upsilon' \in L[\mathfrak{a}_1, \mathfrak{a}_2]$. If $|\Upsilon'|^q$ is a generalized s-type $\mathfrak{m}$-convex function of Raina type on $L[\mathfrak{a}_1, \mathfrak{a}_2]$, then*

$$\begin{aligned}
&\left|\frac{\Upsilon(\mathfrak{a}_2) + \Upsilon(\mathfrak{a}_2 + \mathcal{F}^{\sigma}_{\rho,\lambda}(\mathfrak{a}_1 - \mathfrak{a}_2))}{2} - \frac{1}{\mathcal{F}^{\sigma}_{\rho,\lambda}(\mathfrak{a}_1 - \mathfrak{a}_2)}\int_{\mathfrak{a}_2}^{\mathfrak{a}_2 + \mathcal{F}^{\sigma}_{\rho,\lambda}(\mathfrak{a}_1 - \mathfrak{a}_2)} \Upsilon(x)dx\right| \\
&\leq \frac{|\mathcal{F}^{\sigma}_{\rho,\lambda}(\mathfrak{a}_1 - \mathfrak{a}_2)|}{2}\left(\frac{1}{2(p+1)}\right)^{\frac{1}{p}} \\
&\times \left\{\left(\mathfrak{m}|\Upsilon'(\frac{\mathfrak{a}_1}{\mathfrak{m}})|^q\frac{3-2s}{6} + |\Upsilon'(\mathfrak{a}_2)|^q\frac{3-s}{6}\right)^{\frac{1}{q}} + \left(\mathfrak{m}|\Upsilon'(\frac{\mathfrak{a}_1}{\mathfrak{m}})|^q\frac{3-s}{6} + |\Upsilon'(\mathfrak{a}_2)|^q\frac{3-2s}{6}\right)^{\frac{1}{q}}\right\},
\end{aligned}$$

holds for $\flat \in [0,1]$, $\mathfrak{m} \in (0,1]$ and $s \in [0,1]$.

Proof Suppose that $\mathfrak{a}_1, \mathfrak{a}_2 \in I^\circ$. Since I° is a generalized convex set w.r.t. $\mathcal{F}^{\sigma}_{\rho,\lambda}$, for any $\flat \in [0,1]$, we have $\mathfrak{a}_2 + \flat\, \mathcal{F}^{\sigma}_{\rho,\lambda}(\mathfrak{a}_1 - \mathfrak{a}_2) \in I^\circ$. Using Lemma 2, Hölder-İscan integral inequality and generalized s-type $\mathfrak{m}$-convex function of Raina type of $|\Upsilon'|^q$ and properties of modulus, we have

$$\left|\frac{\Upsilon(a_2)+\Upsilon(a_2+\mathcal{F}^{\sigma}_{\rho,\lambda}(a_1-a_2))}{2}-\frac{1}{\mathcal{F}^{\sigma}_{\rho,\lambda}(a_1-a_2)}\int_{a_2}^{a_2+\mathcal{F}^{\sigma}_{\rho,\lambda}(a_1-a_2)}\Upsilon(x)dx\right|$$
$$\leq\frac{|\mathcal{F}^{\sigma}_{\rho,\lambda}(a_1-a_2)|}{2}\int_0^1|1-2\flat||\Upsilon'(a_2+\flat\mathcal{F}^{\sigma}_{\rho,\lambda}(a_1-a_2))|d\flat$$
$$\leq\frac{|\mathcal{F}^{\sigma}_{\rho,\lambda}(a_1-a_2)|}{2}\left(\int_0^1(1-\flat)|1-2\flat|^p d\flat\right)^{\frac{1}{p}}\left(\int_0^1(1-\flat)|\Upsilon'(a_2+\flat\mathcal{F}^{\sigma}_{\rho,\lambda}(a_1-a_2))|^q d\flat\right)^{\frac{1}{q}}$$
$$+\frac{|\mathcal{F}^{\sigma}_{\rho,\lambda}(a_1-a_2)|}{2}\left(\int_0^1\flat|1-2\flat|^p d\flat\right)^{\frac{1}{p}}\left(\int_0^1\flat|\Upsilon'(a_2+\flat\mathcal{F}^{\sigma}_{\rho,\lambda}(a_1-a_2))|^q d\flat\right)^{\frac{1}{q}}$$
$$\leq\frac{|\mathcal{F}^{\sigma}_{\rho,\lambda}(a_1-a_2)|}{2}\left(\frac{1}{2(p+1)}\right)^{\frac{1}{p}}$$
$$\times\left(|\Upsilon'(a_2)|^q\int_0^1(1-\flat)(1-(s\flat))d\flat+\int_0^1(1-\flat)m|\Upsilon'(\frac{a_1}{m})|^q(1-(s(1-\flat)))d\flat\right)^{\frac{1}{q}}$$
$$+\frac{|\mathcal{F}^{\sigma}_{\rho,\lambda}(a_1-a_2)|}{2}\left(\frac{1}{2(p+1)}\right)^{\frac{1}{p}}\left(|\Upsilon'(a_2)|^q\int_0^1\flat(1-(s\flat))d\flat+\int_0^1 m|\Upsilon'(\frac{a_1}{m})|^q\flat(1-(s(1-\flat)))d\flat\right)^{\frac{1}{q}}$$
$$\leq\frac{|\mathcal{F}^{\sigma}_{\rho,\lambda}(a_1-a_2)|}{2}\left(\frac{1}{2(p+1)}\right)^{\frac{1}{p}}$$
$$\times\left\{\left(m|\Upsilon'(\frac{a_1}{m})|^q\frac{3-2s}{6}+|\Upsilon'(a_2)|^q\frac{3-s}{6}\right)^{\frac{1}{q}}+\left(m|\Upsilon'(\frac{a_1}{m})|^q\frac{3-s}{6}+|\Upsilon'(a_2)|^q\frac{3-2s}{6}\right)^{\frac{1}{q}}\right\},$$

which is the required proof. ■

Corollary 8 *If $m=1$ and $s=1$ in Theorem 13, then*

$$\left|\frac{\Upsilon(a_2)+\Upsilon(a_2+\mathcal{F}^{\sigma}_{\rho,\lambda}(a_1-a_2))}{2}-\frac{1}{\mathcal{F}^{\sigma}_{\rho,\lambda}(a_1-a_2)}\int_{a_2}^{a_2+\mathcal{F}^{\sigma}_{\rho,\lambda}(a_1-a_2)}\Upsilon(x)dx\right|$$
$$\leq\frac{|\mathcal{F}^{\sigma}_{\rho,\lambda}(a_1-a_2)|}{4}\left(\frac{1}{p+1}\right)^{\frac{1}{p}}\left[\left(\frac{|\Upsilon'(a_1)|^q}{3}+\frac{2|\Upsilon'(a_2)|^q}{3}\right)^{\frac{1}{q}}+\left(\frac{2|\Upsilon'(a_1)|^q}{3}+\frac{|\Upsilon'(a_2)|^q}{3}\right)^{\frac{1}{q}}\right].$$

Corollary 9 *If we put $s=m=1$ and $\mathcal{F}^{\sigma}_{\rho,\lambda}(a_1-a_2)=a_1-a_2$ in Theorem 13, we get inequality (4.4) in [18].*

Theorem 14 *Suppose I° is a generalized convex set w.r.t. $\mathcal{F}^{\sigma}_{\rho,\lambda}$ and $\Upsilon: I^\circ\subseteq\mathbb{R}\to\mathbb{R}$ is a differentiable mapping on I°, $a_1,a_2\in I^\circ$ with $a_1<a_2$, $q\geq 1$ and suppose that $\Upsilon'\in L[a_1,a_2]$. If $|\Upsilon'|^q$ is a generalized s−type m−convex function of Raina type on $L[a_1,a_2]$, then*

$$\left|\frac{\Upsilon(a_2)+\Upsilon(a_2+\mathcal{F}^{\sigma}_{\rho,\lambda}(a_1-a_2))}{2}-\frac{1}{\mathcal{F}^{\sigma}_{\rho,\lambda}(a_1-a_2)}\int_{a_2}^{a_2+\mathcal{F}^{\sigma}_{\rho,\lambda}(a_1-a_2)}\Upsilon(x)dx\right|$$
$$\leq\frac{|\mathcal{F}^{\sigma}_{\rho,\lambda}(a_1-a_2)|}{2}\left(\frac{1}{2}\right)^{2-\frac{2}{q}}$$
$$\times\left\{\left(m|\Upsilon'(\frac{a_1}{m})|^q k_1(s)+|\Upsilon'(a_2)|^q k_2(s)\right)^{\frac{1}{q}}+\left(m|\Upsilon'(\frac{a_1}{m})|^q k_2(s)+|\Upsilon'(a_2)|^q k_1(s)\right)^{\frac{1}{q}}\right\},$$

holds for $\flat\in[0,1]$, $m\in(0,1]$ and $s\in[0,1]$. Where

$$k_1(s)=\int_0^1(1-\flat)|1-2\flat|(1-(s(1-\flat)))d\flat=\int_0^1\flat|1-2\flat|(1-(s\flat)))d\flat,$$

$$k_2(s)=\int_0^1\flat|1-2\flat|(1-(s(1-\flat)))d\flat=\int_0^1(1-\flat)|1-2\flat|(1-(s\flat))d\flat.$$

Proof Suppose that $a_1,a_2\in I^\circ$. Since I° is a generalized convex set w.r.t. $\mathcal{F}^{\sigma}_{\rho,\lambda}$, for any $\flat\in[0,1]$, we have $a_2+\flat\mathcal{F}^{\sigma}_{\rho,\lambda}(a_1-a_2)\in I^\circ$. Suppose that $q>1$. Using Lemma 2, improved power-mean integral inequality and generalized s−type m−convex function of Raina type of $|\Upsilon'|^q$ and properties of modulus, we have

$$\begin{aligned}
&\left|\frac{\Upsilon(a_2)+\Upsilon(a_2+\mathcal{F}^{\sigma}_{\rho,\lambda}(a_1-a_2))}{2}-\frac{1}{\mathcal{F}^{\sigma}_{\rho,\lambda}(a_1-a_2)}\int_{a_2}^{a_2+\mathcal{F}^{\sigma}_{\rho,\lambda}(a_1-a_2)}\Upsilon(x)dx\right|\\
&\leq \frac{|\mathcal{F}^{\sigma}_{\rho,\lambda}(a_1-a_2)|}{2}\int_0^1|1-2\flat||\Upsilon'(a_2+\flat\,\mathcal{F}^{\sigma}_{\rho,\lambda}(a_1-a_2))|d\flat\\
&\leq \frac{|\mathcal{F}^{\sigma}_{\rho,\lambda}(a_1-a_2)|}{2}\left(\int_0^1(1-\flat)|1-2\flat|d\flat\right)^{1-\frac{1}{q}}\left(\int_0^1(1-\flat)|1-2\flat||\Upsilon'(a_2+\flat\,\mathcal{F}^{\sigma}_{\rho,\lambda}(a_1-a_2))|^q d\flat\right)^{\frac{1}{q}}\\
&+\frac{|\mathcal{F}^{\sigma}_{\rho,\lambda}(a_1-a_2)|}{2}\left(\int_0^1(\flat|1-2\flat|d\flat\right)^{1-\frac{1}{q}}\left(\int_0^1\flat|1-2\flat||\Upsilon'(a_2+\flat\,\mathcal{F}^{\sigma}_{\rho,\lambda}(a_1-a_2))|^q d\flat\right)^{\frac{1}{q}}\\
&\leq \frac{|\mathcal{F}^{\sigma}_{\rho,\lambda}(a_1-a_2)|}{2}\left(\frac{1}{2}\right)^{2-\frac{2}{q}}\\
&\times\left\{\left(|\Upsilon'(a_2)|^q\int_0^1(1-\flat)|1-2\flat|(1-(s\flat))d\flat+\int_0^1(1-\flat)|1-2\flat|m|\Upsilon'(\frac{a_1}{m})|^q(1-(s(1-\flat)))d\flat\right)^{\frac{1}{q}}\right.\\
&+\left.\left(|\Upsilon'(a_2)|^q\int_0^1\flat|1-2\flat|(1-(s\flat)))d\flat+\int_0^1\flat|1-2\flat|m|\Upsilon'(\frac{a_1}{m})|^q(1-(s(1-\flat)))d\flat\right)^{\frac{1}{q}}\right\}\\
&\leq \frac{|\mathcal{F}^{\sigma}_{\rho,\lambda}(a_1-a_2)|}{2}\left(\frac{1}{2}\right)^{2-\frac{2}{q}}\\
&\times\left\{\left(m|\Upsilon'(\frac{a_1}{m})|^q k_1(s)+|\Upsilon'(a_2)|^q k_2(s)\right)^{\frac{1}{q}}+\left(m|\Upsilon'(\frac{a_1}{m})|^q k_2(s)+|\Upsilon'(a_2)|^q k_1(s)\right)^{\frac{1}{q}}\right\}.
\end{aligned}$$

For the case $q=1$, we apply the same technique step by step as used in the Theorem 10. This completes the proof. ∎

Corollary 10 *If we put* $m=1$ *and* $s=1$ *in Theorem 14, then*

$$\begin{aligned}
&\left|\frac{\Upsilon(a_2)+\Upsilon(a_2+\mathcal{F}^{\sigma}_{\rho,\lambda}(a_1-a_2))}{2}-\frac{1}{\mathcal{F}^{\sigma}_{\rho,\lambda}(a_1-a_2)}\int_{a_2}^{a_2+\mathcal{F}^{\sigma}_{\rho,\lambda}(a_1-a_2)}\Upsilon(x)dx\right|\\
&\leq \frac{|\mathcal{F}^{\sigma}_{\rho,\lambda}(a_1-a_2)|}{8}\left[\left(\frac{|\Upsilon'(a_1)|^q}{4}+\frac{3|\Upsilon'(a_2)|^q}{4}\right)^{\frac{1}{q}}+\left(\frac{3|\Upsilon'(a_1)|^q}{4}+\frac{|\Upsilon'(a_2)|^q}{4}\right)^{\frac{1}{q}}\right].
\end{aligned}$$

Corollary 11 *If we put* $s=m=1$ *and* $\mathcal{F}^{\sigma}_{\rho,\lambda}(a_1-a_2)=a_1-a_2$ *in Theorem 14, we get inequality (4.5) in [18].*

Note: We pass the some comments regarding comparison on the above estimations of the mentioned lemma. On Lemma 2, we examined Theorem 11 and Theorem 13, in which we used the Hölder and Hölder-İscan inequality. On the comparison, Theorem 13 gives a better result as compared to Theorem 11. Similarly, on Lemma 2, we examined Theorem 12 and Theorem 14, in which we used power mean and improved power mean inequality. On the comparison, Theorem 14 gives a better result as compare to Theorem 12.

6 Conclusion

In the development of this paper, some results have been established that generalize, from the definition of Raina integral operator and the use of s-type m-convex function. In particular, those concerning the integral inequality of Hermite-Hadamard. Some algebraic properties are attained in relation to the newly introduced definition. In addition, we described the novel variant of Hermite-Hadamard type inequality in the manner of a generalized s-type m-convex function of Raina type. Our attaining results in the order of lemma can be considered as refinements and remarkable extensions to the new family of generalized convex functions of Raina type. In the future, we hope the results of this paper and the new idea can be extended in different directions like fractional calculus, quantum calculus, time scale calculus, etc. We hope the consequences and techniques of this article will energize and inspire the researcher to explore a more interesting sequel in this area.

Declarations

Consent for publication

Not applicable.

Conflicts of interest

The authors declare that they have no known competing financial interests or personal relationships that could have appeared to influence the work reported in this paper.

Funding

The authors declare that there is no funding source for the reported research.

Author's contributions

M.T.: Conceptualization, Methodology, Software, Writing-Reviewing and Editing. H.A.: Supervision, Investigation, Data Curation, Writing-Original draft preparation. S.K.S.: Visualization, Investigation, Methodology, Software, Writing-Reviewing and Editing. All authors discussed the results and contributed to the final manuscript.

Acknowledgement

Not applicable.

References

[1] Hardy, G.H., Little, J.E. and Polya, G. Inequalities. *Cambridge, UK. Cambridge University Press.* Cambridge mathematical library, (1952).
[2] Kadakal, H. Hermite-Hadamard type inequalities for trigonometrically convex functions. *Scientific Studies and Research. Series Mathematic and İnformatics,* 28(2), 19-28, (2018).
[3] Niculescu, C.P. and Persson, L.E. Convex functions and their applications.*Springer, New York,* (2006).
[4] Tariq, M. New Hermite-Hadamard type inequalities via p-harmonic exponential type convexity and applications. *Universal Journal of Mathematics and Applications,* 4(2), 59-69, (2021).
[5] Özcan, S. and İşcan, İ. Some new Hermite-Hadamard type integral inequalities for the s-convex functions and theirs applications. *Journal of Inequalities and Applications,* 2019(201), 1-14, (2019).
[6] Tariq, M., Nasir, J., Sahoo, S.K. and Mallah, A.A. A note on some Ostrowski type inequalities via generalized exponentially convex function. *Journal of Mathematical Analysis and Modeling,* 2(2), 1-15, (2021).
[7] Khan, M.A., Chu, Y.M., Khan, T.U. and Khan, J. Some new inequalities of Hermite-Hadamard type for s-convex functions with applications. *Open Math,* 15(1), 1414-1430, (2017).
[8] Butt, S.I., Tariq, M., Aslam, A., Ahmad, H. and Nofel, T.H. Hermite-Hadamard type inequalities via generalized harmonic exponential convexity. *Journal of Function Spaces,* 1-12, (2021).
[9] Xi, B.Y. and Qi, F. Some integral inequalities of Hermite-Hadamard type for convex functions with applications to means. *Journal of Function Spaces,* 1-14, (2012).
[10] Butt, S.I., Kashuri, A., Tariq, M., Nasir, J., Aslam, A. and Geo, W. Hermite-Hadamard-type inequalities via n-polynomial exponential-type convexity and their applications. *Advances in Difference Equations,* 508, (2020).
[11] Butt, S.I., Kashuri, A., Tariq, M., Nasir, J., Aslam, A. and Geo, W. n-polynomial exponential-type p-convex function with some related inequalities and their application. *Heliyon,* 6(11), (2020).
[12] Hadamard, J. Étude sur les propriétés des fonctions entiéres en particulier d'une fonction considéréé par Riemann. *Journal of Mathematics. Pures. Appl,* 58, 171-215, (1893).
[13] Raina, R.K. On generalized Wright's hypergeometric functions and fractional calculus operators. *East Asian Mathematical Journal,* 21(2), 191-203, (2005).
[14] Cortez, M.J.V., Liko, R., Kashuri, A. and Hernández, J.E.H. New quantum estimates of trapezium-type inequalities for generalized ϕ-convex functions. *Mathematics,* 7(11), 1047-1066, (2019).
[15] Cortez, M.J.V., Kashuri, A. and Hernández, J.E.H. Trapezium-type inequalities for Raina's fractional integrals operator using generalized convex functions.*Symmetry,* 12(6), 1034, (2020).
[16] Rashid, S., İşcan, İ., Baleanu, D. and Chu, Y.M. Generation of new fractional inequalities via n-polynomials s-type convexity with applications. *Advances in Difference Equations,* Article ID 264
[17] Barani, A., Ghazanfari, A.G. and Dragomir, S.S. Hermite-Hadamard inequality for functions whose derivatives absolute values are preinvex. *Journal of Inequalities and Applications,* 2012(1), 1-9, (2012).
[18] Toplu, T., Kadakal, M. and İşcan, İ. On n-polynomial convexity and some related inequalities. *AIMS Math,* 5(2), 1304-1318, (2020).

Mathematical Modelling and Numerical Simulation with Applications, 2021, 1(1), 44–55

https://www.mmnsa.org
ISSN Online: 2791-8564 / Open Access
https://doi.org/10.53391/mmnsa.2021.01.005

RESEARCH PAPER

Stability analysis of an incommensurate fractional-order SIR model

Bahatdin Daşbaşı [1,*,†]

[1]Kayseri University, Faculty of Engineering, Architecture and Design, Department of Engineering Basic Sciences, 38039, Kayseri, Turkey

[*]Corresponding Author
[†]bdasbasi@kayseri.edu.tr (Bahatdin Daşbaşı)

Abstract

In this paper, a fractional-order generalization of the susceptible-infected-recovered (SIR) epidemic model for predicting the spread of an infectious disease is presented. Also, an incommensurate fractional-order differential equations system involving the Caputo meaning fractional derivative is used. The equilibria are calculated and their stability conditions are investigated. Finally, numerical simulations are presented to illustrate the obtained theoretical results.

Key words: *SIR* mathematical model; incommensurate order differential equation; fractional-derivative; stability analysis
AMS 2020 Classification: 34A08; 34D20; 34K60; 92C50; 92D30

1 Introduction

The topic of fractional calculus (FC) has gained considerable popularity and importance in the last three decades, mainly because of its wide variety of applications in science and engineering. Also, it has been found that many systems can be described with fractional differential equations in many interdisciplinary fields [1]. Fractional-order differential equation (FODE) models have advantages over classical ordinary differential equation (ODE) and/or delayed differential equation models because integer derivatives are used to obtain information about only local properties of a state, while fractional derivatives describe the entire space. In other words, in FODE models, the next precise location for a physical phenomenon depends not only on the current situation, but also on all historical situations. Thus, these models not only give more realistic biological models involving memory but also expand the stability region of states [2]. Fractional-order systems (FOSs) are can be considered in two parts, as commensurate FOS (CFOS) and incommensurate FOS (IFOS) according to the derivative orders in the system. CFOS can be considered as a special case of derivative orders in IFOS [3]. Given the fact that the stability theorem of fractional differential equations favors stability analysis and controller synthesis, this motivates us to adopt stability criteria for the field of incommensurate fractional-order nonlinear systems and give sufficient conditions for determining stability [4]. Therefore, modeling of biological dynamics with IFOS is more comprehensive in terms of predicting the behavior of the system [5]. Furthermore, theorems of existence, uniqueness and dependence upon initial conditions according to some special conditions of IFOS are given in [6, 7].
There are many recent studies in the literature on the stability of IFOS [8, 9, 10, 11]. In addition, modeling and stability analysis of biological systems by IFOS has been frequently discussed in the literature recently [12, 13, 5, 7, 14] and CFOS [15, 16, 17, 18, 19, 20, 21, 22, 23, 24] .
In the field of epidemiology, many schemes have been developed to mathematically model various infectious epidemics. Compartment models such as SIR modeling, which divide communities into certain main classes, are the most widely used models. The interactions between these classes are mainly determined by certain pre-mathematical formulas. The classical SIR epidemiological model was first introduced by Kermack and McKendrick in 1927. This ordinary differential equation system (ODES) models the

➤ **Received:** 17.09.2021 ➤ **Revised:** 28.09.2021 ➤ **Accepted:** 29.09.2021 ➤ **Published:** 30.09.2021

spread of an epidemic in a population. More recently, there has been increased interest in extending SIR models through the inclusion of fractional derivatives [27]. Modified SIR mathematical modeling through CFOS are in recent years analyzed in [28, 29, 30]. In here, the time-dependent changes in sizes of susceptible, infected and recovered individuals in a population in case of an infectious disease were investigated by mathematically modeling with IFOS. An innovation has been presented to the literature in terms of the use of IFOS in the model. In addition, the results were supported by numerical studies.
The remainder of the article is arranged as follows:

- In Section 2, the existence of equilibrium points of the proposed model and their stabilities are analyzed.
- In Section 3, the mathematical formulation of the proposed SIR model is presented. Furthermore, the threshold parameter is presented.
- Section 4 proposes the stability conditions of the mentioned biological system.
- Section 5 backs up the qualitative analysis results of the proposed IFOS. In this respect, numerical simulations are performed.
- The article ends in Section 6 with some concluding remarks.

2 Preliminaries and definitions

In here, it is given some basic definitions and notations with respect to follows: FODE with Caputo derivatives and locally asymptotically stability (LAS) of the equilibrium point of an n-dimensional FOS, respectively.

Definition 1 *According to the definition of Caputo sense, the fractional derivative of the function $f(t)$ is defined as*

$$^{C}D_t^{\alpha}\left(f(t)\right) = \frac{1}{\Gamma(n-\alpha)}\left(\frac{d}{dt}\right)^n \int_a^t (t-x)^{n-\alpha-1}\left(\frac{d}{dx}\right)^n f(x)\,dx,\ n-1<\alpha\leq n, \tag{1}$$

where $\Gamma(.)$ is the Gamma function, which is described by $\Gamma(x) = \int_0^\infty t^{x-1}e^{-t}dt$, $f\colon (0,+\infty)\to\mathbb{R}$ and $\alpha>0$ [31].

The Caputo fractional order sense is used in this study.

Remark 1 *The nonlinear FOS can be defined as following*

$$\frac{d^{\overline{\alpha}}X(t)}{dt^{\overline{\alpha}}} = F(t, X(t)), \tag{2}$$

where it is considered initial conditions by $X(0)=X_0$, the state vectors by $X(t)=[x_1(t), x_2(t), \ldots, x_n(t)]^T\in\mathbb{R}^n$, the functions by $F=[f_1, f_2, \ldots, f_n]^T\in\mathbb{R}^n$, $f_i\colon [0,+\infty)\ \mathrm{x}\mathbb{R}^n\to\mathbb{R}$, $(i=1,2,\ldots,n)$ and the derivative-orders by $\overline{\alpha}=[\alpha_1, \alpha_2, \ldots, \alpha_n]^T$ such that $\frac{d^{\overline{\alpha}}X(t)}{dt^{\overline{\alpha}}} = \left[\frac{d^{\alpha_1}x_1(t)}{dt^{\alpha_1}}, \frac{d^{\alpha_2}x_2(t)}{dt^{\alpha_2}}, \ldots, \frac{d^{\alpha_n}x_n(t)}{dt^{\alpha_n}}\right]^T$ [32].

For the rest of the article, α_i is in $(0,1|$.

Definition 2 *For system (2), autonomous IFOS can be presented as*

$$\frac{d^{\overline{\alpha}}X(t)}{dt^{\overline{\alpha}}} = F(X(t)),\ X(0)=X_0. \tag{3}$$

Also, the equilibrium point of system (3) is found from $F\left(\overline{X}\right)=0$ for $\overline{X}=(\overline{x_1}, \overline{x_2}, \ldots, \overline{x_n})$ [6].

Lemma 1 *Eigenvalues λ_i for $i=1,2,\ldots,m(\alpha_1+\alpha_2+\cdots+\alpha_n)$ of system (3) are obtained from*

$$det\left(diag\left(\lambda^{m\alpha_1}, \lambda^{m\alpha_2}, \ldots, \lambda^{m\alpha_n}\right) - J\left(\overline{X}\right)\right) = 0, \tag{4}$$

where m is the smallest of the common multiples of the denominators of rational numbers $\alpha_1, \alpha_2, \ldots, \alpha_n$ and $J\left(\overline{X}\right) = \left.\frac{\partial F}{\partial X}\right|_{X=\overline{X}}$. If all eigenvalues λ_i obtained from equation (4) satisfy

$$|arg(\lambda_i)| > \frac{\pi}{2m}, \tag{5}$$

then $\overline{X}$ is LAS for system (3) [33, 34].

As a result, Figure 1 shows the stability conditions of the incommensurate order SIR model given in (3), where $\alpha_1 \neq \alpha_2 \neq \cdots \neq \alpha_n < 1$ and λ_i for $i=1,2,\ldots,m(\alpha_1+\alpha_2+\cdots+\alpha_n)$.

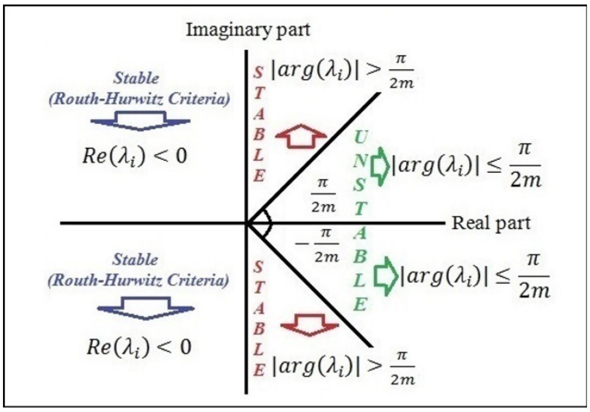

Figure 1. Regions of stability and instability of the equilibrium point in terms of the roots of the characteristic equation of the system (3) [5].

3 The SIR model through IFOS

We consider a *SIR* epidemic disease model. Define the following dependent-time t:

Table 1. State variables and their meanings

State Variable	Meaning
$S(t)$	The susceptible individuals at the t-time
$I(t)$	The infected symptomatic individuals at the t-time
$R(t)$	The recovered individuals at the t-time

Therefore, the dynamics is governed by a system of three FODE as follows:

$$\begin{aligned} \frac{d^{\alpha_1} S(t)}{dt^{\alpha_1}} &= \Lambda + \nu R - \eta IS - (\mu + b) S, \\ \frac{d^{\alpha_2} I(t)}{dt^{\alpha_2}} &= \eta IS - (\gamma + d + b) I, \\ \frac{d^{\alpha_3} R(t)}{dt^{\alpha_3}} &= \mu S + \gamma I - (\nu + b) R, \end{aligned} \tag{6}$$

where $t \geq 0$, $\alpha_i \in (0,1]$ for $i = 1,2,3$. Also, the initial conditions are $S(t_0) = S_0 > 0$, $I(t_0) = I_0 > 0$ and $R(t_0) = R_0 > 0$ for $t > t_0$. Restrictions are imposed on the parameters to ensure that solutions are nonnegative. Therefore, the following conditions hold

$$\Lambda,\ \nu,\ \eta,\ \mu,\ b,\ \gamma,\ d > 0. \tag{7}$$

In Table 2, it is illustrated parameters with their meaning.

Table 2. Parameters and their meanings in the proposed model

Parameter	Meaning
Λ	The constant birth number in the overall population
ν	The immunity loss rate of recovered individuals
η	The contact number, the average number of successful contacts resulting in infection and made by one infected individual
μ	Rate of the vaccinated susceptible individuals
b	The death rate due to the different conditions other than the disease for the overall population.
γ	Recovery rate of the infected individual
d	Average fatality rate of the infected individual due to infectious disease

Therefore, Figure 2 is obtained from system (6).

Definition 3 *The baseline reproduction number, often denoted as $\mathcal{R}_0$, describes the average number of secondary infections caused by an infected individual in a fully susceptible population. This number indicates whether the infection will spread to the population or not [35].*

For the proposed model, it is described this parameter as

$$\mathcal{R}_0 = \frac{\eta}{(\gamma + d + b)} \frac{\Lambda}{b} \frac{(b + \nu)}{(b + \nu + \mu)}. \tag{8}$$

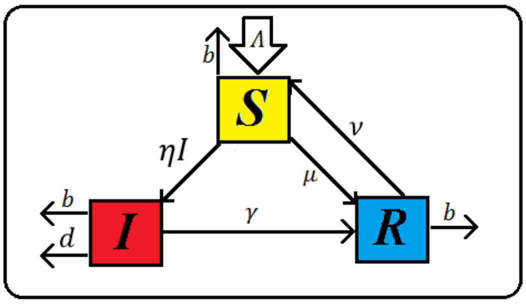

Figure 2. The movement of the individuals between compartments in the proposed model

It is clear that

$$\mathcal{R}_0 > 0, \tag{9}$$

due to the inequalities in (7).

4 Stability analysis

Proposition 1 *Let us consider the equations,* $\frac{d^{\alpha_1} S(t)}{dt^{\alpha_1}} = 0$, $\frac{d^{\alpha_2} I(t)}{dt^{\alpha_2}} = 0$, $\frac{d^{\alpha_3} R(t)}{dt^{\alpha_3}} = 0$, *for equilibrium points. The proposed model has two types of the equilibrium points. These are disease free equilibrium point* $E_0\left(\frac{\Lambda}{b}\frac{(b+\nu)}{(b+\nu+\mu)}, 0, \frac{\Lambda}{b}\frac{\mu}{(b+\nu+\mu)}\right)$ *and the endemic equilibrium* $E_1(S^*, I^*, R^*)$ *when*

$$\mathcal{R}_0 > 1. \tag{10}$$

In here, it is

$$\begin{cases} S^* = \frac{(\gamma+d+b)}{\eta}, \\ I^* = \frac{S^*(\mathcal{R}_0-1)(b+\nu+\mu)}{\left(\gamma+d+b+\nu\frac{d}{b}+\nu\right)}, \\ R^* = \left(\frac{S^*(\mathcal{R}_0-1)(b+\nu+\mu)}{\left(\gamma+d+b+\nu\frac{d}{b}+\nu\right)} + \frac{S^*}{\gamma}\mu\right)\frac{\gamma}{(b+\nu)}. \end{cases} \tag{11}$$

Proposition 2 *Considering the proposed model in* (6)*, there are follows.*

i. *Let* $\alpha_1 = \alpha_2 = \alpha_3 \leq 1$. *For CFOS, it is satisfied the followings:*

a) *If* $\mathcal{R}_0 < 1$, *the equilibrium point* E_0, *namely trivial disease-free equilibrium, is LAS.*
b) *If*

$$\left(\left(\eta I^* + (\mu+b)\right) + (\nu+b)\right)\left(\eta I^*\left((\nu+b)+\eta S^*\right) + b(\mu+\nu+b)\right) - \eta I^*\left((\nu+b)\eta S^* + \gamma\nu\right) > 0, \tag{12}$$

then the equilibrium point E_1, *existing biologically meaning when* $\mathcal{R}_0 > 1$, *is LAS.*

ii. *For IFOS in system* (6), *where* $\alpha_1 \neq \alpha_2 \neq \alpha_3 < 1$, *it is satisfied the followings:*

a) *If* $\mathcal{R}_0 < 1$ *and all roots* λ_i *for* $i = 1, 2, \ldots, m(\alpha_1+\alpha_3)$ *founded from the equation*

$$\lambda^{m(\alpha_1+\alpha_3)} + \lambda^{m\alpha_1}(\nu+b) + \lambda^{m\alpha_3}(\mu+b) + b(\mu+\nu+b) = 0$$

satisfy Routh-Hurwitz stability criteria [36] or the condition $|\arg(\lambda_i)| > \frac{1}{m}\frac{\pi}{2}$ *[37] as seen inequalities* (5)*, then the equilibrium point* E_0 *is LAS.*
b) *Let* $\mathcal{R}_0 > 1$. *If all roots* λ_i *for* $i = 1, 2, \ldots, m(\alpha_1+\alpha_2+\alpha_3)$ *founded from the equation* $\lambda^{m(\alpha_1+\alpha_2+\alpha_3)} + \lambda^{m(\alpha_1+\alpha_2)}(\nu+b) + \lambda^{m(\alpha_2+\alpha_3)}(\eta I^* + (\mu+b)) + \lambda^{m\alpha_2}(\eta I^*(\nu+b) + b(\mu+\nu+b)) + \lambda^{m\alpha_3}(\gamma+d+b)\eta I^* + \eta I^*((\gamma+d+b)(\nu+b)+\gamma\nu) = 0$ *satisfy Routh-Hurwitz stability criteria or the condition* $|\arg(\lambda_i)| > \frac{1}{m}\frac{\pi}{2}$, *then the equilibrium point* E_1 *is LAS.*

Proof By the equations in (6), the Jacobian matrix evaluated at the equilibrium point $E_i\left(\bar{S},\ \bar{I},\bar{R}\right)$ for $i=0,1$ is

$$J\left(E_i\right)=\begin{pmatrix} -\left(\eta\bar{I}+(\mu+b)\right) & -\eta\bar{S} & \nu \\ \eta\bar{I} & \left(\eta\bar{S}-(\gamma+d+b)\right) & 0 \\ \mu & \gamma & -(\nu+b) \end{pmatrix}. \tag{13}$$

i. The system in (6) translates to CFOS, when $0<\alpha_1=\alpha_2=\alpha_3\leq 1$.

a) For E_0, the eigenvalues are obtained by considering the equation $Det\left(J_{(S,I,\ R)=E_0\left(\frac{\Lambda}{b}\frac{(b+\nu)}{(b+\nu+\mu)},0,\frac{\Lambda}{b}\frac{\mu}{(b+\nu+\mu)}\right)}-\lambda I_{3x3}\right)=0$. Accordingly, it is

$$(\lambda-(\gamma+d+b)(\mathcal{R}_0-1))\left(\lambda^2+\lambda((\nu+b)+(\mu+b))+(\mu+\nu+b)\right)=0. \tag{14}$$

Therefore, the eigenvalues obtained from equation in (14) are determined as followings:

$$\lambda_1=(\gamma+d+b)(\mathcal{R}_0-1), \tag{15}$$

and λ_2 and λ_3 are found by solving the equation

$$\lambda^2+\lambda((\nu+b)+(\mu+b))+(\mu+\nu+b). \tag{16}$$

It can be observed that $((\nu+b)+(\mu+b))>0$ and $(\mu+\nu+b)>0$, due to inequalities in (7). The LAS conditions for E_0 are provided for the eigenvalues λ_2 and λ_3. Thus, it is sufficient to examine the sign of λ_1. If

$$\mathcal{R}_0<1, \tag{17}$$

then λ_1 is a negative real number due to inequalities (7). Routh-Hurwitz stability conditions are satisfied. In this case, E_0 is LAS.

b) Let $\mathcal{R}_0>1$. There is positive equilibrium point. Charasteristic equation obtained from $Det\left(J_{(S,I,\ R)=E_1(S^*,I^*,R^*)}-\lambda I_{3x3}\right)=0$ for the equilibrium point E_1 is founded as

$$\lambda^3+a_1\lambda^2+a_2\lambda+a_3=0, \tag{18}$$

where

$$a_1=(\eta I^*+(\mu+b)+(\nu+b)),\ a_2=\left(\eta I^*\left((\nu+b)+\eta S^*\right)+b(\mu+\nu+b)\right),\ a_3=\eta I^*\left((\nu+b)\eta S^*+\gamma_I\nu\right). \tag{19}$$

Let us consider that Routh-Hurwitz stability criteria. It is already clear that $a_1,a_3>0$ due to inequalities in (7) and (9). In addition, we have

$$a_1a_2-a_3=((\eta I^*+(\mu+b))+(\nu+b))\left(\eta I^*\left((\nu+b)+\eta S^*\right)+b(\mu+\nu+b)\right)-\eta I^*\left((\nu+b)\eta S^*+\gamma\nu\right).$$

If

$$((\eta I^*+(\mu+b))+(\nu+b))\left(\eta I^*\left((\nu+b)+\eta S^*\right)+b(\mu+\nu+b)\right)-\eta I^*\left((\nu+b)\eta S^*+\gamma\nu\right)>0, \tag{20}$$

then $a_1a_2-a_3>0$. Hence, E_1 is LAS when inequality in (20) is satisfied.

ii. In case of $0<\alpha_1\neq\alpha_2\neq\alpha_3<1$, we have IFOS of (6). In this sense, the determinant found by the equation

$$det\left(diag\left(\lambda^{m\alpha_1},\ \lambda^{m\alpha_2},\lambda^{m\alpha_3}\right)-J_{(x_1,\ x_2,\ldots,\ x_n)=(\overline{x_1},\overline{x_2},\ldots,\overline{x_n})}\right)=0 \tag{21}$$

is

$$\begin{vmatrix} \lambda^{m\alpha_1}+\left(\eta\bar{I}+(\mu+b)\right) & -\eta\bar{S} & \nu \\ \eta\bar{I} & \lambda^{m\alpha_2}-\left(\eta\bar{S}-(\gamma+d+b)\right) & 0 \\ \mu & \gamma_I & \lambda^{m\alpha_3}+(\nu+b) \end{vmatrix}=0. \tag{22}$$

a) Firstly, if the determinant in (22) evaluates in the point $E_0\left(\frac{\Lambda}{b}\frac{(b+\nu)}{(b+\nu+\mu)},0,\frac{\mu}{(\nu+b)}\frac{\Lambda}{b}\frac{(b+\nu)}{(b+\nu+\mu)}\right)$ or $E_0\left(\frac{(\gamma+d+b)}{\eta}\mathcal{R}_0,0,\frac{\mu}{(\nu+b)}\frac{(\gamma+d+b)}{\eta}\mathcal{R}_0\right)$ with respect to (8), then it is achieved the equations:

$$\lambda^{m\alpha_2}-(\gamma+d+b)(\mathcal{R}_0-1)=0, \tag{23}$$

and

$$\left(\lambda^{m\alpha_1} + (\mu + b)\right)\left(\lambda^{m\alpha_3} + (\nu + b)\right) - \mu\nu = 0. \tag{24}$$

These equations are examined as the followings: Taking into consideration the equation in (23), it is found that $\lambda^{m\alpha_2} = (\gamma + d + b)(\mathcal{R}_0 - 1)$. If

$$\mathcal{R}_0 < 1, \tag{25}$$

then $\lambda^{m\alpha_2}$ is a negative real number due to inequalities in (7). Otherwise, at least one root of (23) would be a positive real number, in which case the equilibrium point E_0 would be unstable. By De-Moivre formulas, we have $\lambda^{m\alpha_2} = \overbrace{(\gamma + d + b)(1 - \mathcal{R}_0)}^{>0 \text{ due to } (7),(25)} cis\pi$, and so, $\lambda_k = \left[(\gamma + d + b)(1 - \mathcal{R}_0)\right]^{\frac{1}{m\alpha_2}} cis\left(\frac{\pi + 2k\pi}{m\alpha_2}\right)$ for $k = 0, 1, 2, \ldots, (m\alpha_2 - 1)$, such that $cis\pi = \cos\pi + i\sin\pi$, $i = \sqrt{-1}$. Also, we have

$$\begin{cases} |arg(\lambda_0)| = \dfrac{\pi}{m\alpha_2}, \\ |arg(\lambda_1)| = \dfrac{3\pi}{m\alpha_2}, \\ \vdots \\ \left|arg\left(\lambda_{(m\alpha_2 - 1)}\right)\right| = \dfrac{(2m\alpha_2 - 1)\pi}{m\alpha_2}. \end{cases} \tag{26}$$

Considering the conditions $|arg(\lambda)| > \frac{\pi}{2m}$ for the stability of the equilibrium point, the stability condition for E_0 is given as $\frac{\pi}{m\alpha_2}, \frac{3\pi}{m\alpha_2}, \ldots, \frac{(2m\alpha_2 - 1)\pi}{m\alpha_2} > \frac{\pi}{2m}$, and so,

$$\begin{cases} \alpha_2 < 2, \\ \alpha_2 < 6, \\ \vdots \\ \alpha_2 < 2(2m\alpha_2 - 1). \end{cases} \tag{27}$$

Inequalities in (27) have been always provided since the derivative-orders $0 < \alpha_1, \alpha_2, \alpha_3 \leq 1$ in (6) are already satisfied. On the other hand, we have considered the equation (24)). If this equation is arranged, then

$$\lambda^{m(\alpha_1 + \alpha_3)} + \lambda^{m\alpha_1}(\nu + b) + \lambda^{m\alpha_3}(\mu + b) + b(\mu + \nu + b) = 0 \tag{28}$$

is obtained. If the eigenvalues, which are the roots of equation (28), satisfy Routh-Hurwitz stability condition or the conditions $|arg(\lambda_i)| > \frac{\pi}{2m}$ for $i = 1, 2, \ldots, m(\alpha_1 + \alpha_3)$, then E_0 is LAS.
b) Let $\mathcal{R}_0 > 1$. In this case, the equilibrium point E_1 emerges as positive definite. By calculating the determinant (22) at this equilibrium point, it is obtained the following characteristic equation

$$\begin{aligned} &\lambda^{m(\alpha_1 + \alpha_2 + \alpha_3)} + \lambda^{m(\alpha_1 + \alpha_2)}(\nu + b) + \lambda^{m(\alpha_2 + \alpha_3)}(\eta I^* + (\mu + b)) + \\ &\lambda^{m\alpha_2}(\eta I^*(\nu + b) + b(\mu + \nu + b)) + \\ &\lambda^{m\alpha_3}(\gamma + d + b)\eta I^* + \eta I^*((\gamma + d + b)(\nu + b) + \gamma\nu) = 0. \end{aligned} \tag{29}$$

When the signs of the terms of the last equation are examined according to Descartes' sign rule [38], it is clear that the equation does not have a positive real root. This does not disturb the stability of the equilibrium point. Therefore, if the eigenvalues λ_i for $i = 1, 2, \ldots, m(\alpha_1 + \alpha_2 + \alpha_3)$, which are the roots of the equation (29), satisfy Routh-Hurwitz stability condition or the conditions $|arg(\lambda_i)| > \frac{1}{m}\frac{\pi}{2}$, the equilibrium point E_1 is LAS.

Therefore, the proof is completed. ■
As a result, it can be reached to Table 3.

Corollary 1 *Let us consider Table 3. If $\mathcal{R}_0 < 1$ and some additional conditions are satisfied, then the equilibrium point E_0, always existing, is LAS. However, the equilibrium point E_1 biologically exists when $\mathcal{R}_0 > 1$. In this context, it can be said the followings:*

i. *In case the unexistence of E_1, E_0 can be a stable equilibrium point,*
ii. *In case the unstability of E_0, where $\mathcal{R}_0 > 1$, E_1 exists.*

Therefore, these two points cannot be stable under the same conditions.

Table 3. The existence conditions for the equilibrium points of system (6) and the stability conditions of these points according to different states of its derivative orders

Equilibrium Point	The existence condition	Derivative-orders	Stability conditions
$E_0\left(\frac{\Lambda}{b}\frac{(b+\nu)}{(b+\nu+\mu)},0,\frac{\Lambda}{b}\frac{\mu}{(b+\nu+\mu)}\right)$	Always	$\alpha_1=\alpha_2=\alpha_3\leq 1$	If $\mathcal{R}_0<1$
$E_0\left(\frac{\Lambda}{b}\frac{(b+\nu)}{(b+\nu+\mu)},0,\frac{\Lambda}{b}\frac{\mu}{(b+\nu+\mu)}\right)$	Always	$\alpha_1\neq\alpha_2\neq\alpha_3$, $\alpha_1,\alpha_2,\alpha_3\in(0,1)$	If $\mathcal{R}_0<1$ and all roots λ_i for $i=1,2,\ldots,m(\alpha_1+\alpha_3)$ founded from the equation $\lambda^{m(\alpha_1+\alpha_3)}+\lambda^{m\alpha_1}(\nu+b)+\lambda^{m\alpha_3}(\mu+b)+b(\mu+\nu+b)=0$ satisfy Routh-Hurwitz stability criteria or the condition $\lvert arg(\lambda_i)\rvert>\frac{1}{m}\frac{\pi}{2}$.
$E_1(S^*,I^*,R^*)$	$\mathcal{R}_0>1$	$\alpha_1=\alpha_2=\alpha_3\leq 1$	$((\eta I^*+(\mu+b))+(\nu+b))(\eta I^*((\nu+b)+\eta S^*)+b(\mu+\nu+b))-\eta I^*((\nu+b)\eta S^*+\gamma\nu)>0$,
$E_1(S^*,I^*,R^*)$	$\mathcal{R}_0>1$	$\alpha_1\neq\alpha_2\neq\alpha_3$, $\alpha_1,\alpha_2,\alpha_3\in(0,1)$	If all roots λ_i for $i=1,2,\ldots,m(\alpha_1+\alpha_2+\alpha_3)$ founded from the equation $\lambda^{m(\alpha_1+\alpha_2+\alpha_3)}+\lambda^{m(\alpha_1+\alpha_2)}(\nu+b)+\lambda^{m(\alpha_2+\alpha_3)}(\eta I^*+(\mu+b))+\lambda^{m\alpha_2}(\eta I^*(\nu+b)+b(\mu+\nu+b))+\lambda^{m\alpha_3}(\gamma+d+b)\eta I^*+\eta I^*((\gamma+d+b)(\nu+b)+\gamma\nu)=0$ satisfy Routh-Hurwitz stability criteria or the condition $\lvert arg(\lambda_i)\rvert>\frac{1}{m}\frac{\pi}{2}$,
where $\mathcal{R}_0$ is in (8) and the components S^*, I^* and R^* of E_1 are in (11).			

5 Numerical results

To highlight the stability analysis results of this work using the proposed model for both CFOS and IFOS, two numerical examples are investigated. To do this, it is examined the behavior of the solutions of the model by valuing the parameters. It has been used Matlab R2012b. The parameter values are given in Table 4.

Table 4. The considered values of the parameters

Parameter	Value[1]	Value[2]	Unit
Λ	100	1000	individuals
ν	0.001	0.01	day $^{-1}$
η	0.0001	0.0001	day $^{-1}$
μ	0.045	0.05	day $^{-1}$
b	0.0032	0.15	day $^{-1}$
γ	0.25	0.25	day $^{-1}$
d	0.022	0.022	day $^{-1}$
α_1	0.9	0.8	Rational number
α_2	0.9	0.6	Rational number
α_3	0.9	0.4	Rational number
Value[1] is used in numerical study 1. **Value**[2] is used in numerical study 2.			

Numerical study 1

Consider Value[1] in Table 4. It is found as $\mathcal{R}_0\approx 0.969$. This only means the existence of the equilibrium point $E_0(2668,0,28582)$. In addition, since $\mathcal{R}_0<1$, it is seen that the equilibrium point E_0 for CFOS ($\alpha_1=\alpha_2=\alpha_3=0.9$) is stable according to Table 3 . This situation with initial conditions $[S_0\ I_0\ R_0]=[1000\ 1000\ 10000]$ can be seen in Figures 3 and 4.

Numerical study 2

When the values in Table 4 are used, the threshold parameter is found as $\mathcal{R}_0\approx 1.2$. Also, the trivial equilibrium point is $E_0(5079,0,1587)$. Since $\mathcal{R}_0>1$, the positive equilibrium point $E_1(4220,409,1958)$ exists and E_0 is an unstable point according to Table 3. Only the stability of E_1 can be examined.

Derivatives-orders are given as $[\alpha_1\ \alpha_2\ \alpha_3]=[0.8\ 0.6\ 0.4]$. Since m is the least common multiple of the denominators of derivative-orders, it is 5. Equation (29) translates to

$$\lambda^9+0.16\lambda^7+0.2409\lambda^5+0.038044\lambda^3+0.0172598\lambda^2+0.002863818=0. \tag{30}$$

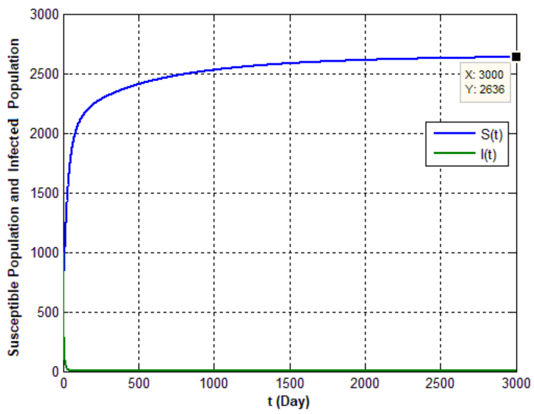

Figure 3. Time-dependent variation of susceptible and infectious populations for CFOS in (6)

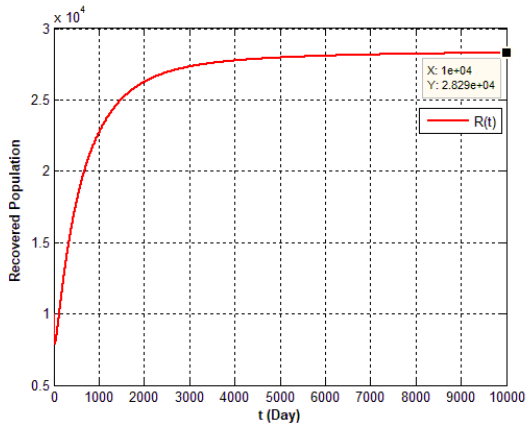

Figure 4. Time-dependent variation of the recovered population for CFOS in (6)

Roots of (30) are

$$\lambda_1 = -0.4990 + 0.5267i,$$

$$\lambda_2 = -0.4990 - 0.5267i,$$

$$\lambda_3 = 0.5039 + 0.4542i,$$

$$\lambda_4 = 0.5039 - 0.4542i,$$

$$\lambda_5 = -0.4042,$$

$$\lambda_6 = 0.2018 + 0.3738i,$$

$$\lambda_7 = 0.2018 - 0.3738i,$$

$$\lambda_8 = -0.0047 + 0.4025i,$$

$$\lambda_9 = -0.0047 - 0.4025i.$$

Also, we have

$$arg\lambda_1 = 133.4530°,$$

$$arg\lambda_2 = 226.5470°,$$

$$arg\lambda_3 = 42.0305°,$$

$$arg\lambda_4 = 317.9695°,$$

$$arg\lambda_5 = 180°,$$

$$arg\lambda_6 = 61.6371°,$$

$$arg\lambda_7 = 298.3629°,$$

$$arg\lambda_8 = 90.6690°,$$

$$\lambda_9 = 269.3310°.$$

Eigenvalues λ_i for $i = 1, 2, \dots, 9$ are greater than $\frac{\pi}{2m} = 18°$. Therefore E_1 is LAS.

Let the initial conditions by $[S_0\ I_0\ R_0] = [10000\ 100\ 100]$. In this case, the numerical simulation is obtained along the following Figures 5, 6 and 7.

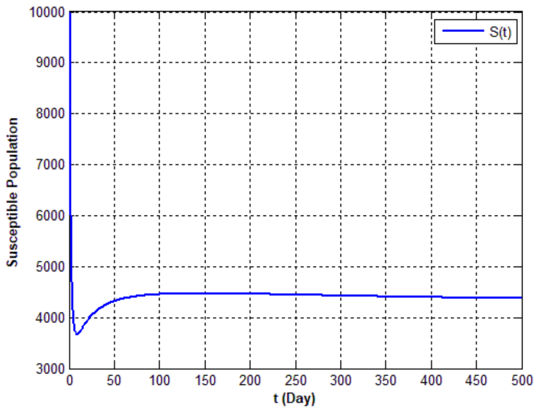

Figure 5. Time-dependent variation of susceptible population for IFOS in (6)

6 Conclusions

In this study, it is suggested the newly IFOS SIR model including the three time-dependent variables: susceptible, infected and recovered individuals in a population. This model proposed in system (6) is the form of nonlinear IFOS with the Caputo fractional derivative, accepted as rational numbers in the interval (0, 1]. In this context, the general situation regarding the stability of proposed model was investigated. Considering the derivative-orders, a new perspective was presented to the literature.

The model has an infection-free equilibrium point $E_0\left(\frac{\Lambda}{b}\frac{(b+\nu)}{(b+\nu+\mu)}, 0, \frac{\Lambda}{b}\frac{\mu}{(b+\nu+\mu)}\right)$ and a positive equilibrium point $E_1\left(S^* = \frac{(\gamma+d+b)}{\eta}, I^* = \frac{S^*(\mathcal{R}_0-1)(b+\nu+\mu)}{\left(\gamma+d+b+\nu\frac{d}{b}+\nu\right)}, R^* = \left(\frac{S^*(\mathcal{R}_0-1)(b+\nu+\mu)}{\left(\gamma+d+b+\nu\frac{d}{b}+\nu\right)} + \frac{S^*}{\gamma}\mu\right)\frac{\gamma}{(b+\nu)}\right)$. For these equilibrium points, their existence were analyzed according to the threshold parameter $\mathcal{R}_0$ and their stability were examined according to both $\mathcal{R}_0$ and eigenvalues obtained from characteristic equation roots. These results about the stability analysis are summarized in Table 3. In general, the *SIR* models in literature trying to explain the infection progress in a population with respect to the only parameter R_0. According to qualitative analysis of our model, it was found followings:

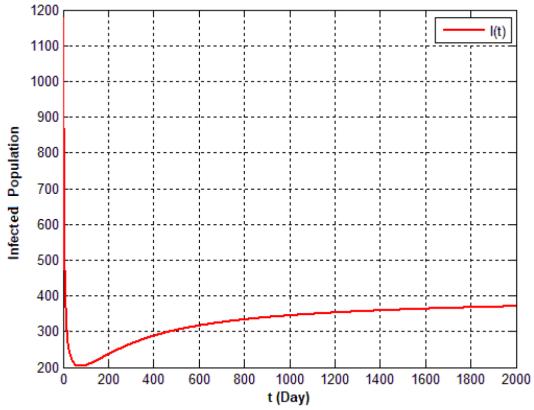

Figure 6. Time-dependent variation of infected population for IFOS in (6)

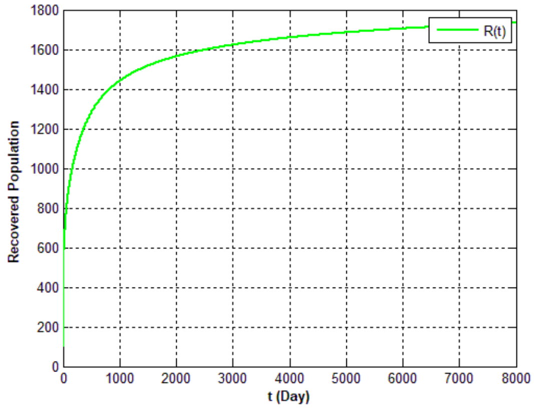

Figure 7. Time-dependent variation of recovered population for IFOS in (6)

i. Disease-free equilibrium point always exists and is LAS,

$$\begin{cases} \text{If } R_0 < 1 & \text{in case of } \alpha_1 = \alpha_2 = \alpha_3 \leq 1. \\ \text{If } R_0 < 1 \text{ and } (28) \text{ meet conditions } |arg\,(\lambda_i)| > \frac{\pi}{2m} & \text{in other cases.} \end{cases}$$

ii. Positive equilibrium point exists when R_0>1. This point is LAS,

$$\begin{cases} \text{If } R_0 > 1 \text{ (also the existence condition)} & \text{in case of } \alpha_1 = \alpha_2 = \alpha_3 \leq 1. \\ \text{If } (29) \text{ meet conditions } |arg\,(\lambda_i)| > \frac{\pi}{2m} & \text{in other cases.} \end{cases}$$

In numerical studies, the results of the qualitative analysis given in Table 3 are supported by graphics for the proposed SIR model. For this, the stability of E_0 for CFOS is shown in the first numerical study, while the stability of E_1 for IFOS is shown in the second numerical study.

Declarations

Consent for publication

Not applicable.

Conflicts of interest

The author declares that there is no known competing financial interests or personal relationships that could have appeared to influence the work reported in this paper.

Funding

The author declares that there is no funding source for the reported research.

Author's contributions

The research was carried out by the author and he accepts that the contributions and responsibilities belong to the author.

Acknowledgements

Not applicable.

References

[1] Yavuz, M., Ozdemir, N. & Baskonus, H. Solutions of partial differential equations using the fractional operator involving Mittag-Leffler kernel. *The European Physical Journal Plus*, 133(6), 1-11, (2018).
[2] Kashkynbayev, A. & Rihan, F. Dynamics of Fractional-Order Epidemic Models with General Nonlinear Incidence Rate and Time-Delay. *Mathematics*, 9(15), 1829, (2021).
[3] Razminia, A., Majd, V. & Baleanu, D. Chaotic incommensurate fractional order Rössler system: active control and synchronization. *Advances In Difference Equations*, 2011(1), 1-12, (2011).
[4] Ji, Y., Lu, J. & Qiu, J. Stability of equilibrium points for incommensurate fractional-order nonlinear systems. *2016 35th Chinese Control Conference (CCC)*, pp. 10453-10458, (2016,July).
[5] Daşbaşi, B. Stability analysis of the hiv model through incommensurate fractional-order nonlinear system. *Chaos, Solitons & Fractals*, 137, 109870, (2020).
[6] Deng, W., Li, C. & Guo, Q. Analysis of fractional differential equations with multi-orders. *Fractals*, 15(02), 173-182, (2007).
[7] Hamou, A.A., Azroul, E. & Hammouch, Z. On dynamics of fractional incommensurate model of Covid-19 with nonlinear saturated incidence rate, *medRxiv*, (2021).
[8] Wang, Y. & Li, T. Stability analysis of fractional-order nonlinear systems with delay. *Mathematical Problems In Engineering*, (2014).
[9] Petras, I. Stability of fractional-order systems with rational orders. *ArXiv Preprint ArXiv:0811.4102*, (2008).
[10] Rivero, M., Rogosin, S.V., Tenreiro Machado, J.A. & Trujillo, J.J. Stability of fractional order systems. *Mathematical Problems In Engineering*, (2013).
[11] Brandibur, O., Garrappa, R. & Kaslik, E. Stability of Systems of Fractional-Order Differential Equations with Caputo Derivatives. *Mathematics*, 9(8), 914, (2021).
[12] Lekdee, N., Sirisubtawee, S. & Koonprasert, S. Bifurcations in a delayed fractional model of glucose–insulin interaction with incommensurate orders. *Advances In Difference Equations*, 2019(1), 1-22, (2019).
[13] Debbouche, N., Ouannas, A., Batiha, I.M. & Grassi, G. Chaotic Dynamics in a Novel COVID-19 Pandemic Model Described by Commensurate and Incommensurate Fractional-Order Derivatives. (2021).
[14] Wang, X., Wang, Z. & Xia, J. Stability and bifurcation control of a delayed fractional-order eco-epidemiological model with incommensurate orders. *Journal Of The Franklin Institute*, 356(15), 8278-8295, (2019).
[15] Veeresha, P. A Numerical Approach to the Coupled Atmospheric Ocean Model Using a Fractional Operator.*Mathematical Modelling and Numerical Simulation with Applications (MMNSA)*, 1(1), 1-10, (2021).
[16] Yavuz, M., & Yaşkıran, B. Conformable Derivative Operator in Modelling Neuronal Dynamics. *Applications & Applied Mathematics*, 13(2), 803-817, (2018).
[17] Yokuş, A. Construction of Different Types of Traveling Wave Solutions of the Relativistic Wave Equation Associated with the Schrödinger Equation. *Mathematical Modelling and Numerical Simulation with Applications (MMNSA)*, 1(1), 24-31, (2021).
[18] Yavuz, M., & Sene, N. Fundamental calculus of the fractional derivative defined with Rabotnov exponential kernel and application to nonlinear dispersive wave model. *Journal of Ocean Engineering and Science*, 6(2), 196-205, (2021).
[19] Hammouch, Z., Yavuz, M., & Özdemir, N. Numerical Solutions and Synchronization of a Variable-Order Fractional Chaotic System. *Mathematical Modelling and Numerical Simulation with Applications (MMNSA)*, 1(1), 11-23, (2021).
[20] Sene, N. Fractional diffusion equation described by the Atangana-Baleanu fractional derivative and its approximate solution. *Journal of Fractional Calculus and Nonlinear Systems*, 2(1), 60-75, (2021).
[21] Al-Mdallal, Q.M., Hajji, M.A., & Abdeljawad, T. On the iterative methods for solving fractional initial value problems: new perspective. *Journal of Fractional Calculus and Nonlinear Systems*, 2(1), 76-81, (2021).
[22] Yavuz, M., Coşar, F. Ö., Günay, F., & Özdemir, F. N. A new mathematical modeling of the COVID-19 pandemic including the vaccination campaign. *Open Journal of Modelling and Simulation*, 9(3), 299-321, (2021).
[23] Yavuz, M., Sulaiman, T.A., Yusuf, A. & Abdeljawad, T. The Schrödinger-KdV equation of fractional order with Mittag-Leffler nonsingular kernel. *Alexandria Engineering Journal*, 60(2), 2715-2724, (2021).
[24] Nazir, G., Zeb, A., Shah, K., Saeed, T., Khan, R.A. & Khan, S.I.U. Study of COVID-19 mathematical model of fractional order via modified Euler method. *Alexandria Engineering Journal*, 60(6), 5287-5296, (2021).
[25] Zarin, R., Ahmed, I., Kumam, P., Zeb, A. & Din, A. Fractional modeling and optimal control analysis of rabies virus under the convex incidence rate. *Results in Physics*, 28, 104665, (2021).
[26] Alqudah, M.A., Abdeljawad, T., Zeb, A., Khan, I.U. & Bozkurt, F. Effect of Weather on the Spread of COVID-19 Using Eigenspace Decomposition. *Cmc-Computers Materials & Continua*, 3047-3063, (2021).
[27] Angstmann, C.N., Henry, B.I. & McGann, A.V. A fractional-order infectivity and recovery SIR model. *Fractal And Fractional*, 1(1), 11, (2017).
[28] Liu, N., Fang, J., Deng, W. & Sun, J.W. Stability analysis of a fractional-order SIS model on complex networks with linear treatment function. *Advances In Difference Equations*, 2019(1), 1-10, (2019).
[29] Alqahtani, R.T. Mathematical model of SIR epidemic system (COVID-19) with fractional derivative: stability and numerical analysis. *Advances In Difference Equations*, 2021(1), 1-16 (2021).
[30] Naik, P.A., Yavuz, M., Qureshi, S., Zu, J. & Townley, S. Modeling and analysis of COVID-19 epidemics with treatment in

fractional derivatives using real data from Pakistan. *The European Physical Journal Plus*, 135(10), 1-42, (2020).
[31] Tavares, D., Almeida, R. & Torres, D.F. Caputo derivatives of fractional variable order: numerical approximations. *Communications In Nonlinear Science And Numerical Simulation*, 35, 69-87, (2016).
[32] Tavazoei, M.S. & Haeri, M. Chaotic attractors in incommensurate fractional order systems. *Physica D: Nonlinear Phenomena*, 237(20), 2628-2637, (2008).
[33] Odibat, Z.M. Analytic study on linear systems of fractional differential equations. *Computers & Mathematics With Applications*, 59(3), 1171-1183, (2010).
[34] Owolabi, K.M. Riemann-Liouville fractional derivative and application to model chaotic differential equations. *Progress in Fractional Differentiation and Applications*, 4, 99-110, (2018).
[35] Alshomrani, A.S., Ullah, M.Z. & Baleanu, D. Caputo SIR model for COVID-19 under optimized fractional order. *Advances In Difference Equations*, 2021(1), 1-17, (2021).
[36] Daşbaşı, B. & Öztürk, İ. Mathematical modelling of bacterial resistance to multiple antibiotics and immune system response. *SpringerPlus*, 5(1), 1-17, (2016).
[37] Daşbaşı, B. Stability analysis of mathematical model including pathogen-specific immune system response with fractional-order differential equations. *Computational And Mathematical Methods In Medicine*, (2018).
[38] Daşbaşı, B. Çoklu Kesirli Mertebeden Diferansiyel Denklem Sistemlerinin Kalitatif Analizi, Analizdeki Bazi Özel Durumlar ve Uygulamasi: Av-Avci Modeli. *Fen Bilimleri ve Matematik'te Akademik Araştırmalar* (1. B., S. 127-157). Içinde Ankara: Gece Kitaplığı, (2018).